IN VITRO EXPERIMENTAL FLOW ANALYSIS INSIDE AN ARTERIOVENOUS GRAFT TO VEIN CONNECTION

by

Ayşe Büşra ŞENGÜL

A thesis submitted to

the Graduate Institute of Sciences and Engineering

of

Fatih University

in partial fulfillment of the requirements for the degree of

Master of Science

in

Environmental Engineering

August 2007
Istanbul, Turkey

APPROVAL PAGE

I certify that this thesis satisfies all the requirements as a thesis for the degree of Master of Science.

Assist. Prof. Dr. Sami GÖREN
Head of Department

This is to certify that I have read this thesis and that in my opinion it is fully adequate, in scope and quality, as a thesis for the degree of Master of Science.

Assist. Prof. Dr. Nurullah ARSLAN
Supervisor

Examining Committee Members

Assist. Prof. Dr. Nurullah ARSLAN ……..

Assist. Prof. Dr. Sami GÖREN ……..

Assist. Prof. Dr. Omar ALAGHA ……..

It is approved that this thesis has been written in compliance with the formatting rules laid down by the Graduate Institute of Sciences and Engineering.

Assist. Prof. Dr. Nurullah ARSLAN

Director

August 2007

IN VITRO EXPERIMENTAL FLOW ANALYSIS INSIDE AN ARTERIOVENOUS GRAFT TO VEIN CONNECTION

Ayşe Büşra ŞENGÜL

M. S. Thesis – Environmental Engineering
August 2007

Supervisor: Assist. Prof. Dr. Nurullah ARSLAN

ABSTRACT

We present experimental results inside an upscaled end-to-side model of a human arteriovenous (AV) graft using laser Doppler anemometry (LDA) under steady flow conditions. This work is to understand better the importance of biomechanical forces in the development of intimal hyperplasia (IH) within these grafts. We measured the turbulence level and Wall shear stresses (WSS) inside an in vitro model representing an AV arteriovenous graft to vein connection. The steady flow had maximum and mean Reynolds numbers of 2400 and 1400 based on the graft diameter. The flow division was 80% entering from the graft inlet and 20% entering from the distal vein segment (DVS) for flow meaurements. Measurements were made at twenty nine axial locations in the plane of bifurcation at the venous anastomosis (VA). At Reynolds 2400, the velocity profiles were blunt at the inlet of the arteriovenous graft. High turbulence levels and WSS were found in the proximal vein segment (PVS). A separation region was observed at the toe side of the

arteriovenous graft. Strong secondary flows were found at the inlet graft and inside the PVS. These regions are considered critical regions for medical applications because of the lower WSS values and higher turbulence levels. The blockage of the graft was mostly seen in this region. We find that this model was implanted with considered very poor geometrical approach. The patency rate of these types geometrical connections will be very low. The results of this study show the flow field inside an AV graft to be complex.

Keywords: Arteriovenous graft, Dialysis, In vitro model, Laser Doppler anemometry, Steady flow

ARTERIOVENOUS GRAFT – TOPLARDAMAR BAĞLANTI BÖLGESİNDEKİ AKIŞIN DENEYSEL OLARAK ARAŞTIRILMASI

Ayşe Büşra ŞENGÜL

Yüksek Lisans Tezi – Çevre Mühendisliği
Ağustos 2007

Tez Yöneticisi: Yrd.Doç. Dr. Nurullah ARSLAN

ÖZ

Akış ölçümleri, graft bağlantı bölgesinde laser Doppler anemometri kullanılarak sürekli akış şartlarında deneysel olarak yapıldı. Bu çalışma graft içerisindeki hücre büyümesinden kaynaklanan biomekanik güçlerin önemini daha iyi anlamak için yapılmıştır. Arteriovenüz graft modelinin ifade eden deneysel çalışmada duvar kayma gerilimi ve türbülans seviyesi ölçülmüştür. Graft çapına bağlı olarak maksimum ve ortalama Reynolds sayıları 2400 ve 1400 olarak belirlenmiştir. Akış ölçümleri için akışın %80'i graft girişine %20'side merkezden uzak damar kısmına dağıtılmıştır. Ölçümler toplardamar bölgesindeki çatallaşma kısmında 13 eksende yapılmıştır. Toplardamar bağlantısında dağınık hız profilleri gözlemlenmiştir. Merkeze yakın damar kısmında yüksek türbülans dalgalanmaları ve yüzey gerilim stresi bulunmuştur. Toplardamar bağlantısının çatal kısmında ayrılma bölgesi gözlemlendi. Merkeze yakın damar kısmının girişinde ve içinde kuvvetli ikincil akışlar bulundu. Bu bölgedeki eylemsizlik kuvvetinden dolayı düşük gerilim stres değerleri ve yüksek türbülans meydana gelmiştir. Bu nedenle tibbi uygulamalarda kritik bölgeler olarak düşünülür. Graft tıkanması çoğunlukla bu bölgede oluşur. Bu modelin geometrik açıdan yetersiz olduğu bulunmuştur. Bu tip

geometrik bağlantılarda damarın açık kalma oranı çok düşük olacaktır. Bu çalışma sonucunda toplardamar bağlantı bölgesindeki akış alanının karmaşık olduğu görülmüştür.

Anahtar Kelimeler: Toplardamar bağlantı bölgesi, Diyaliz, In vitro, Laser Doppler anemometri, Sürekli akış

DEDICATION

This is dedication to my loving husband Abdülkadir,
my father, my mother and my brothers

ACKNOWLEDGEMENT

I wish to thank many people who, in one way or another, made this thesis possible. First of all to my supervisor Assist. Prof. Dr. Nurullah ARSLAN, I am really very much grateful for his scientific guides, motivation, providing a critical atmosphere for discussion, for his patience and for all the time and efforts he devoted for me. It was really a great pleasure for me to conduct this thesis under his supervision.

I also want to thank to Assist Prof. Sami GÖREN for their supporting to my research endeavors.

My thanks also go to Erkan KABACALI and İlhan GENÇHELLAÇ for their technical helping during the construction of experimental setup.

I would also like to thank to TÜBİTAK Health Science Research Group (SBAG) for funding my thesis and supporting my research financial with the project number of SBAG- 104S531.

I also want to thank Dr. Kazım BEŞİRLİ, Assoc. Prof. Hikmet KOCABAŞ, Dr. Mehmet Halit YILMAZ, and Dr. Sinan TRABLUS for their helping to supply in vivo data for the research.

I express my thanks and appreciation to my husband, Abdülkadir ŞENGÜL for his understanding, motivation and patience.

TABLE OF CONTENTS

LIST OF FIGURES

LIST OF TABLE

LIST OF ABBREVIATIONS

ABBREVIATION

AA	:	Arterial Anastomosis
AV	:	Arteriovenous
AVF	:	Arterovenous Fistula
AVLG	:	Arteriovenous Fistula Loop Graft
CFD	:	Computational Fluid Dynamics
DOS	:	Distal Outlet Segment
DVS	:	Distal Vein Segment
EMF	:	Electromagnetic Flow Meter
ESRD	:	End-Stage Renal Disease
FFT	:	Fast Fourier Transform
LDA	:	Laser Doppler Anemometry
LDV	:	Laser Doppler Vibrometer
OSI	:	Osillatory Index
PG	:	Pressure Gradient
PM	:	Photomultiplier
POS	:	Proximal Outlet Segment
PR	:	Pressure Ratio
PTFE	:	Polytetrafluorethylene
PVS	:	Proximal Vein Segment
RI	:	Resistance Index
VA	:	Venous Anastomosis
VAIH	:	Venous Anastomotic Inimal Hyperplasia
VWV	:	Vein Wall Vibration
WSS	:	Wall Shear Stress
WSSG	:	Wall Shear Stress Gradiant

CHAPTER 1

INTRODUCTION

1.1 BACKROUND

Patients with end-stage renal disease (ESRD) would die within a few weeks or months if not sustained by some form of dialysis theraphy or a kidney transplant [1]. According to the National Kidney Foundation about 20 million Americans are currently affected by kidney and urological disease and millions more are at risk. In the US., approximately 300,000 patients suffer from ESRD; 85% of these patients will be treated by hemodialysis. In the absence of a kidney transplant these patients will require artificial hemodialysis for their lifetime.[2]. In 1995, Medicare was expected to spend nearly $8 billion, or over 4% of all total spending, on such patients. That is about $40,000 per beneficiary pear year [3] With the constant increase in the number of people with cronic failure who have undergone dialysis in Turkey has rapidly grown. According to the results of these statistical studies, the number of patients who underwent dialysis during the 2003 showed approximately 30,000 patients are treated by hemodialysis [4].

For some patients, kidney transplantation is the preferred treatment. While the transpalantation is an attractive solution in principle, there are many difficulties in its implementation, especially the severe shortage of appropriately matched donor kidneys [3].

Kidney transplants are seldom performed in elderly people. In 1985, only 56 (1 percent) of the 6,938 kidney transplants performed in the US were performed in patients aged 65 to 74 years, and only 3 were performed in patients 75 years and

older [3]. In 2003, only 1 percent of the 6,195 kidney transplants performed in the Turkey we performed in patients aged 65 to 74 years, and only 2 were performed in patients 75 years and older [4]. At present, renal dialysis is the only widely used ESRD treatment for elderly persons.

Healthy kidneys clean your blood by removing excess fluid, minerals, and wastes. They also make hormones that keep your bones strong and your blood healthy. When your kidneys fail, harmful wastes build up in your body, your blood pressure may rise, and your body may retain excess fluid and not make enough red blood cells. When this happens, you need treatment to replace the work of your failed kidneys. Hemodialysis do exactly removes waste, salt and extra water to prevent them from building up in your blood. Keep a safe level of certain chemicals in your blood. Help to control blood pressure [5].

Patients with end-stage renal disease require a renal replacement therapy such as hemodialysis. The blood flow through the artificial kidney required to obtain efficient hemodialysis is about 350 ml/min. As the mean blood flow through blood vessels in the limbs does not reach 350 ml/min, a vascular access is constructed [6-8].

Hemodialysis requires a direct artery-vein access that is easy to locate and that will provide optimal blood flow during treatment. Unfortunately, a number of hemodialysis patients do not have adequate vessels to form a fistula (a connection) between a vein and an artery; therefore, a synthetic graft must be inserted. Synthetic grafts like polytetrafluorethylene (PTFE) grafts are the most widely used types of vascular access in US. PTFE grafts are easily inserted, easily maintained, have moderate resistance to infection and a low incidence of aneurysm formation. Typically, these grafts are placed as a straight connection or as a loop in either the forearm or arm (Figure 1.1) [9]. This loop connects an artery to a vein and allows for easy access during hemodialysis treatment.

In patients with small or poor blood vessels such as diabetic and elderly, a PTFE graft is often the access of choice because the blood vessels of these patients do not allow the creation of a native arteriovenous (AV) fistula (Figure 1.2) [7]. In Europe, the commonly used vascular accesses like central venous catheters (10% of the cases),

arterovenous fistula (AVF) (60%), and acess graft (30%) are used to deliver this flow rate [10]. In Turkey the commonly used vascular accesses like central venous catheters (3.5% of the cases), AVF (87.5%), and acess graft (3.5%) and other (repeated surgery 5.5%) are used to deliver this flow rate [4]. Despite the lower primary patency rate for the AVF (20-30% early failures), AVF have a higher secondary patency rate (50-78% after 3 year) than PTFE-grafts (40-59% after 3 year) [10]. The main reason for PTFE-graft failure is stenosis (Figure 1.3) development at the venous anastomosis (VA) leading to thrombosis [10].

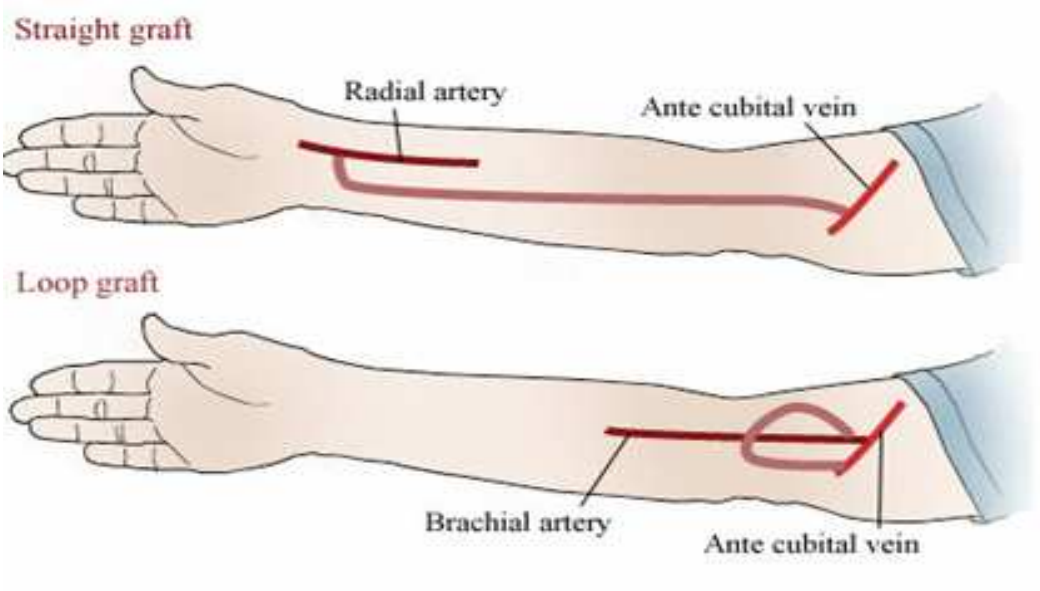

Figure 1.1 Two types of AV graft construction, straight and loop [11].

If you have small veins that won't develop properly into a fistula, you can get a vascular access that uses a synthetic tube implanted under the skin in your arm. The tube becomes an artificial vein that can be used repeatedly for needle placement and blood access during hemodialysis. A graft doesn't need to develop as a fistula does, so it can be used sooner after placement, often within 2 or 3 weeks. Compared with fistulas, grafts tend to have more problems with clotting or infection and need replacement sooner, but a well-cared-for graft can last for several years.

For hemodialysis patients, an AV connection is constructed from an artery to a vein to provide an access site. By bypassing the high-resistance vessels, high flow rates can be achieved that are necessary for efficient hemodialysis. In the US., the majority of AV connections are constructed by using PTFE grafts. Unfortunately, more than half of the AV grafts fail and require surgical reconstruction within three years. The prevalent cause of these graft failures is venous anastomotic inimal hyperplasia (VAIH)-a stenosis, or narrowing of the vein, downstream of the graft [1].

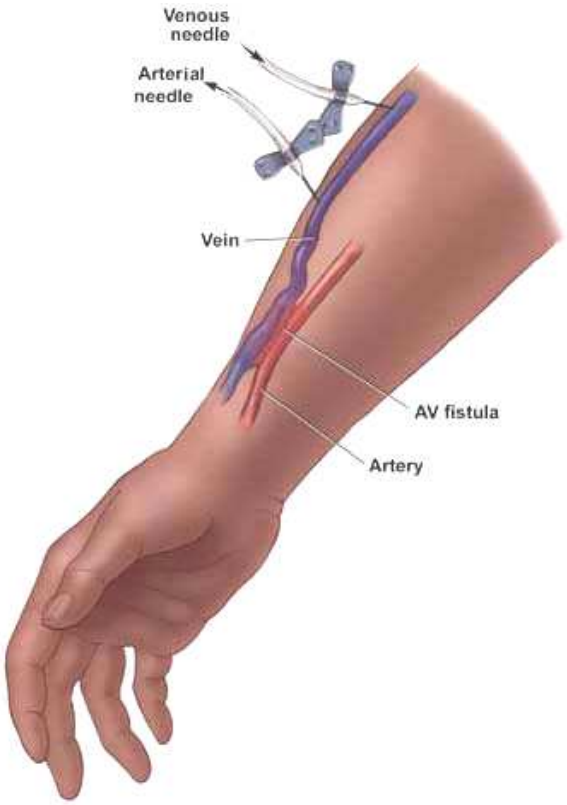

Figure 1.2 An AVF is a surgical connection between an artery and a vein, usually in the forearm [12].

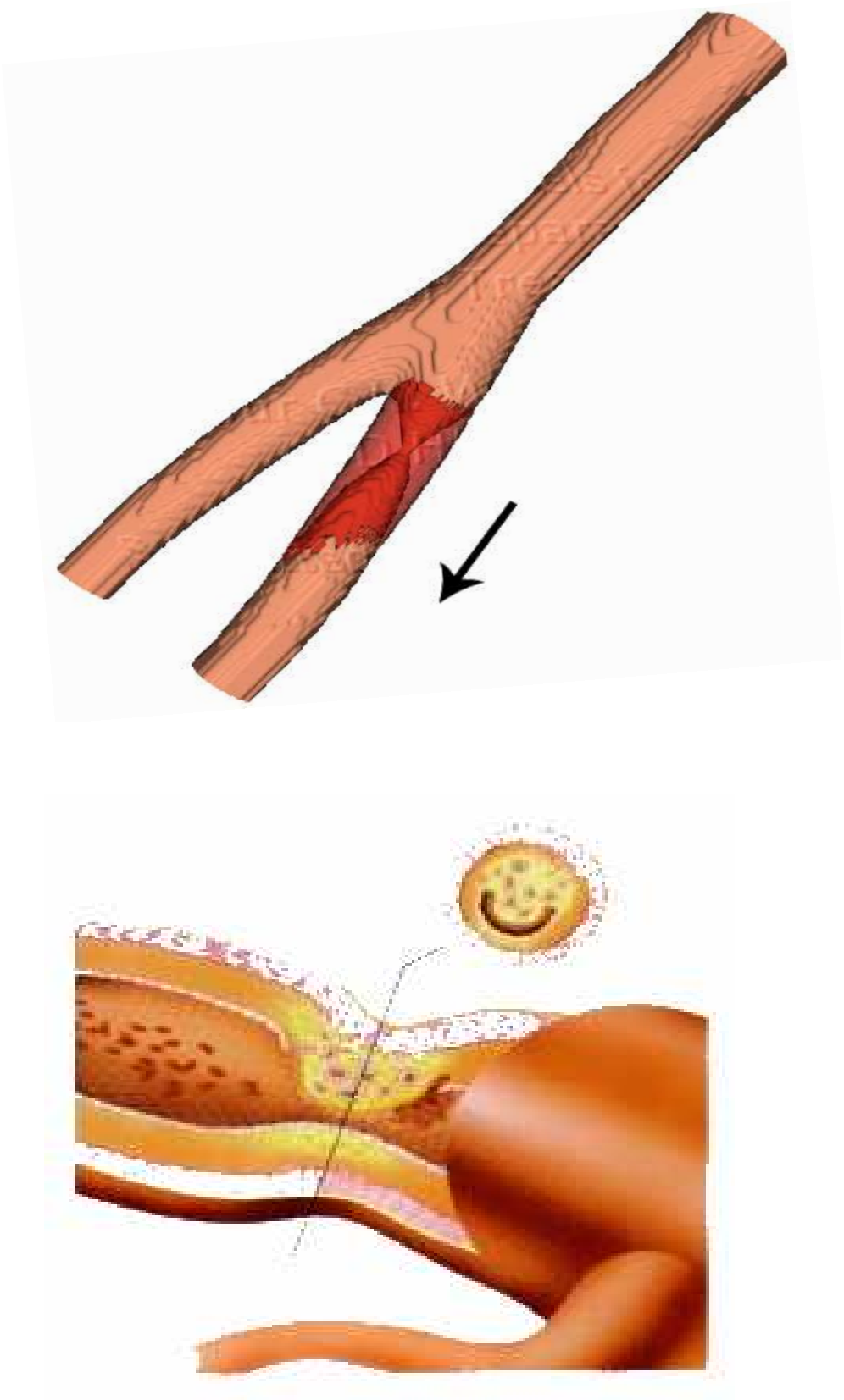

Figure 1.3 Sketch of stenosis or narrowing of the vein [9].

Changes in the VA geometry can greatly affect fluid dynamic variables. The surgeon has some degree of control over this geometry during graft construction. A further understanding of the relationship between AV graft failure and fluid dynamic variables may lead to a prediction of graft performance. This may lead to geometric designs, which extend the function period before AV graft failure occurs.

This research is an experimental study to analyze the hemodynamics inside an upscaled model of an AV graft quantitatively. The velocities in the bifurcation plane of the model are measured using laser Doppler anemometry (LDA). The turbulence level and Wall shear stress (WSS) are calculated quantitatively. The in vivo values of velocity at the inlet of the AV graft and geometry were measured using color Doppler ultrasound at the Cerrahpaşa Hospital of The University of İstanbul.

Several experimental studies have employed in vitro and in vivo models representing the anastomoses to investigate the hemodynamic environment and its relationship with graft failure.

Prostetic AV grafts are more prone to failure as a result of anastomotic intimal hyperplasia than any other type of vascular graft. In PTFE hemodialysis access grafts hyperplasia causes more than 50% of all failures, and graft patency at 1 year is less than 80% [13]. Toward that end, study examined the effect of tapered AV grafts using canine in vivo model. Untapered 6 mm diameter polytetrafluoraethylene grafts were paired with 4 to 7 mm taper or 7 to 4 mm taper grafts [13-16]. Several hemodynamic variables were assesses at multiple locations, and venous intimal-medial thickness was measured at locations corresponding to the hemodynamic measurements. Color Doppler imaging demonstrated energy transfer out of the vessel in form of perivascular tissue vibration signal. Differences among graft types were noted for pressure, flow velocity, tissue vibration, and venous intimal-medial thickness. They concluded that graft geometry can have a significant impact on hemodynamic factors and venous intimal-medial hyperplasia in arteriovenous loop grafts. Flow disturbances appear to cause energy transfer through the vessel wall and into perivascular tissue. Kinetic energy transfer in the form of perivascular tissue vibration was quantitated in vivo and correlates strongly with venous intimal-medial thickness [13]. In one canine study placed a Teflon tape just after the arterial anastomosis to create different levels of tissue vibration in two venous

anastomoses. They found a greater degree of intimal-medial thickening in the anastomosis in which tissue vibration was more severe. They found tissue vibration to be most severe near the venous anastomosis. They concluded from their measurements that turbulence was a mojor factor in the development of venous intimal-medial thickening in AV grafts. They also correlated Reynolds number with intimal thickening at the venous anastomosis [14]. In another study examined the effect of tapered AV grafts using a canine in vivo model. The size of the graft was 4 mm in a diameter at the arterial end to a 7 mm in diameter at the venous end. In another group of animals, the tapered grafts were reversed with the 7 mm end placed at the arterial anastomosis. This created a situation where volumetric flow rates were similar, flow velocities and the degree of turbulence were volumetric flow rates were similar, but flow velocities and degree of turbulence were different. In comparing different graft types, they reported that the 4-7 mm taper grafts demonstrated less perivascular tissue vibration than did the 7-4 mm or 6 mm straight grafts. They also found oscillating boundary layer separation in the hood of the graft, but not in the vein itself where hyperplasia commonly occurs.

IHT is a frequent cause of prosthetic by-pass graft failure. Induction and progression of IHT is thought to involve a number of mechanisms related to variations in the flow field, injury and the prosthetic nature of the conduit [17]. Study was designed to examine the relative contribution of WSS and injury to the junction of IHT at defined regions of experimental end-to-side prosthetic anastomoses. The distribution of IHT was determined at the distal end-to-side anastomosis of seven canine iliofemoral PTFE grafts after 12 weeks of implantation. An upscaled transparent model easy constructed using the in vivo anastomotic geometry, and WSS was determined at 24 axial locations from LDA measurements of the near wall velocity under conditions of pulsatile flow. The model was constructed from a Sylgard elastomer (Dow Corning, Midland, MI) and scaled up nine times to increase the spatial resolution. Dynamic similarity between the original graft and the scaled-up model was ensured by maintaining physiologic Reynolds and Womersley numbers. The WSS values were estimated from the near wall velocity measurements. The fluid was mixture of 42% water and 58% glycerin by weight in order to match the refractive index of the Sylgard model.

A canine animal study was conducted to simulate the hemodynamic environment of a human AV graft [1]. In vivo measurements were obtained for vein-wall vibration (VWV), graft geometry, and blood flow rate. In order to investigate the complex flow structure at the venous anastomosis of an AV graft, which is thought to induce these vibrations, a computational fluid dynamic study was conducted by direct numerical simulation under pulsatile flow and geometry conditions based on the animal study. The simulation technique employs the spectral element method, which is a high-order discretizetion ideally suited to the simulation of transitional flows in complex domains. The minimum and maximum Reynolds numbers entering the graft, based on average velocities, were 875 and 1,235, respectively. While velocity and pressure fluctuations are clearly present in the numerical simulations, their magnitude and frequency do not correlate well with the in vivo VWV meaurements. Potential reasons for this discrepancy are threefold. First, a quiescent inflow condition was used in the present computations; a more realistic inflow condition might alter the velocity fluctuations significantly. Second, simulations were conducted with a rigid geometry; compliance may play an important role in flow stability within an AV graft. Third, the fow split between the graft and vein inlet may also an important role in the stability of the flow structures.

Boundary layer separation in models of side-to-end anastomoses used clinically in axillofemoral and femorofemoral grafting [18]. Boundary layer separation occurs when momentum causes a fluid to flow against a local pressure gradient. Models of side-to-end anastomoses were constructed from Dacron grafting material and from clear plastic blocks and tubing. Water from a gravity head tank was used as a steady-flow source and inlet water temperature was monitored continuously. Flow was measured by timed collection. Inlet Reynold’s numbers from 300 to 5,000 were studied. Fluid energy loss across the anastomosis was small and physiologically insignificant. Local adverse pressure gradients were demonstrated near the anastomosis. Flow visualization studies demonstrated characteristic areas of boundary layer separation in the region of the adverse pressure gradients. The separation region involved both the main limb and the side arm. The separation forms a shell or ring of slow-moving fluid around the mainstream. Preliminary studies with pulsatile flow and with blood demonstrate that boundary layer separation occurs under clinical flow conditions. Boundary layer

separation may play a role in the development of anastomotic hyperplasia and atherosclerotic deposits in the vicinity of surgical anastomoses.

Transition in a pipe flow with a superimposed sinusoidal modulation has been studied in a straight circular water pipe using LDA techniques [19]. The experiments were carried out in a Plexiglass pipe. Water entered the pipe from a constant head tank through a bell-shaped contraction. A 35 mW He-Ne laser in conjuction with a counter-type signal processor (TSI Model 1990) was used in the dual-beam forward-scattering mode to obtain the longtitudinal velocity signal. Natural seeding of the water was enough to ensure a continouos velocity signal of the anolog output of the counter. The temperature of the water was kept constant (24 ^{o}C) to ensure a constant value of the viscosity.

The phasic velocity field in the vicinity of the venous anastomosis in a hemodialysis angioaccess arteriovenous fistula loop graft (AVLG) is investigated employing a LDA system. Detailed LDA velocity profiles are obtained by sectional survey performed in a transparent, elastic flow model which was fabricated to represent the geometry of the AVLG system under physiological pressure and flow waveforms. The transparent flow model was installed in a small rectangular plexiglass box with an open top and flat optic glass. The space between the model and the box walls was filled with the same analog fluid to minimize laser beam refraction. The blood analog fluid used in this study was a solution of 32.7% glycerol and 5.2% $CaCI_2$ in distlled water. The geometry of the flow model was based on a silicone rubber cast obtained from an experimental dog model. Distribution of velocity profiles is obtained. The distribution of WSS in the model is computed from the slope of the local velocity profiles near the wall. The relationship between the results obtained by flow visualization and the LDA measurements is discussed [20].

Flow dynamic study of the AVLG system using three elastic, transparent bench-top flow models, which were based on the geometry of silicone rubber casts obtained at different times from a chronic animal model [21]. Each model thus represented a different stage of the lesion development. Flow visualization and LDA surveys of the flow field confirmed that the hydrodynamic factors favour lesion development near the stagnation point opposite the anastomotic toe, where the momentum of the imping jet

stream, combined with the oscillating WSS generated in the vicinity of the stagnation point, acts in both directions. The accumulation of tracer particles in the region of flow separation is belived to be a combined contribution from the hydraulic forces and the inward motion of the vessel wall.

Flow behavior in models of end-to-side vascular graft anastomoses was studied for steady and pulsatile flow conditions [22]. They constructed models to simulate geometry employed in experimental studies on inimal thickening in a canine model. Sylgard model of the anastomotic region was constructed. Reynolds numbers, division of flow in the outflow tracts and the pulsatile waveform employed were taken from measurements obtained in the canine model. Flows in the scaled-up, transparent models were visualized with white, neutrally buoyant particles which were photographed under laser illumination and also recorded on video tape under bright incandescent light. Strong, three-dimentional helical patterns which formed in the anastomotic junction were prominent features of the flow fields. Regions of low wall shear, oscillatory wall shear and long particle residence time were identified from the flow visualization experiments. Comparisons with the limited qualitative data available on inimal thickening in vascular graf anastomoses suggest a relation between localization of vascular inimal thickening and those surfaces experiencing low shear and long particle residence time.

Measurements of turbulent flow through a constricted tube with a 75% constriction have been performed with LDA [23]. The Reynolds numbers changed from 5,000 to 15,000. Velocity profiles, root mean square, turbulence velocities, and energy spectra were recorded along with determination of the wall pressure variation and the length of the recirculation region. Results showed extremely high level of turbulence within the recirculation region.

Flow structures were visualized in a transparent polyurethane model of proximal side-to-end vascular anastomoses, using planar illumination of suspended tracer particles. Both the effects of geometry and flow division were determined under steady and pulsatile flow conditions, for anastomosis angles 15, 30, and 45 degrees. The flow patterns were highly three-dimentional and were characterized by a series of vortices in the fully occluded distal artery and two helical vortices aligned with the axis of the

graft. In steady flow, above a critical Reynolds number, the flow changed from a laminar regime to one displaying time-dependent behavior. In particular, significant fluctuating velocity components were observed in the distal artery and particles were shed periodically from the occuled artery into the graft. Pairs of asymmetry flow patterns were also observed in the graft, before the onset of the time-dependent flow regime. The critical Reynolds number ranged from 427 to 473 and appeared to be independent of anastomosis angle. The presence of a patent distal artery had a significant effect on the overall flow pattern and led to the formation of a large recicurlation region at the toe of the anastomosis. The main structures observed in the steady flow, such as vortices in the distal artery and helical flow in the graft, were also seen during the pulsatile cycle. However, the secondary flow components in the graft were more pronounced in pulsatile flow particularly during deceleration of the flow waveform. At higher mean Reynolds numbers, there was also a greater mixing between fluid in the occluded arterial section and that in the graft [24].

A pulsatile flow in vitro model of the distal end-to-side anastomosis of an arterial bypass graft was used to examine the effects that different flow ratios between the proximal outlet segment (POS) and the distal outlet segment (DOS) have on the flow patterns and the distributions of hemodynamic factors in the anastomosis [25]. Sylgard model was constructed. The flow system consisted of a steady flow pump, a pulsatile air pump, a timer-controlled solenoid valve, a compliance chamber, variable resistor, a test section, and a return tank. A concentration Dextran by weigh in distled water was used as the circulating fluid obtain the required kinematic viscosity 0.15 cm^2/s. To achieve minimum refraction between the viewing box, which was made of 3-mm-thick Plexiglass, and the test section, mineral oil with a refractive index of 1.468 was used to fill the viewing box. Amberlite particles were tracked by flow visualization to determine overall flow patterns and velocity measurements were made with two-dimentional LDA to obtain detailed hemodynamic factors along the artery floor and the graft hood regions. These factors included WSS, spatial wall shear stress gradiant (WSSG), and osillatory index (OSI). Statistical analysis was used to compare these hemodynamic factors between cases having different POS:DOS flow ratios. The results showed that changes in POS:DOS flow ratios had a great influence on the flow patterns in the anastomosis. With an increase in proximal outlet flow, the range of location of the

stagnation point along the artery floor decreased, while the extent of flow separation along the graft hood increased.

Turbulent flow measurements were conducted inside an upscaled end-to-side model of a human arteriovenous graft using LDA under steady and pulsatile flow conditions [3, 26, 27]. Turbulence intensity, Reynolds stress, and mean velocities have been measured for steady and pulsatile flow. AV graft-vein junctions flow conditions and vessel diameters were determined using Color Doppler ultrasound measurements were conducted within one month of graft construction. The PTFE AV graft connected the brachial artery to the basilic vein near the patient's elbow. The model material was transparent elastomer (Slygard 184, Dow Corning). The fluid employed, a mixture of 42% water and 58% gylcerine by weight, was chosen the index of refractive of the Slygard model. A heater/mixer in the downstream tank was used to keep the fluid temperature at 23±0.5ºC during experiments. Reynolds numbers for steady flow were 1060, 1820, 2530 and 2720. The peak, mean and minimum Reynolds numbers were 2470, 1762 and 1198 for the pulsatile flow, respectively. The flow division was 90% entering from the graft inlet and 10% entering from the distal vein segment (DVS) for steady flow measurements. It was 85% entering from the graft and 15% entering from the DVS for pulsatile flow measurements. Measurements were made thirteen axial locations in the plane of the bifurcation at the VA. At high Reynolds numbers (>2000), the velocity profiles were blunt at the inlet of the arteriovenous graft. High turbulence fluctuations and Reynolds stress were found in the proximal vein segment (PVS) opposite to the vein side of the anastomosis for steady and pulsatile flows. Steady flow fluctuation values were 20-30% larger than pulsatile flow values for the same instantaneous Reynolds number. A separation region was observed at the toe side of the arteriovenous graft. Strong secondary flows were found at the inlet to and the PVS under steady flow conditions. The results of this research demonstrate the level and distribution of turbulence in an arteriovenous graft for one specific geometry. Turbulence levels in the arteriovenous graft high enough to cause vibration which may stimulate tissue growth. The larger the disturbances at the anastomosis, the greater the release of energy. The velocity and pressure fluctuations that cause perivascular energy transfer through the vessel wall cause cyclic stresses which may trigger biochemical mediators that ultimately result in the development of inimal-medial hyperplasia. While

the levels are not high enough to cause red blood cell damage, platelets may be activated by the high Reynolds stresses.

Hemodialysis patients require a vascular access to deliver sufficient blood flow to the artificial kidney. Of these vascular accesses, 30% are prosthetic graft implants. These grafts are prone to the development of stenosis in the vein due to intimal hyperplasia, subsequently leading to thrombosis [10]. They investigate the hemodynamics in a straight and a tapered PTFE graft and compare the hydrodynamical behavior of both grafts. Two different vascular access geometry models were examined: 6-mm diameter straight graft and 4-7 mm tapered graft. The grafts were sutured to a compliant silicon model of an artery and vein in a loop configuration. Flow rate varied between 500 and 1500 mL/min. Two conditions were tested: 1) contor; mean pressure is 100 mm Hg at the arterial inlet; and 2) low resistance condition: pressure is 20 mm Hg at the venous outlet. Pulse pressure is 60 mm Hg at the arterial inlet for both conditions. Pressure and flow velocity are measured continuously, while flow rate is measured volumetrically.

Experimental study was to evaluate invasive and noninvasive indices to detect significant stenoses in a vascular access graft [6]. A compliant underarm loop graft in vitro model was built and studied with 50, 65, 80, and 90% stenosis at flow rates of 500, 1000, and 1500 mL/min. The hemodynamic measurements are performed on an in vitro model with a compliant silicon artery and vein (4% RD) and a 6 mm graft (GORE-TEX Stretch Vascular Graft, AZ, USA). The Newtonian blood analog that circulates, is a glycerine-water (40/60%) with density 1103 kg/m^3 and a dynamic viscosity 3.75 mPa.s at 25°C. Flow in the system was pulsatile. Velocity was measured with ultrasound Doppler and the pressure was measured invasively. The resistance index (RI), and pressure ratio (PR) were calculated and compared. A stenosis can be suspected when highly frequency ultrasound velocity signals develop at the venous anastomosis.

Computational fluid dynamics (CFD) whether different arterial anastomositic geometries result in a different hemodynamics at the arterial anastomosis (AA) and (VA) of hemodynamics vascular access grafts [8]. They have studied a 6 mm a graft (CD) and a 4-7 mm graft (TG). A validated three-dimentional CFD model is developed to simulate flow in the two graft types. Only the AA geometry differs. The baundary

conditions applied are a periodic velocity signal at the arterial inlet and a periodic pressure wave at the venous outlet. Flow rate is set to 1000 ml/min. The time dependent Navier-Stokes equations are solved. WSS, WSSG and pressure gradient (PG) are calculated.

The hemodynamic in the vascular access graft are influenced by the flow aspirated and injected through the two needles during hemodialysis [7]. For the first time, the impact of needle flow on vascular access performance, measured in an in vitro set up, is reported. A vascular access model, consisting of a loop polytetrafluoroethylene graft sewn to a compliant artery and vein, simulated the patient. The extracorporeal circuit was connected to the model. Three mean access flow rates and five roller pump flow rates were studied. Mean, systolic, and diastolic pressure and according pressure drops were derived at 14 loci. This study demonstrates the need for a well-functioning vascular access to perform adequate dialysis and to avoid venous system loading.

LDV was used to compare the levels of turbulence at the venous anastomosis in the presence and absence of a venous needle jet [28]. Considerably higher turbulence was observed downstream of the venous needle, in comparison to graft flow alone without the needle. Turbulent intensities were 5-6 times greater in the presence of the needle, in comparison with graft flow alone. Since hemodialysis patients are exposed to needle turbulence for four hours three times a week, the role of post-venous needle turbulence may be important in the pathogenesis of AV graft complications. A better understanding of the role of needle turbulence in the mechanisms of AV graft failure may lead to improved design of AV graft and venous needels associated with reduced turbulence, and to pharmacological interventions that attenuate IH and graft failure resulting from turbulence.

1.2 IMPORTANCE OF THE STUDY

The major complication observed in grafts is the development of IH near the anastomoses. IH leads stenoses and finally results in a trombosis. Vascular access complication, including stenosis and trombosis at the VA, are a major cause of

morbidity in hemodialysis patients. They account for over 20% of hospitalization, and consume more than 10% of the total cost of core of dialysis patients in the US or about $1.5 bilion/year [29-32]. Patients receiving hemodialysis are usually referred to the dialysis unit three times a week; the exact duration of a hemodialysis session depends on the personal need of the patient. Venous neontimal hyperplasia followed by thrombosis is the major cause of PTFE graft failure. The economic impact of AV access and its related morbidity approaches one billion dollors annually in the US [33]. At present, PTFE grafts are inverted in approximately 207,000 ESRD patients per year in the US, more than 30% of all dialysis patients. The number of dialysis patiets in the US is expected to double by 2010 [34]. Changes in the venous anastomosis geometry can greatly affected fluid dynamic variables. The surgeaon has some degree of control over this geometry during graft construction. A further understanding of the relationship between AV graft failure and fluid dynamic variables may lead to a prediction of graft performance. This may lead to geometric design, which extend the functional period before AV graft failure occurs.

The goal of the present study is to determine the turbulence and WSS levels of the in vitro AV graft. We find that this model was implanted considered with very poor geometrical approach. Further studies should be done on AV grafts with the different geometric design to find the optimum fluid dynamic condition.

CHAPTER 2

EXPERIMENTAL SETUP

2.1 FLOW SYSTEM

An experimental flow system was designed and built to provide the scaled-up model with the desired inlet and outlet conditions. A schematic of this system is shown in Figure 2.1a, a picture of this system is shown in Figure 2.1b and picture of model geometry is shown in Figure 2.1c. A glycerin-water mixture of 60% and 40% water by weight was selected to match the index of refraction of the Pyrex glass model. The Pyrex glass model was installed in a small rectangular plexiglass box with an open top. The space between the model and the box was filled with the same mixture to minimize laser beam refraction. The fluid must be affordable, compatible with the other components of the system, stable in use [35]. This fluid has a refractive index of 1.41, a density of 1.11 g/ml, and a dynamic viscosity of 10.8 centipoise at 20ºC [36].

A 1/5HP centrifugal pump [Type U83B1, FASCO] supplied the pressure head to drive the flow. A PC computer (hp1702) was used to record the flowrate. The flow was monitored by two Electromagnetic Flow Meter (EMF) (Type MAG 5100W) manufactured by SIEMENS Inc. The EMF meters measured the total flow entering the graft model and the flow rate entering from the DVS. The EMF meter was calibrated by the bucket and stopwatch method.

An upstream tank was used to stabilize the flow. After the upstream tank, the fluid enters a 1 meter Plexiglas tube with an inner diameter of 25.4 mm (1 inche). The flow exits the model through the PVS into a downstream tank.

The procedure setup is important to ensure accuracy and repeatability of measurements. An experimental system was designed and constructed to provide upscaled model with the proper inlet and outlet flow conditions. The alignment procedure is the following:

1. Control the valves,
2. Operate the pump,
3. The heater/cooler was adjusted to control the temperature at 24 ºC. Temperature was important because changing the fluid temperature 1 ºC changed the fluid viscosity approximately three percent,
4. Control the flowmeter to measure the total flow entering the graft model and the flow rate entering from the DVS.
5. Traverse controller is operated.
6. Signal p rocessor is operated.
7. LDA measurement must be made to match the refraction indices of all the materials exposed to the laser beam. The laser probe was focused at the beam entering point on one side of the box and then at the existing point on the opposite side. The distance between these two points was measured. The laser beam coming from laser probe was focused at the measurement point lacated at the midplane of the model.
8. The laser beams are very important to obtain correct finge spacing inside the ellipsoidal beam-crossing section to find the particle velocities. Laser beams are checked if the surfaces of two beams are perpendicular to each other

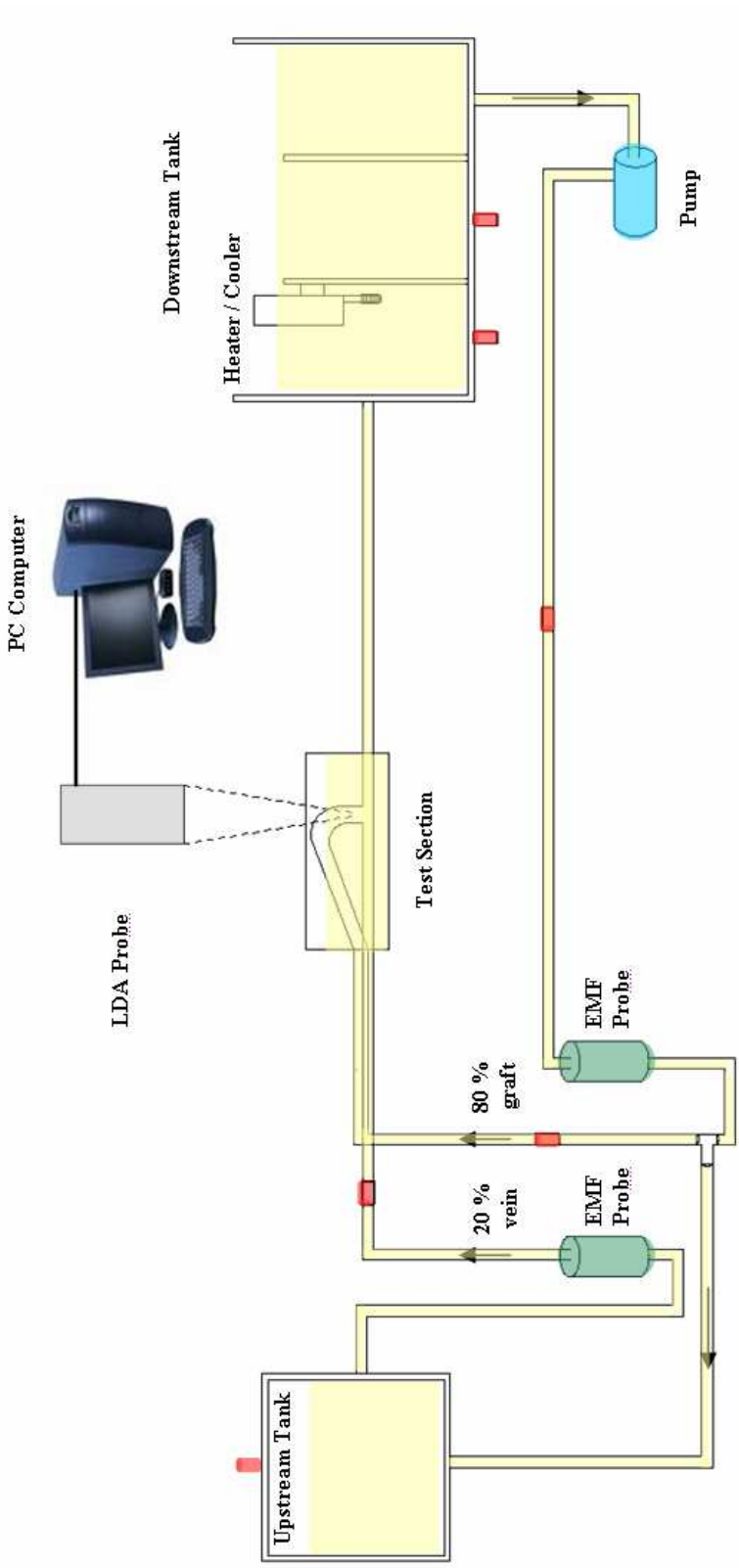

Figure 2.1a Schematic of experimental flow system

Figure 2.1b Picture of experimental flow system

Figure 2.1c Picture of model geometry

Temperature differences between air in the room and the fluid caused local changes in the fluid temperature inside the entrance tube. While the fluid is heated (or cooled) at the outer radius of the tube, the viscosity and density variations created locally were large enough to cause the steady flow profile to become skewed The second chamber in the downstream tank had a heater (LAUDA, Type T/P Nr: VD3029) to control the fluid temperature. The heater was adjusted to control the temperature 24±0.5ºC. The accuracy of the fluid temperature was important because changing the fluid temperature 1ºC changed the fluid viscosity approximately three percent. A mercury thermometer was also used to monitor the room ambient temperature to insure that it was also maintained at 24±0.5ºC.

2.2 FLOW CONDITION (*IN VIVO* MEASUREMENT)

The measurements were conducted at the Cerrahpaşa Hospital and İstanbul Training and Research Hospital. Measurements were made using a color Doppler ultrasound device and BT angiography. The basic geometry of the venous anastomosis was measured in the plane of the bifurcation as shown in the three Duplex ultrasounda images Figures 2.3a and 2.3b. The results of the ultrasound study are summarized in Table 2.1.

Measuring ultrasound, Doppler and BT angiography to obtain geometry and flow conditions from three different patients who are grafted with AV:

For this purpose, at first, graft diameter, daimeters of graft arterial and venous junction regions, graft wall and the existence of stenosis in lumen and native arterial venous vascular sections are investigated by gray scale US. At the same time, flow in the graft, the characteristics of the flow at the ends of graft arterial and venous, the existence of turbulence inside the graft or anastomosis regions are searched by using color Doppler US. Flow speed, Pulsatility index (PI), Resistivity index (RI) values inside the graft and arterial venous anastomosis regions are calculated separately numerically and spectrally.

Table 2.1 Parameter of Color Doppler ultrasound measurements taken on a dialysis patient's AV Graft

Parameter	PTFE Graft Value
Diameter (mm)	5.2
Mean Velocity (m/s)	1
Peak Velocity (m/s)	1.5
Mean Flowrate (ml/sec)	21
Peak Flowrate (m/sec)	32
Mean Reynolds Number	1560
Peak Reynolds Number	2340

Flowrate values computed from $Q = V_{ave}A$

Reynolds number: $Re = \rho VD/\mu$

Properties of blood used in calculation: μ=0.35 g/sec/cm, ρ=1.05

The cases which are not suitable for our study are excluded according to US and Doppler results. In one of them there is intense calcification on the graft walls. In the other one, there is hemodynamic stenosis at the venous anastomosis end of the graft.

The three cases we think to be suitable for our study are processed for BT angiography by arranging hemodialysis day. BT is obtained using contrast matter from intravenous path. The obtained and raw pictures are evaluated and their convenience is verified. 3D BT angiography of these three cases is obtained by using post processing and volume rendering technique (VRT). The parameters like graft location, graft diameter, lumen diameters of arterial venous regions, lumen inner structure – wall, the existence of stenosis are compared with US.

As a result, US color Doppler and BT angiography data of the three cases which are suitable for our study are written on a CD. No complication developed in patients after these processes.

Figure 2.2 The image of AV graft to vein connection taken from dialysis patient

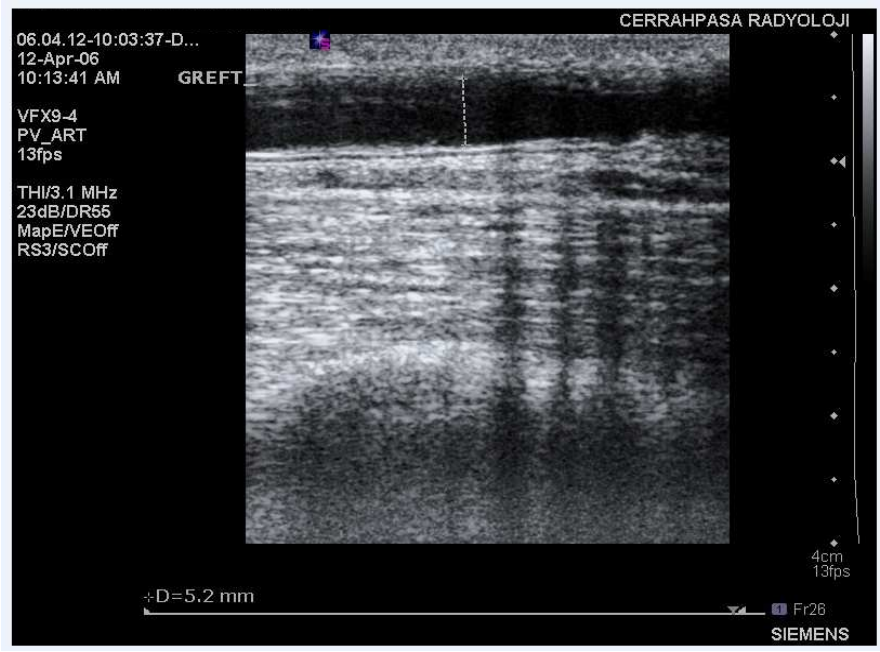

Figure 2.3a The image of AV graft to vein connection taken from the dialysis patients using color Doppler Ultrasonograpy

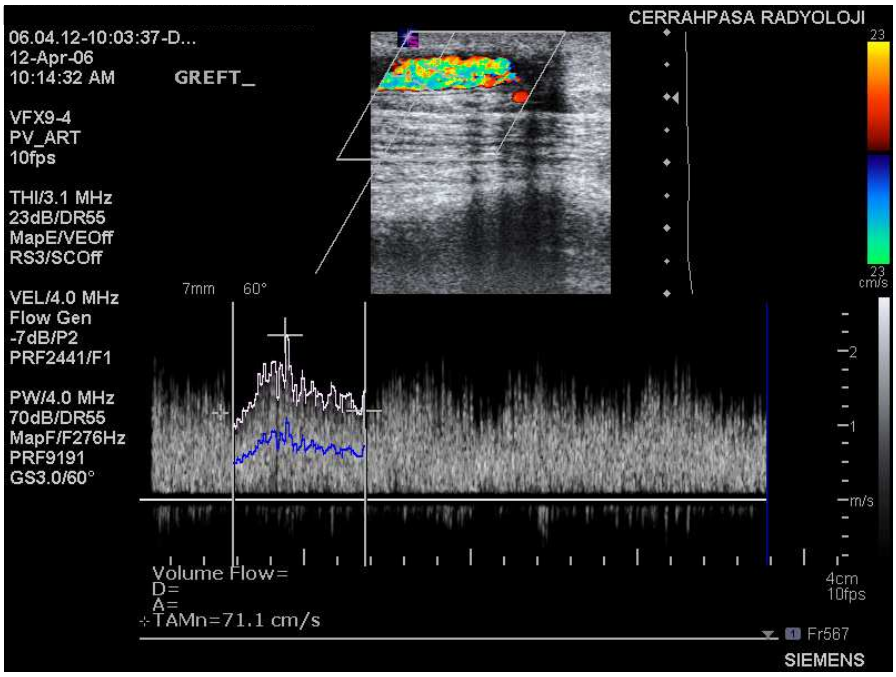

Figure 2.3b The image of AV graft to vein connection taken from the dialysis patients using color Doppler Ultrasonograpy

2.3 LASER DOPPLER ANEMOMETRY (LDA)

Laser Doppler anemometry was used to take velocity measurement inside model. 1-D LDA Flow is a DANTEC Electronics flow explorer type 62N01, FlowExplorer Standard System, comprising 65X11, 62N60 and62S10 BSA Flow Software. Laser output was provided by operating in a wavelength 514.5 nm. The laser beam diameter is 2.5 mm. A one-color laser arrangement is used to measure one components of velocity. In order to measure the velocity direction, color is divided into two beams of equal intensity, and one beam is passed through a Bragg cell in order to shift its frequency by 80 MHz. The Dopller shifted frequency is converted to particle velocity using a software called BSA Flow Software.

The particles used in the flow system are poyyamid seeding particles (PSP) (5µ-10 µ) from the Dantec Dynamic A/S (Code 9080A3011). The number of particles put into tha water-glycerin mixture was determined by the ratio of the total volume of liquid in the system to the probe fringe volume. Ideally, only one particle should be in the probe volume at a given time.

The raw data collected with LDA system is used to calculate the mean velocities, fluctuating velocities (u_{rms}) and Wall shear stress (τ) by using the data processing BSA Flow Software . The scaling between in vivo and in vitro measurements under steady conditions was done by using dynamic similarity ($Re_{vitro}=Re_{vivo}$). The density, kinematix viscosity, and the diameter under in vivo conditions were 1.05 g/cm^3, 3.5 cP, and 5.2 mm, respectively. Under in vitro conditions, the density, kinematic viscosity, and the diameter were 1.06 g/cm^3, 10 cP, and 25.4 mm, respectively.

The basic configuration (Figure 2.4) of an LDA consists of a continuous wave laser, transmitting optics, including a beam splitter and a focusing lens Receiving optics, comprising a focusing lens, an interference filtre and a photodetector, signal conditioner and a signal processor.

The output of the Bragg cell is two beams of equal intensity with frequencies f_0 and f_{shift}. These are focused into optical fibres bringing them to a probe. In the probe, the parallel exit beams from the fibres are focused by a lens to intersect in the probe

volume. The photo-detector converts the fluctuating light intensity to an electrical signal. The Doppler bursts are filtered and amplified in the signal processor

The frequency shift obtained by the Bragg cell makes the fringe pattern move at a constant velocity. Particles which are not moving will generate a signal of the shift frequency f_{shift}. The velocities will generate signal frequencies respectively.

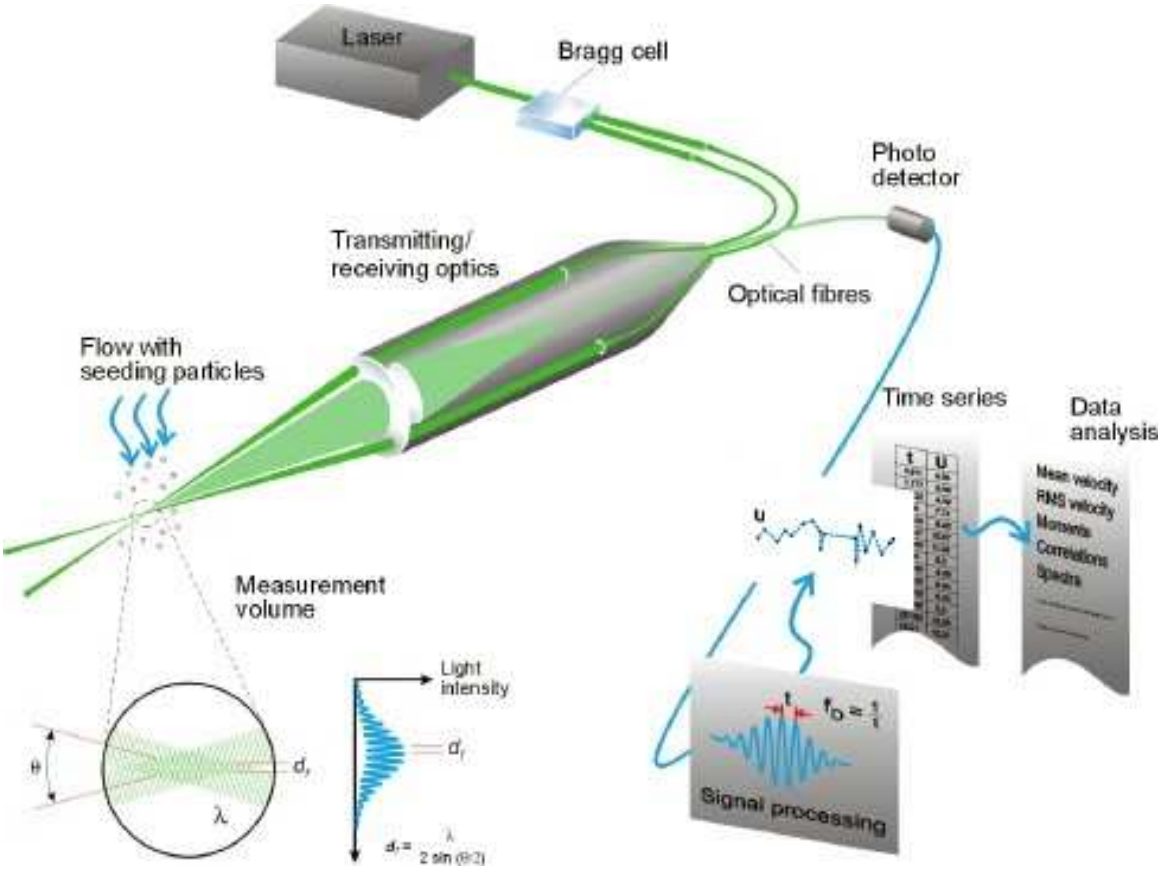

Figure 2.4 LDA Principle [37]

2.4 SELECTION OF PARAMETER

The setting of parameters in the BSA Flow Software program is very important to obtain reliable measurements with laser system. There are three parameters affecting the data rate. They are validation level, Photomultiplier (PM) tube voltage and gain. Validation level is the ratio of signal to noise. It changes from 97-100% in the Dantec system used for these experiments. The PM tube voltage controls the volume of the ellipsoid through which particles pass. The PM tube voltages vary from 1000V to 2000V. Gain setting is related to the size of particles inside the flow. It is set low to get the signal from big particles and set high to get the signal from particles. Since the data rate changes with these parameters we performed two sets of experiments. The first set of the experiments was done near the wall and the second one was in the center of the model. In a bounded flow like the flow is in pipes or channels, the low inertia flow is always near the wall and high inertia flow is in the center. This means that the data rate (the number of the particles passing through a specific location per unit time is low near the wall and high in the center of flow. The PM tube voltage was varied from 1000V to 2000V. And the gain was set to high and low at a specific bandwidth to find the optimum values. These parameters can change for different studies. It is recommended to do this type of study before using the laser Doppler system. For this research; the voltage values were selected between 1000V and 1200V.

2.5 FLOW INLET CONDITION

The inlet conditions were measured before taking data inside the graft geometry to be able to repeat the experiment. Velocity profiles for steady flow were measured upstream of the graft. The measured values for steady flow were then compared to theoretical solutions to gain insight into the accuracy achievable in the system. The velocity profiles at Re=1400 and 2400 for steady flow were measured upstream of the anastomosis parallel to the plane of bifurcation.

2.6 STEADY FLOW

The program BSA Flow Software was used to record the intantenous velocity for steady flow. Two thousand (2000) validated samples were recorded inside flow field and then the mean velocity was found by taking the average of the samples for v component of the velocity. Since the data rate was lower near the wall of the model and data was taken for two minutes. The fluctuation velocity was found by substracting the mean velocity from the intantenous velocity at each time step and then averaged over the specified number of validated samples to find the variables at each measurement location. The notations for mean velocities, fluctuation velocity and Wall shear stress are defined in the following equations.

u_i = instant velocity component of i^{th} particle along x direction

$\bar{u}$ = mean velocity

i = 1, 2, 3,…….N

N = Number of spherical particles passing through the measurement volume.

The equations used for mean velocities, fluctuation velocities and Reynolds stresses are as follows:

Mean value

$$\bar{u} = \frac{\sum_{i=1}^{N} u_i}{N} \tag{2.1}$$

Variance

$$\bar{u}^2 = \frac{\sum_{i=1}^{N} \left(u_i - \bar{u}\right)^2}{N} \tag{2.2}$$

Fluctuation Velocity (u_{rms})

$$u_{rms} = \sqrt{\overline{u}^2} \tag{2.3}$$

Wall Shear stress

μ is the dynamic viscosity

u is the flow velocity parallel to the wall

y is the distance to the wall

$$\tau_w = \mu\left(\frac{\partial u}{\partial y}\right)_{y=0} \tag{2.4}$$

CHAPTER 3

EXPERIMENTAL RESULTS (VELOCITY FIELD)

We present the flow measurements inside an upscaled end-to-side model of a human AV graft to vein using LDA under steady flow conditions. The ratio of the graft inlet flow-rate to the DVS inlet flow-rate was chosen to be Graft:DVS=80:20. Because the flow rate is less than 20% of the total flow rate in the venous anastomosis. Reynolds numbers at mean and maximum are estimated as 1400 and 2400. These Reynolds numbers correspond to flow rates of 1.0 and 1.5 liters/min at mean and maximum for a graft diameter of 5.2 mm, respectively. Velocity and Wall shear stress values are scaled to in vivo values by dynamic similarity,

$$\mathrm{Re}_{vivo}=\mathrm{Re}_{vitro},\ \left(\frac{\rho_{vitro}\mathrm{V}_{vitro}}{\mu_{vitro}}=\frac{\rho_{vivo}\mathrm{V}_{vivo}}{\mu_{vivo}}\right). \tag{3.1}$$

3.1 MEASUREMENTS AT THE MIDPLANE (Re = 1400, Graft:DVS=80:20)

The velocity measurements were performed at the inlet and entrance of the graft, DVS and PVS and inside the graft, DVS and PVS at various positions as shown in Figure 3.2. Turbulence levels and Wall shear stresses were calculated as explained in Cahapter 2.6. The velocity components u, v and w are in the x, y and z directions, respectively. In plane of bifurcation, u is parallel to the floor of the graft and v is perpendicular to the floor, while w is perpendicular to the plane of bifurcation. At each Reynolds number, the one-component LDA measured only u velocity components. This section describes the primary flow field, turbulence levels and WSS at the midplane. It also describes aspects of secondary flow motions.

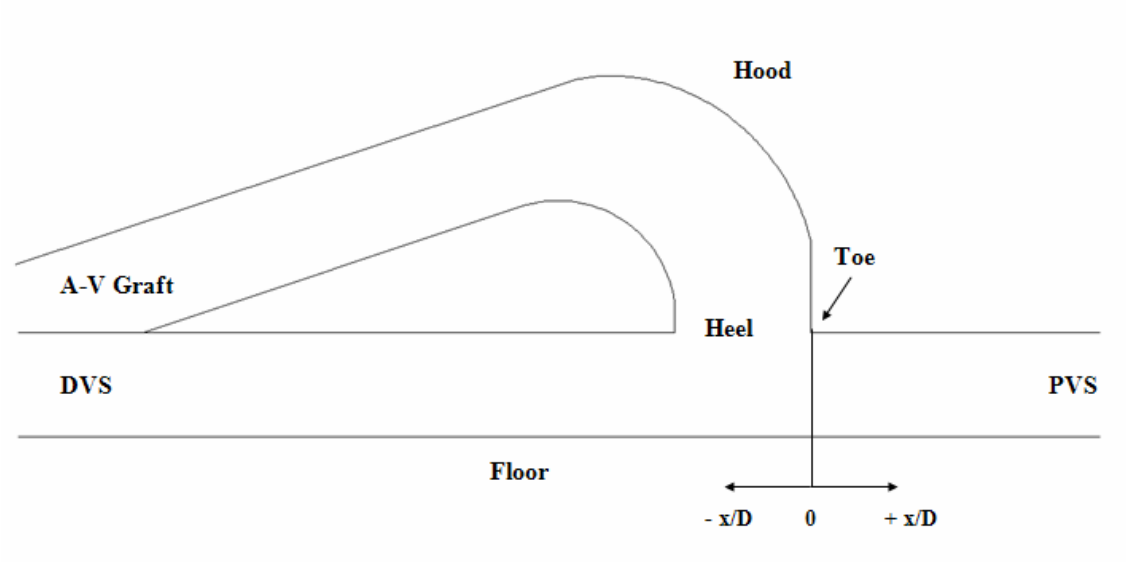

Figure 3.1 Geometry of the venous anastomosis of an A-V graft model.

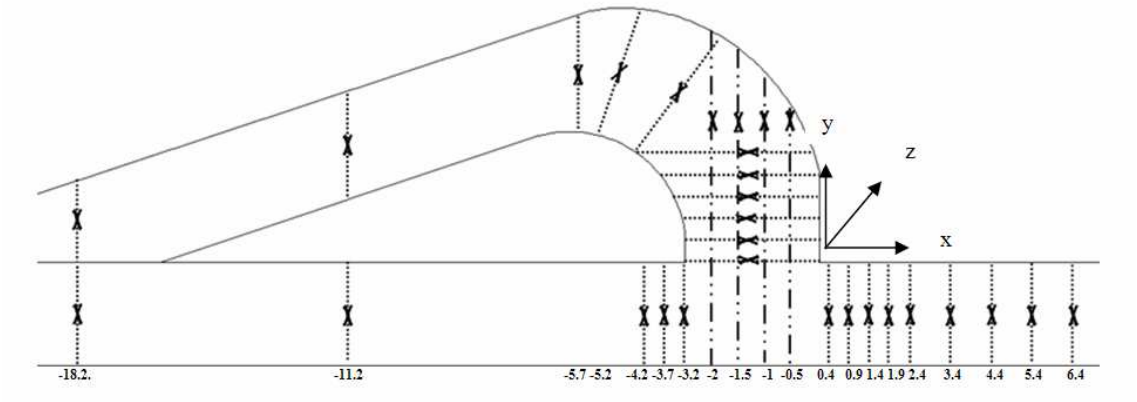

Figure 3.2 Measurement locations under steady flow conditions

At Re=1400, flow enters the model with a fully developed profile from the graft and DVS. The flow entering from the graft meets with the flow entering from DVS in the anastomosis. The profiles at position -18.2, -11.2 and -5.2 have parabolic shapes in the graft (Figure 3.3, 3.4 and 3.5). The graft and DVS entrance velocity profiles along the lines that are parallel to the floor at position -18.2 and -11.2 are shown in Figure 3.2. The maximum fluctuation velocity was u_{rms}=13cm/s which is 4% of mean velocity u_m indicating low turbulence level at the graft inlet. At position -4.2, the velocity profile slightly skewed towards the hood side of the graft (Figures 3.6 and 3.7). The hood side of the graft has more favorable pressure gradient than the heel side, which causes the flow to move toward the hood side. At position 2.5 before entering the anastomosis (in the direction of x), the velocity profile is M shaped which is general characteristic secondary flow in the curved pipes (Figures 3.8, 3.9, 3.10, 3.11, 3.12, and 3.13). The turbulence level at position 0 (in the direction of x) was measured as u_{rms}=20 cm/s which is 1.5% of u_m.

The velocity profile at the inlet of the DVS is parabolic as shown in Figure 3.14, 3.15. At position -4.2 the velocity profile slightly skewed towards the heel side (Figures 3.16, 3.17, 3.18).This can be because of the temperature change between the room and water glycerin mixture inside the model. The maximum fluctuation velocity at the inlet was u_{rms} 4 cm/s.

The velocity profile at the entrance of the PVS is blunt near to the toe side with high velocity gradient near the wall and increased velocity component. A separation region downstream of the toe by a retrograde vector near the wall at position +0.4 (Figures 3.19, 3.20, 3.21, and 3.22). The length of the separation region is estimated to be one diameter. Peak velocity is around 89 cm/s at position of +0.4 and changed to 83 cm/s at position +2.4. Turbulence level, u_{rms}, in the PVS at position +0.4 shown in Figure 3.19 was 33 cm/s which is the 26% of mean velocity. Then the turbulence level, u_{rms}, decreased to the value of ~~18~~ cm/s at position +6.4 through PVS, Figure 3.27. Figures illustrating the mean velocities and fluctuations velocities are shown by Figures 3.23, 3.24, 3.25, 3.26, 3.28, 3.29, 3.30, and 3.31.

At Re=2400, The flow field is similar to the one with Re=1400 in structure but not in magnitude. The velocity profile at the inlet of the graft is still parabolic (Figures

3.3, 3.4 and 3.5). The inlet profile in the DVS is blunt (Figures 3.14 and 3.15). At position -18.2 and -5.2 have blunt shape that is the characteristic of transition/turbulent flow. The graft and DVS entrance velocity profiles along the lines that are again parallel to the floor at position -18.2 and -11.2 are shown in Figure 3.2. The flow entering from graft at position -18.2. The maximum fluctuation velocity was u_{rms}=8 cm/s. which is 10% of mean velocity u_m indicating low turbulence level at the graft inlet. At position -2.5, the velocity profile slightly skewed towards the hood side of the graft (Figures 3.8 and 3.9). At position 2.5 before entering the anastomosis (in the direction of x), the fluctuation velocity profile is again M shaped (Figures 3.8, 3.9, 3.10, 3.11, 3.12 and 3.13). Mean velocity profile is shifted towards the floor side compared to measurements made at 1400 Reynolds number. The turbulence level at position 0 (in the direction of x) was measured as u_{rms}=18 cm/s which is 22% of local mean velocity u_m.

At position -4.2 the velocity profile slightly skewed towards the heel side (Figures 3.16, 3.17 and 3.18). This can be because of the temperature change between the room and water glycerin mixture inside the model. The maximum fluctuation velocity at the inlet was u_{rms} 20 cm/s.

The velocity profiles in the entrance to the PVS are still blunt near the floor side with high velocity gradient near the wall. Seperation is still present on the toe side of the PVS (Figures 3.19, 3.20, 3.21, 3.22 and 3.23). The length of the separation region is still estimated to be one diameter. The magnitude of backflow decreases with increasing Reynold number. The velocity decrease slightly near the center from u_m Figures illustrating the mean velocities and fluctuations velocities are shown by Figures 3.24, 3.25, 3.26, 3.27, 3.28, 3.29, 3.30 and 3.31.

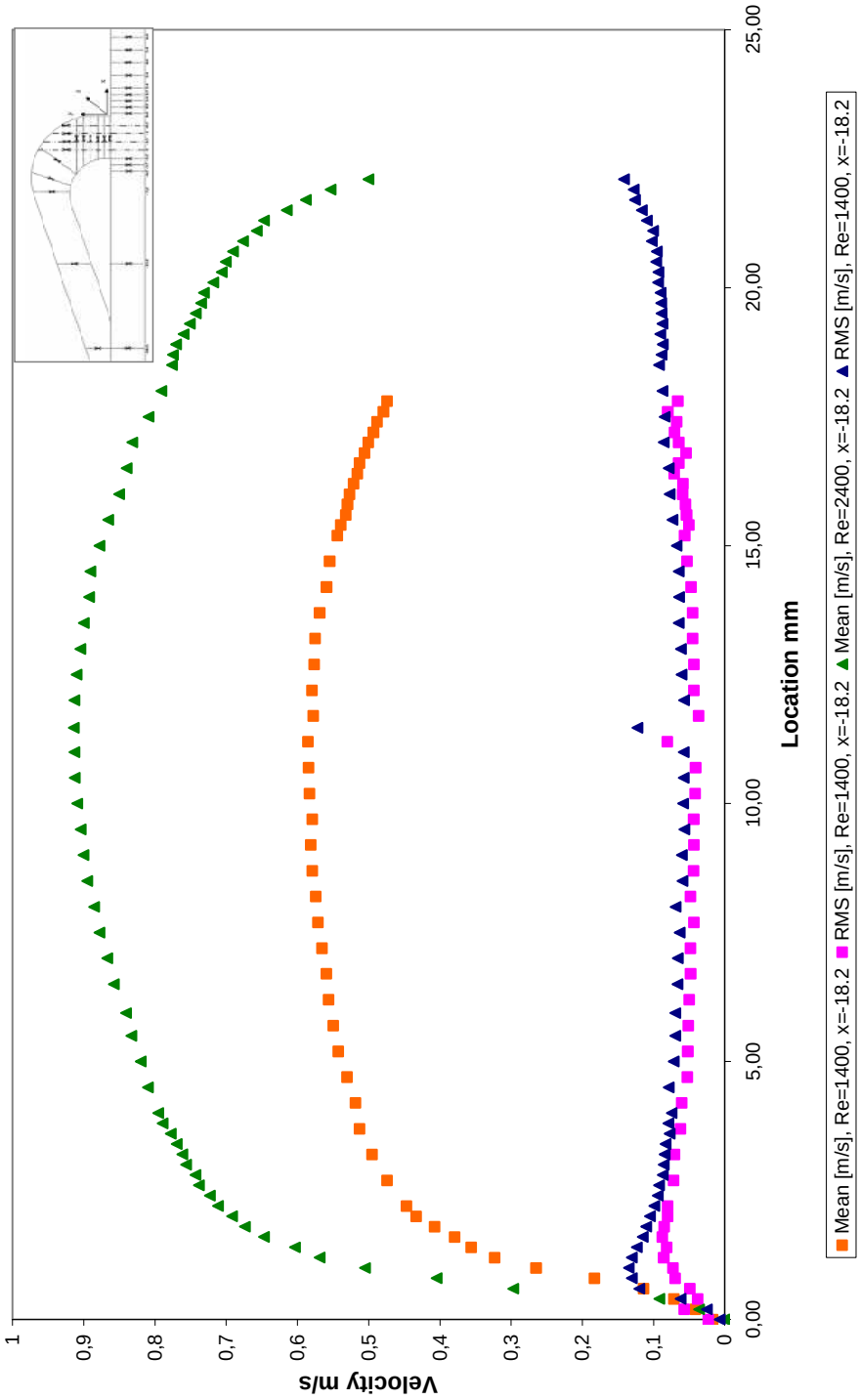

Figure 3.3 Velocity profile measured at the inlet of the Garft Re=1400, 2400, x=-18.2

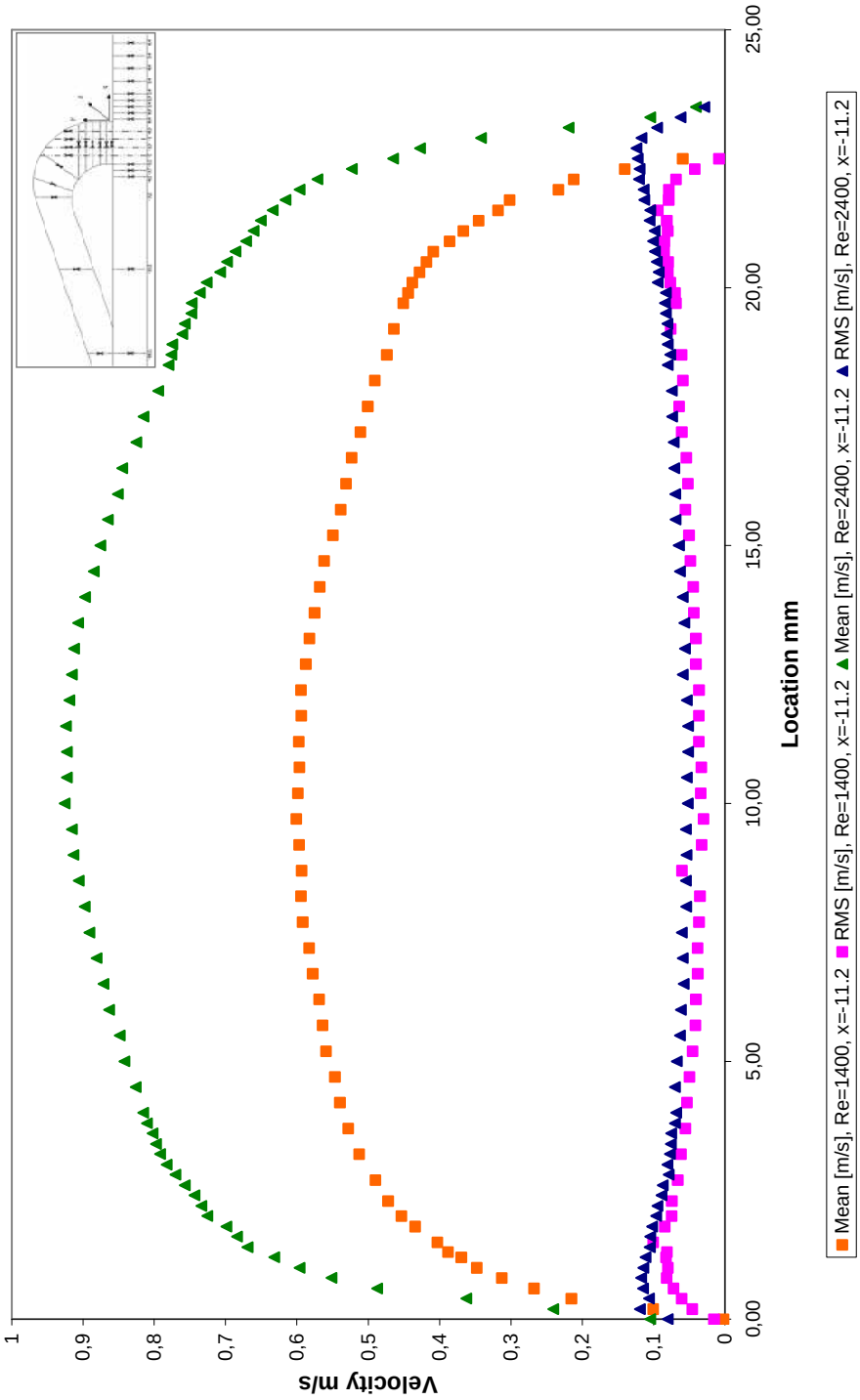

Figure 3.4 Velocity profile measured at the inlet of the Garft Re=1400, 2400, x=-11.2

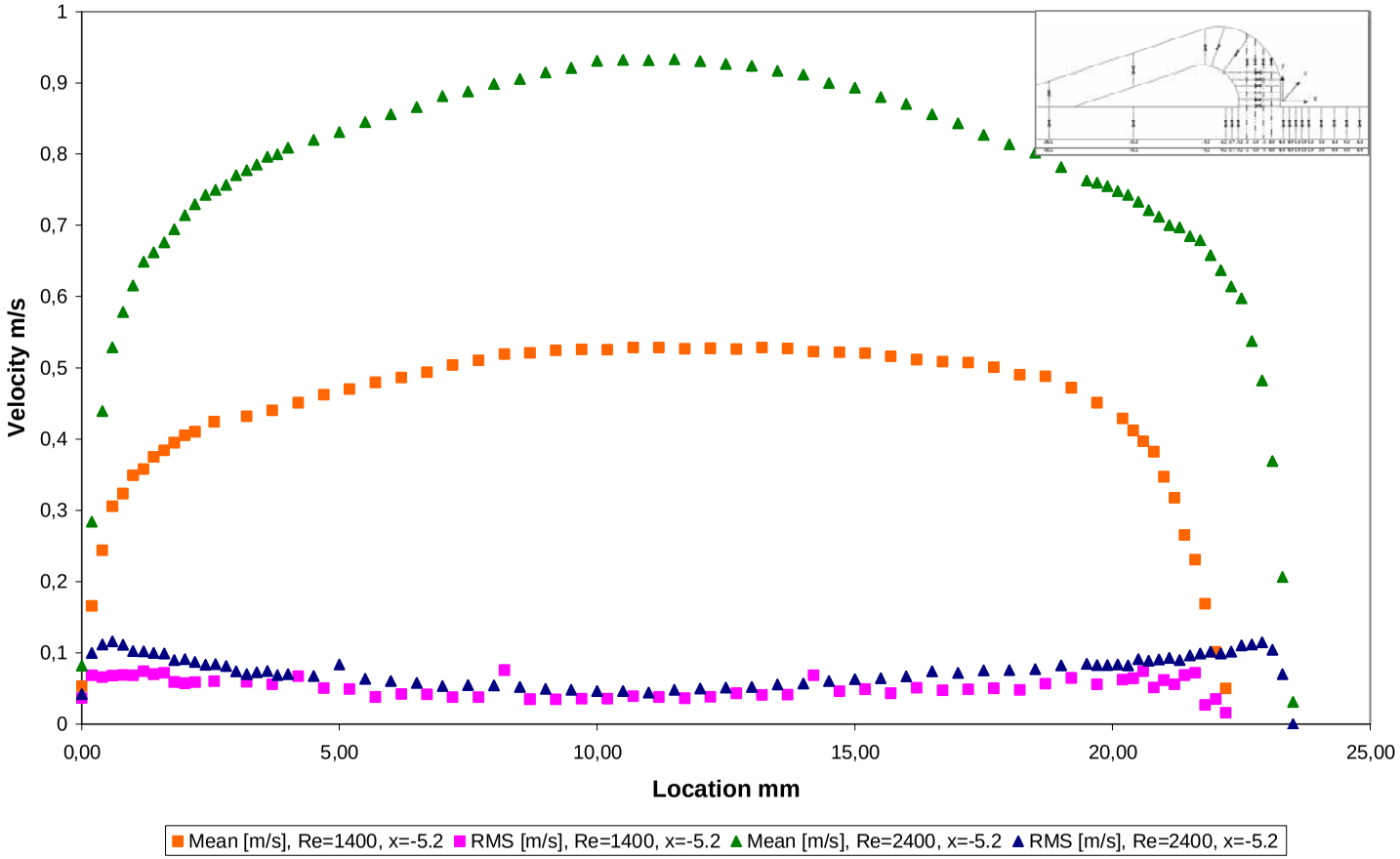

Figure 3.5 Velocity profile measured at the inlet of the Garft Re=1400, 2400, x=-5.2

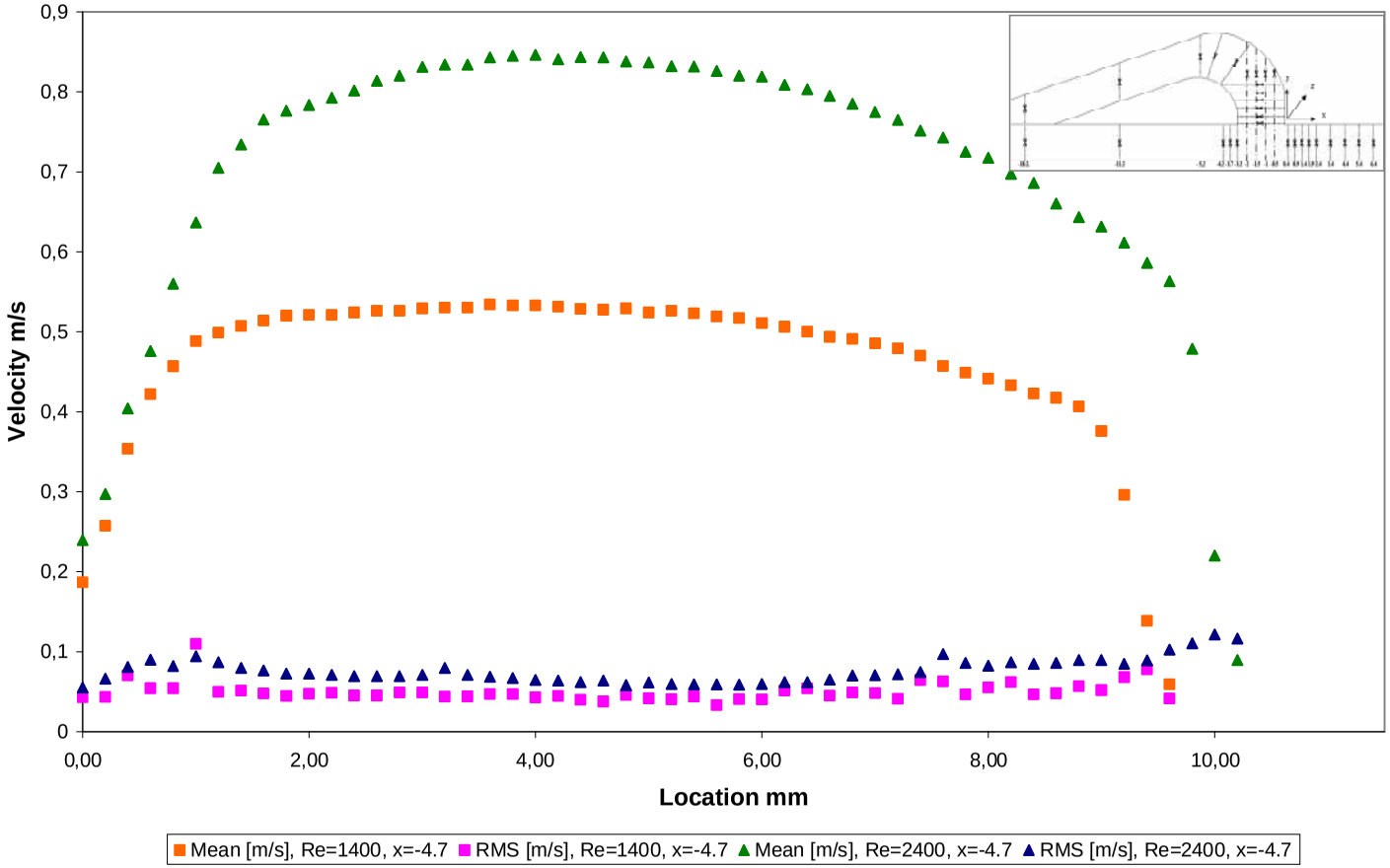

Figure 3.6 Velocity profile measured at the inlet of the Garft Re=1400, 2400, x=-4.7

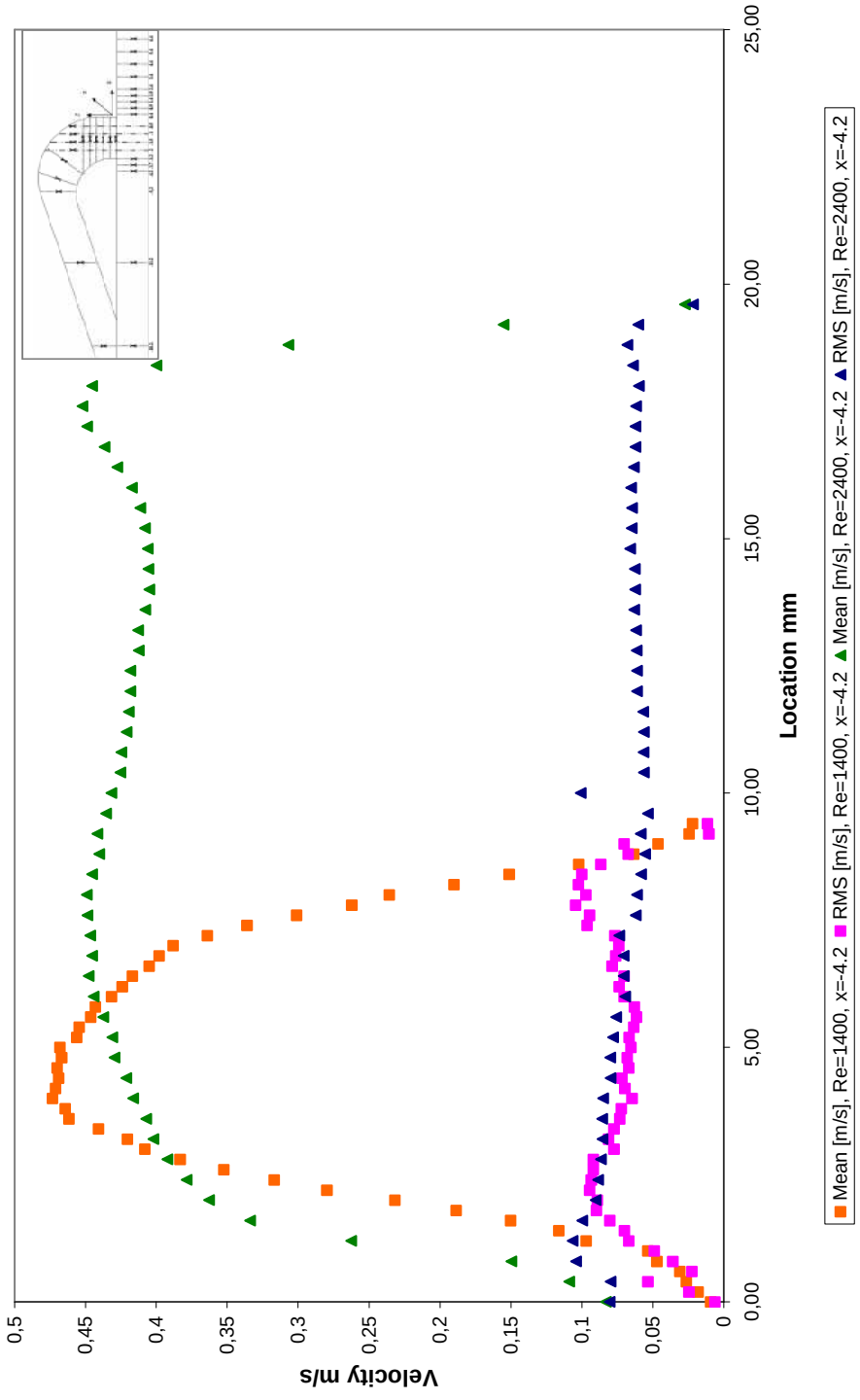

Figure 3.7 Velocity profile measured at the inlet of the Garft Re=1400, 2400, x=-4.2

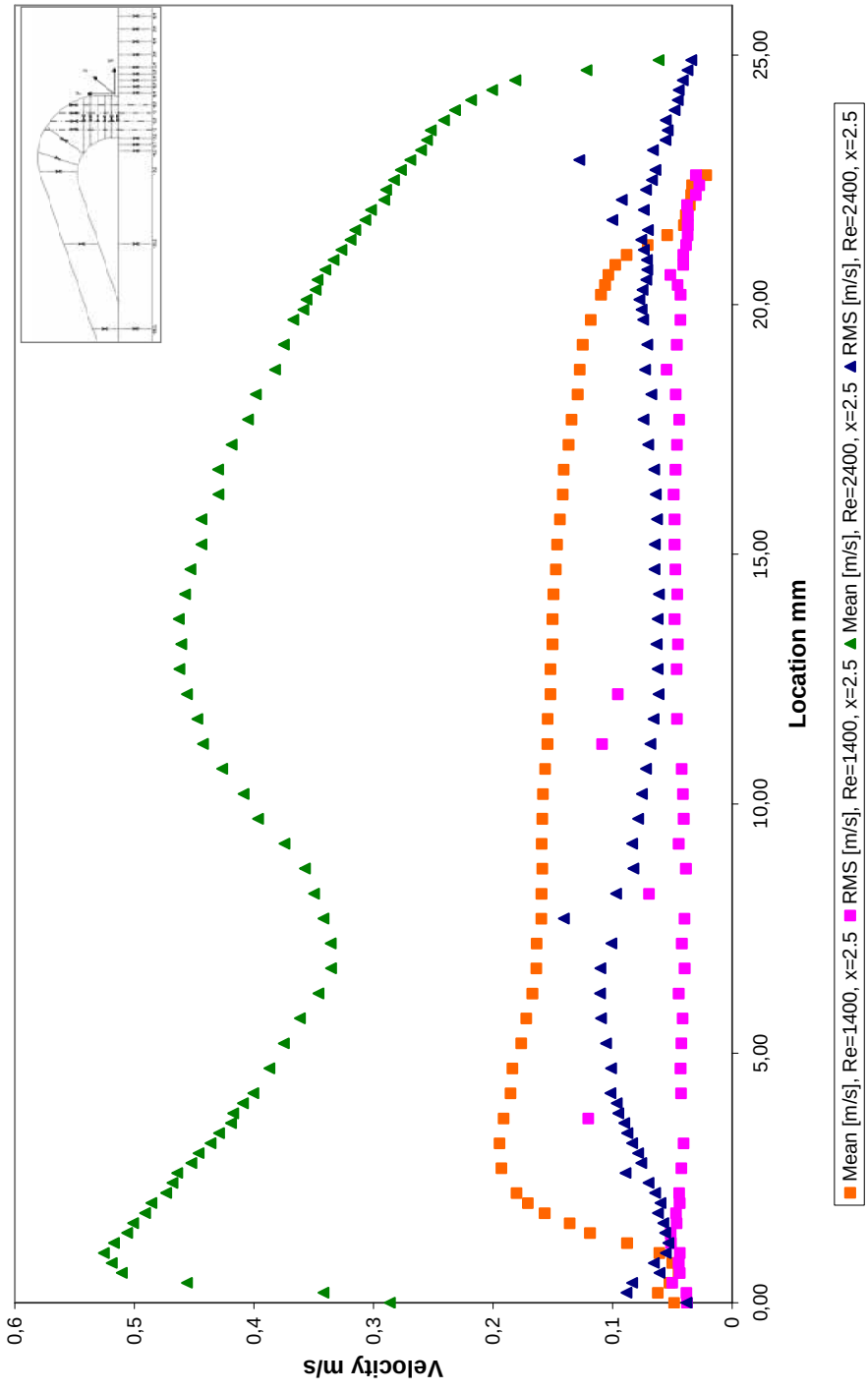

Figure 3.8 Velocity profile measured at the inlet of the Garft Re=1400, 2400, x=2.5

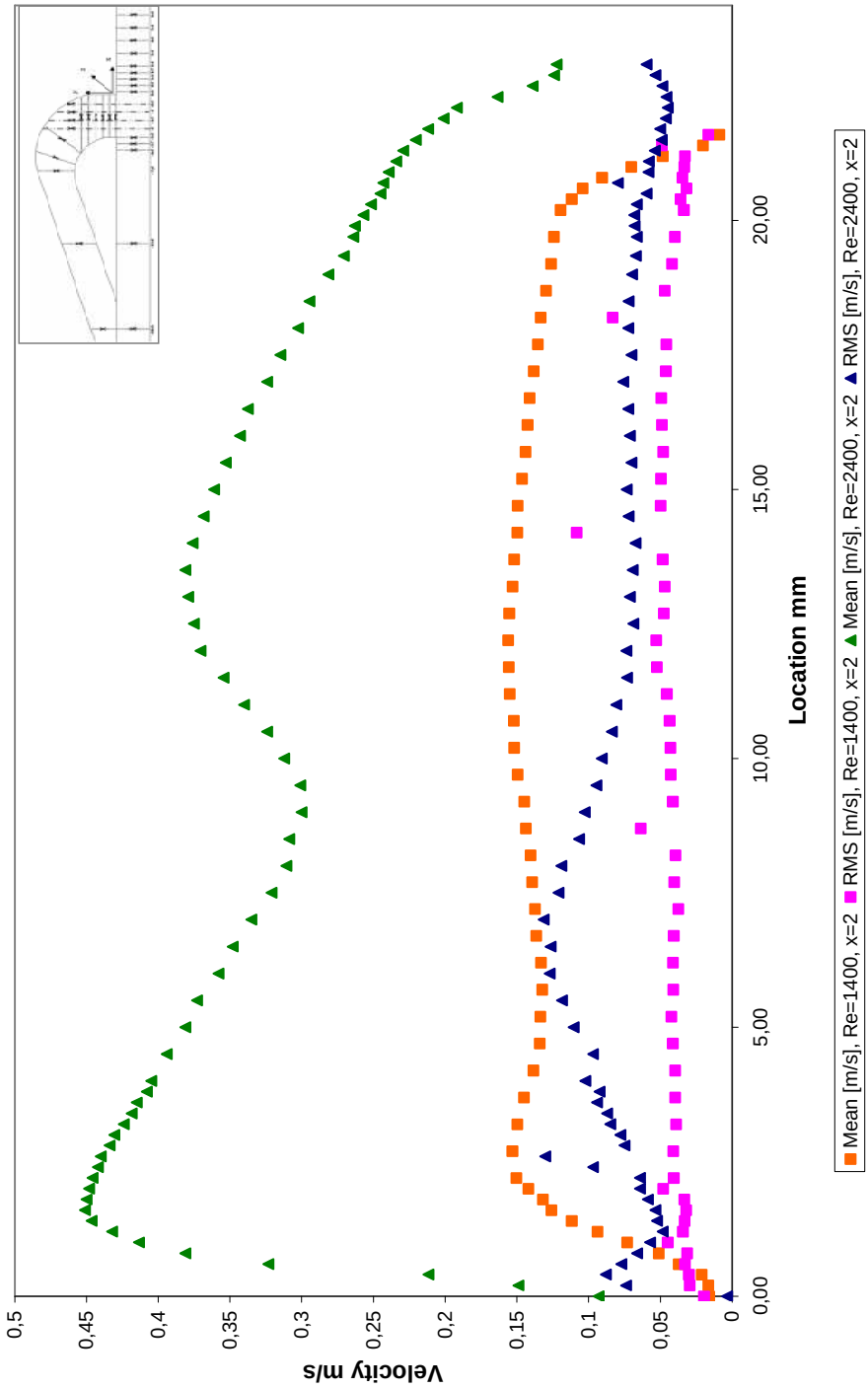

Figure 3.9 Velocity profile measured at the inlet of the Garft Re=1400, 2400, x=2

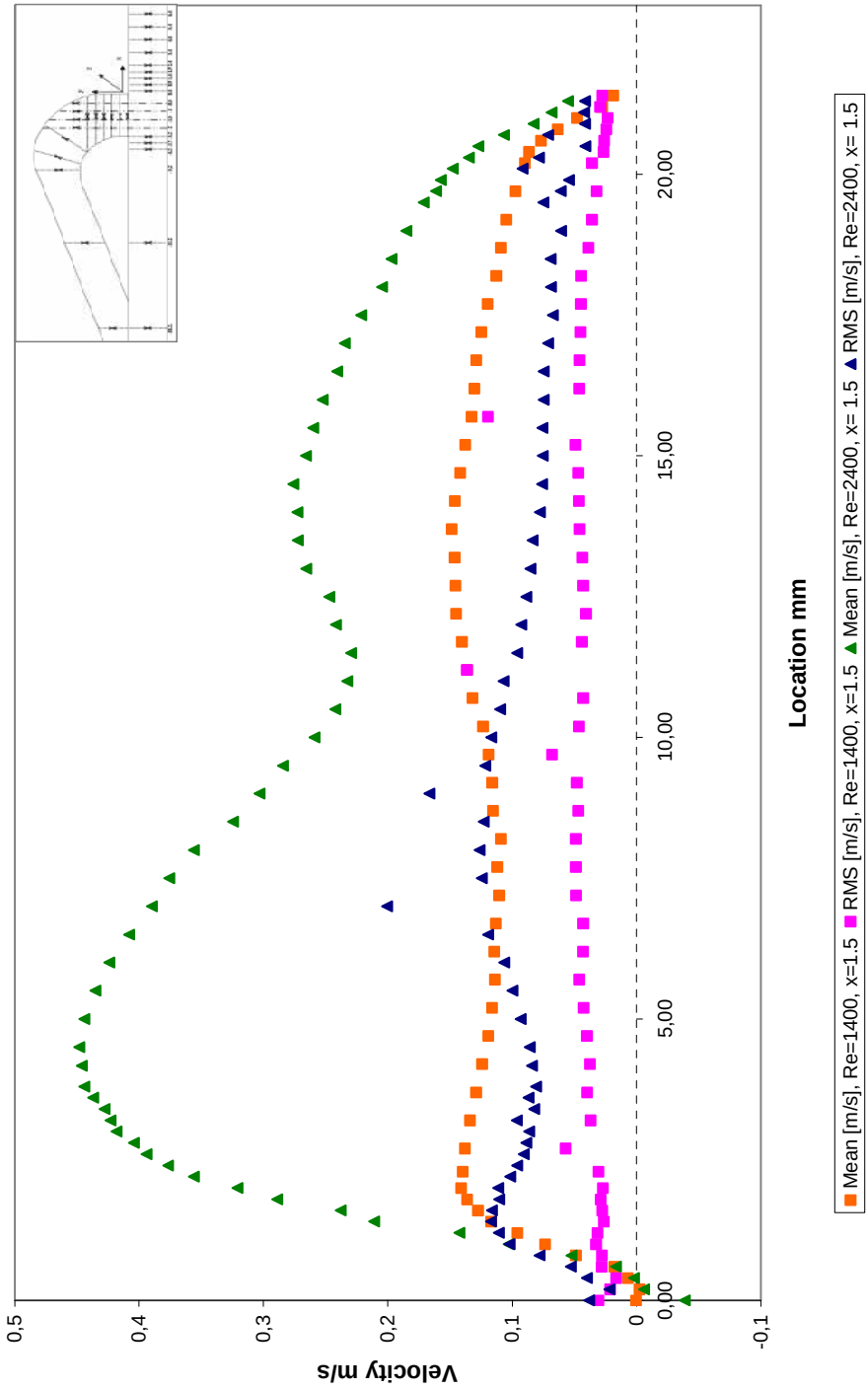

Figure 3.10 Velocity profile measured at the inlet of the Garft Re=1400, 2400, x=1.5

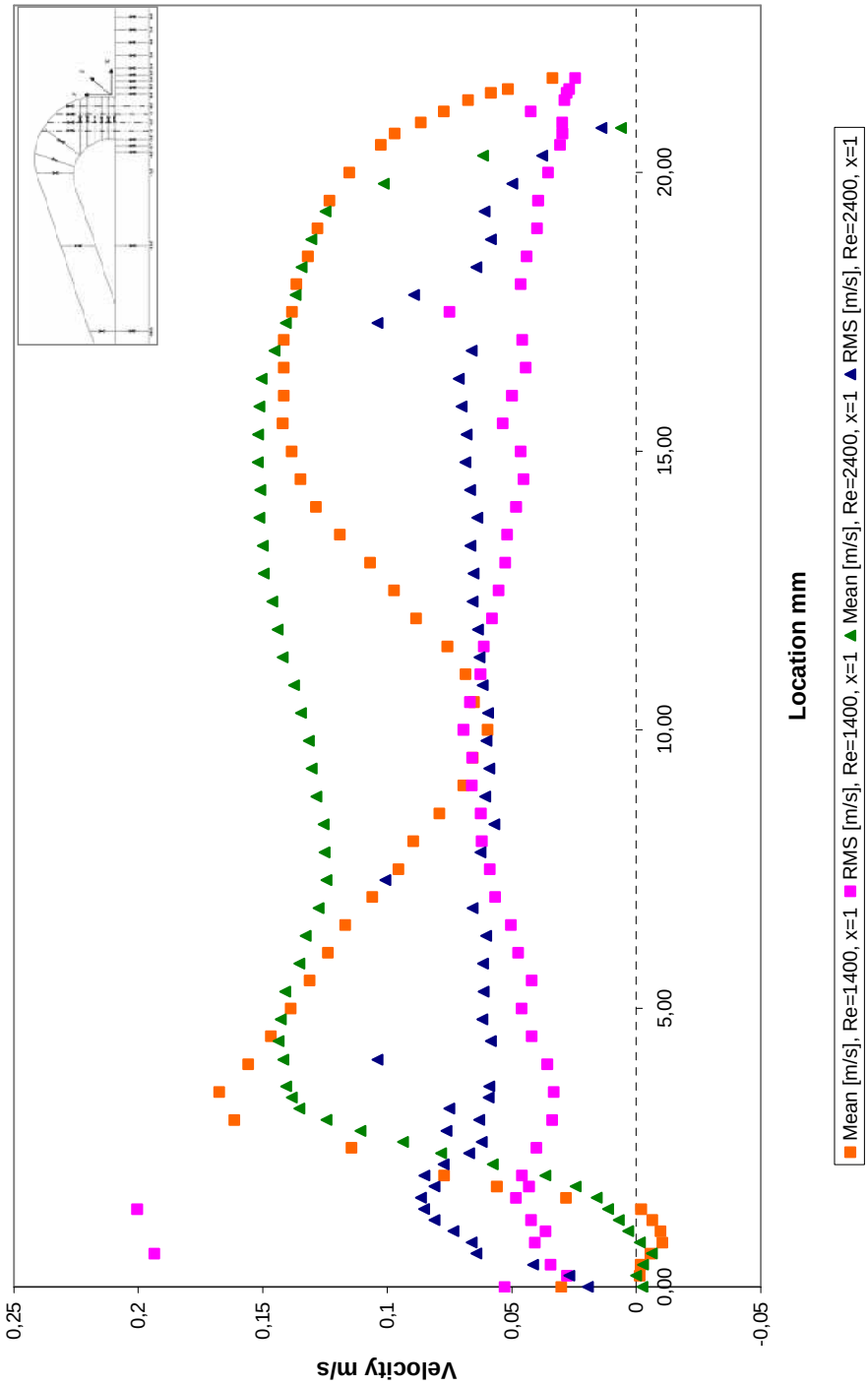

Figure 3.11 Velocity profile measured at the inlet of the Garft Re=1400, 2400, x=1

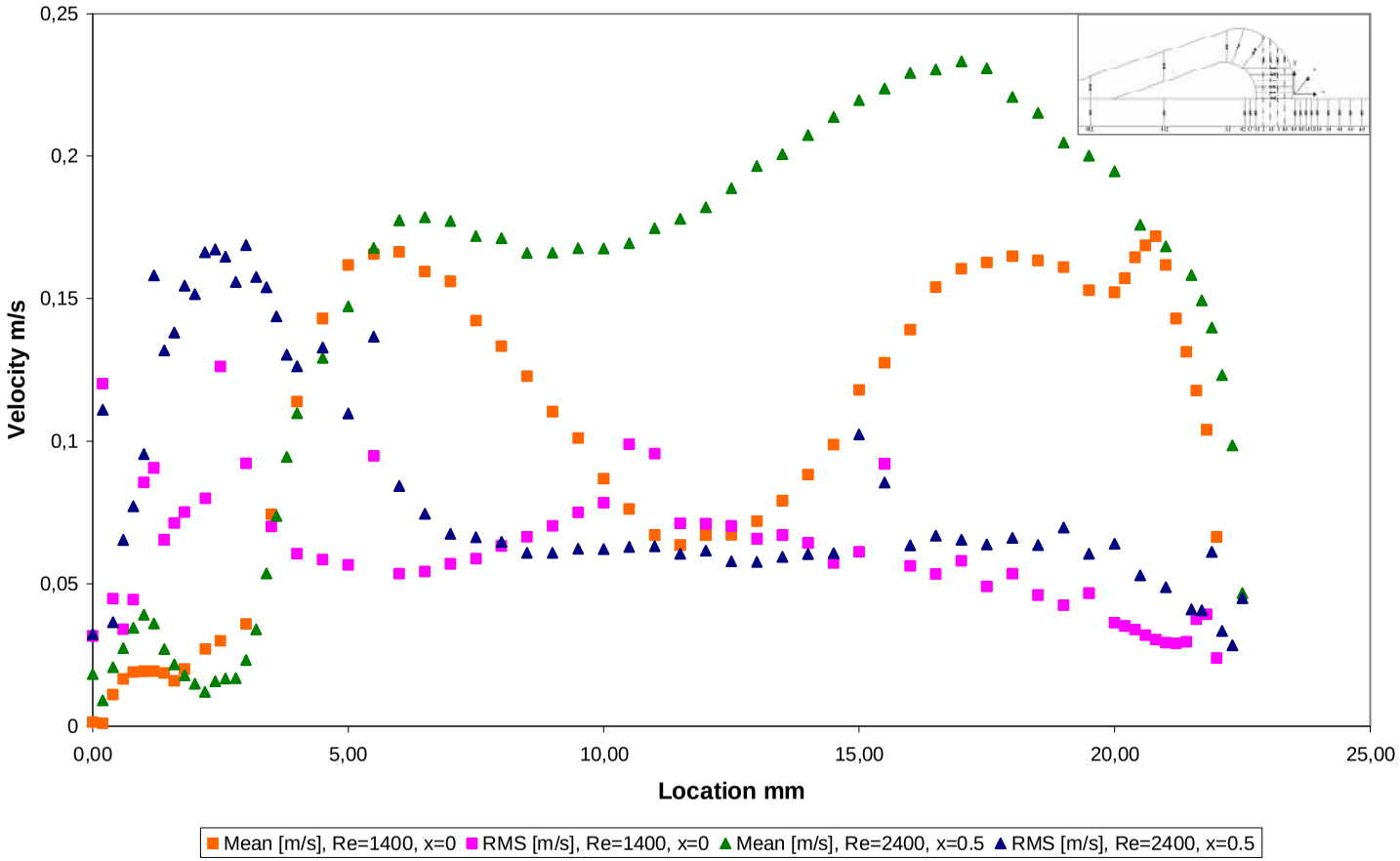

Figure 3.12 Velocity profile measured at the inlet of the Garft Re=1400, 2400, x=0.5

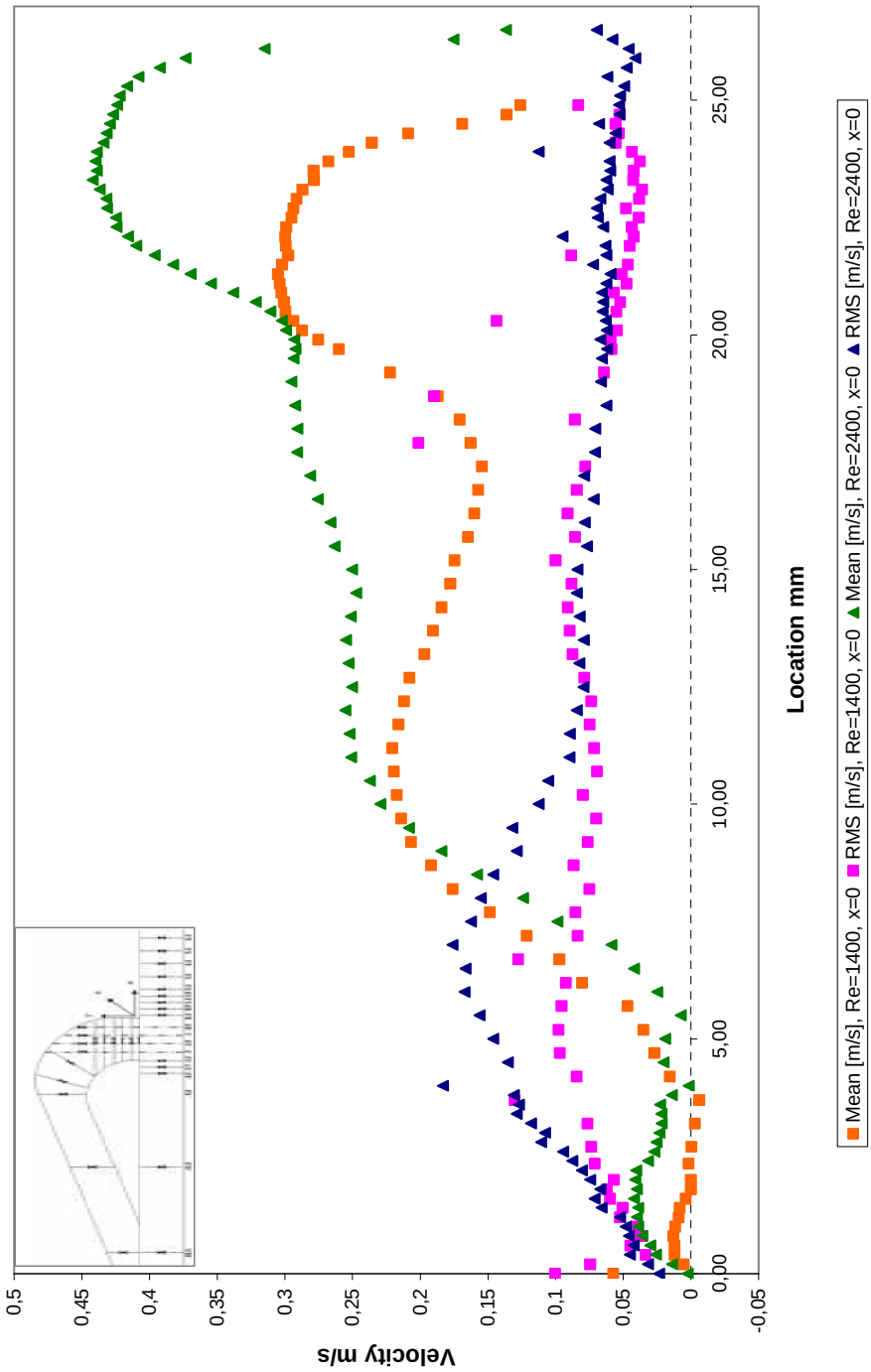

Figure 3.13 Velocity profile measured at the inlet of the Garft Re=1400, 2400, x=0

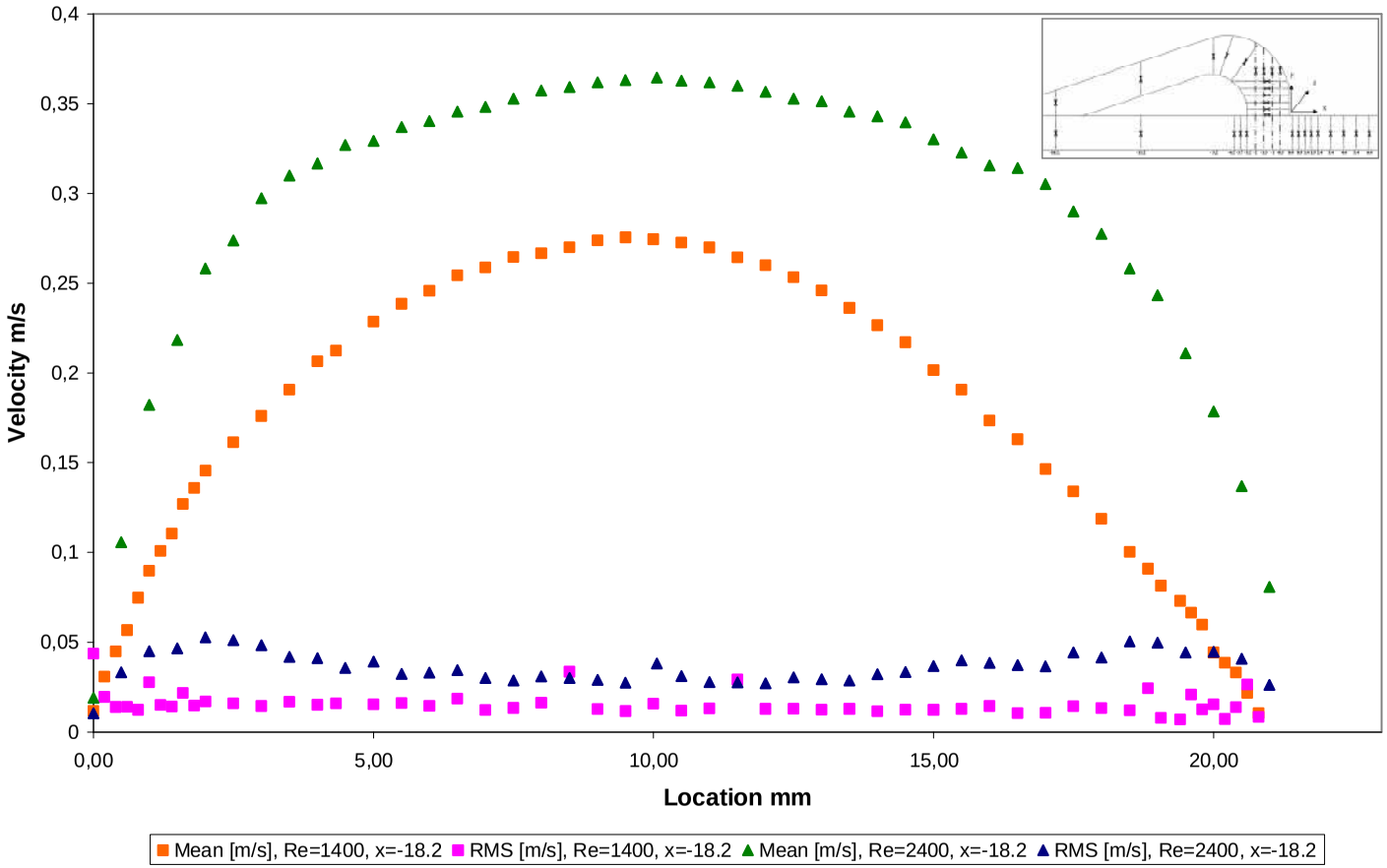

Figure 3.14 Velocity profile measured at the inlet of the DVS Re=1400, 2400, x=-18.2

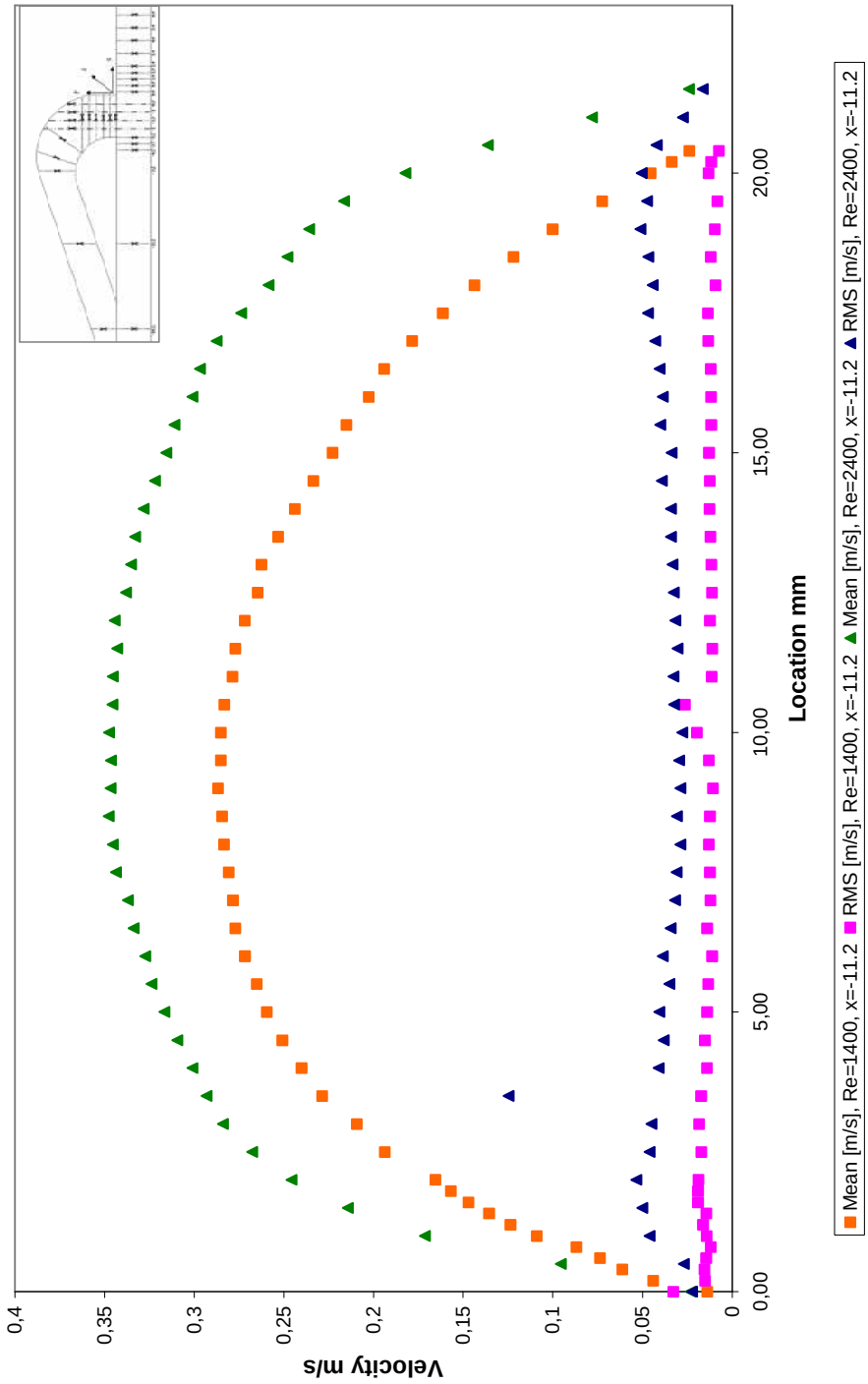

Figure 3.15 Velocity profile measured at the inlet of the DVS Re=1400, 2400, x=-11.2

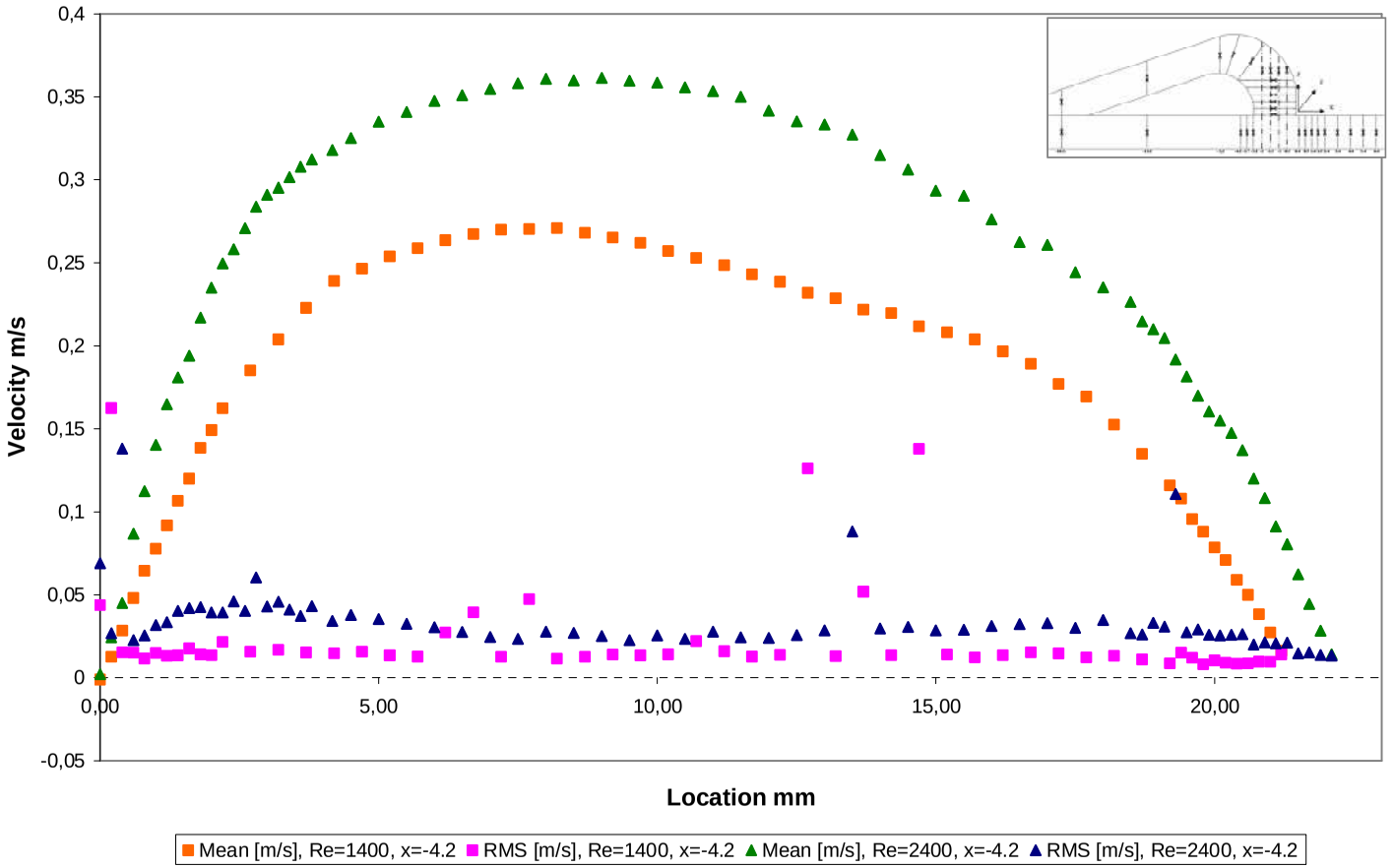

Figure 3.16 Velocity profile measured at the inlet of the DVS Re=1400, 2400, x=-4.2

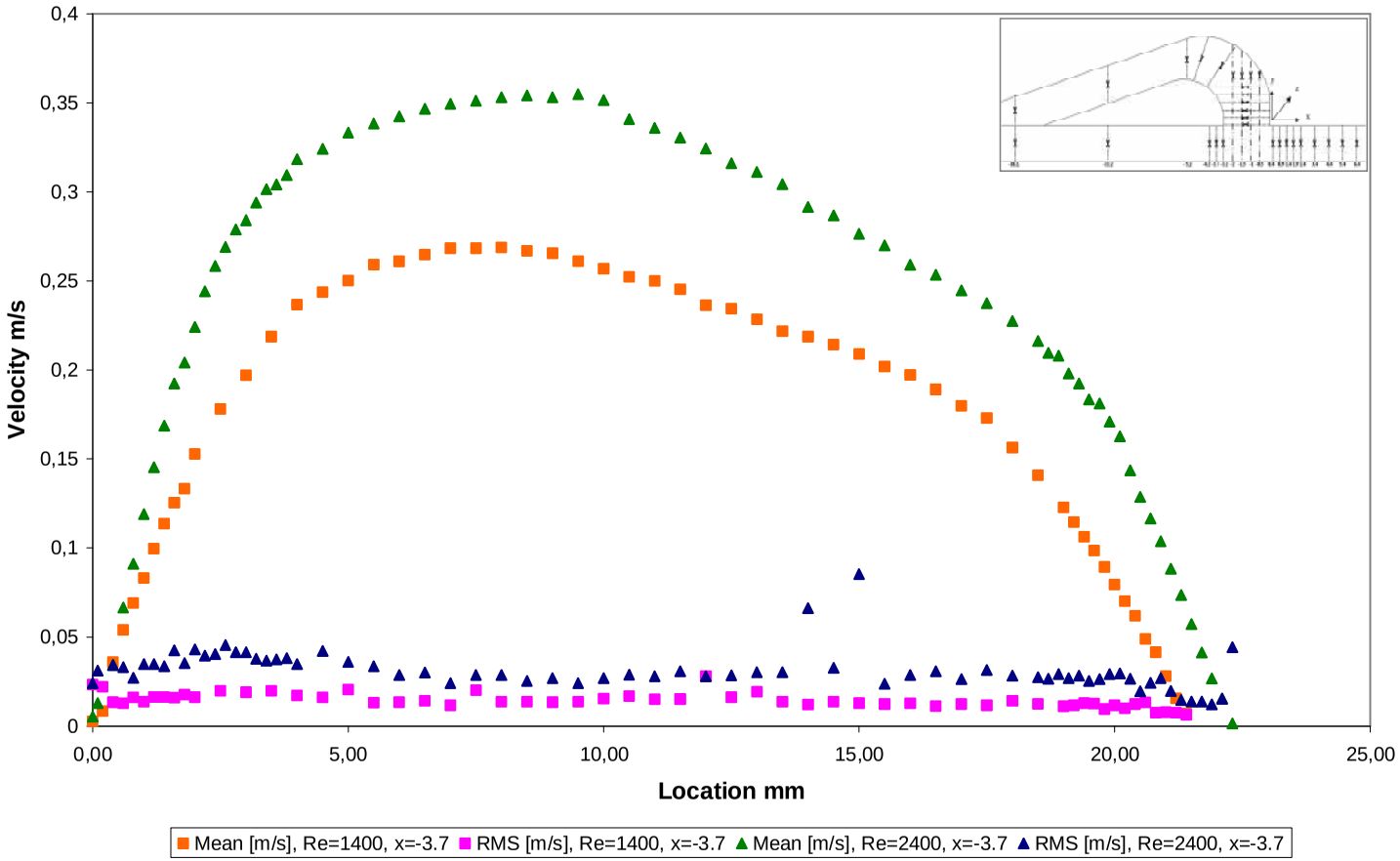

Figure 3.17 Velocity profile measured at the inlet of the DVS Re=1400, 2400, x=-3.7

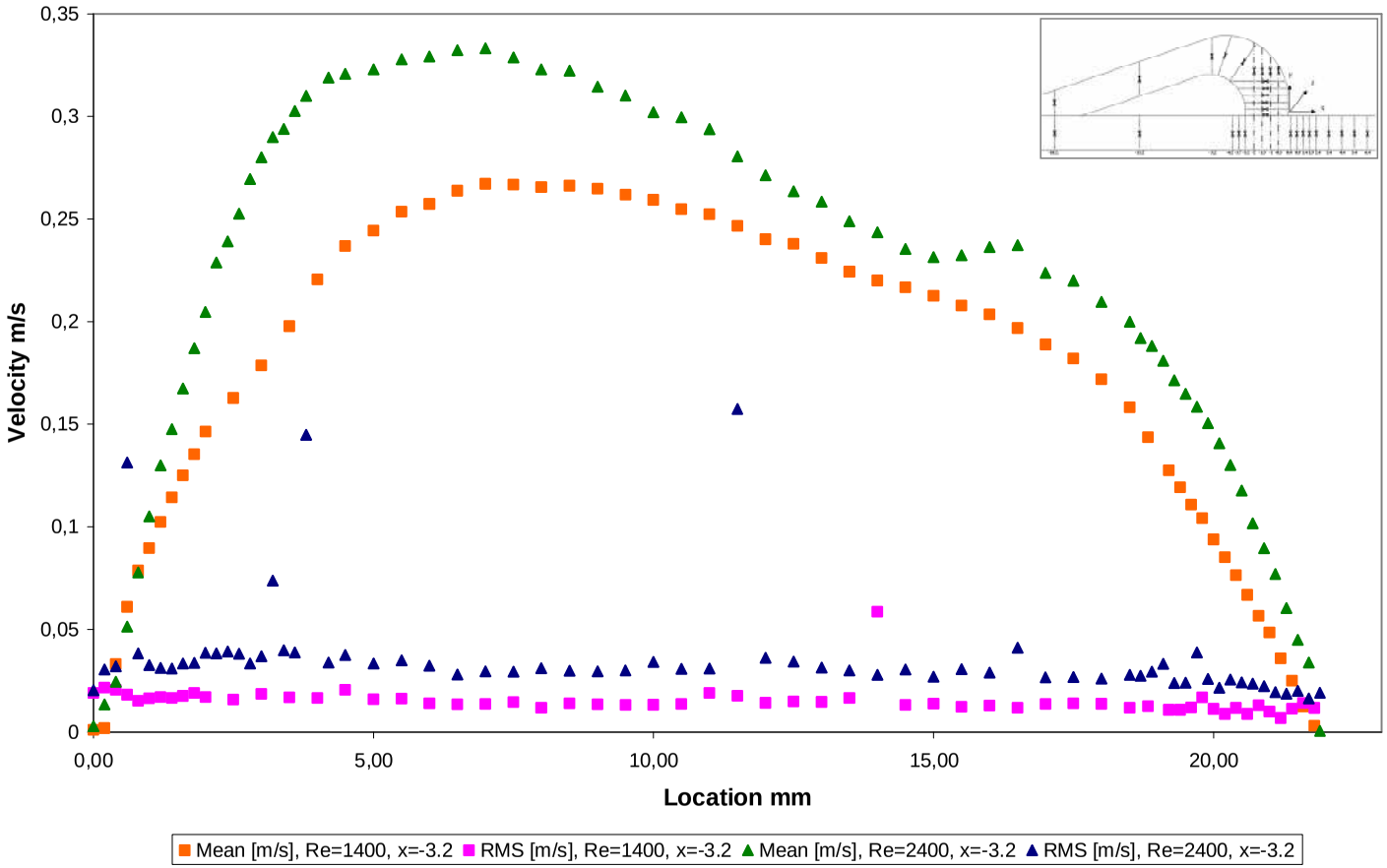

Figure 3.18 Velocity profile measured at the inlet of the DVS Re=1400, 2400, x=-3.2

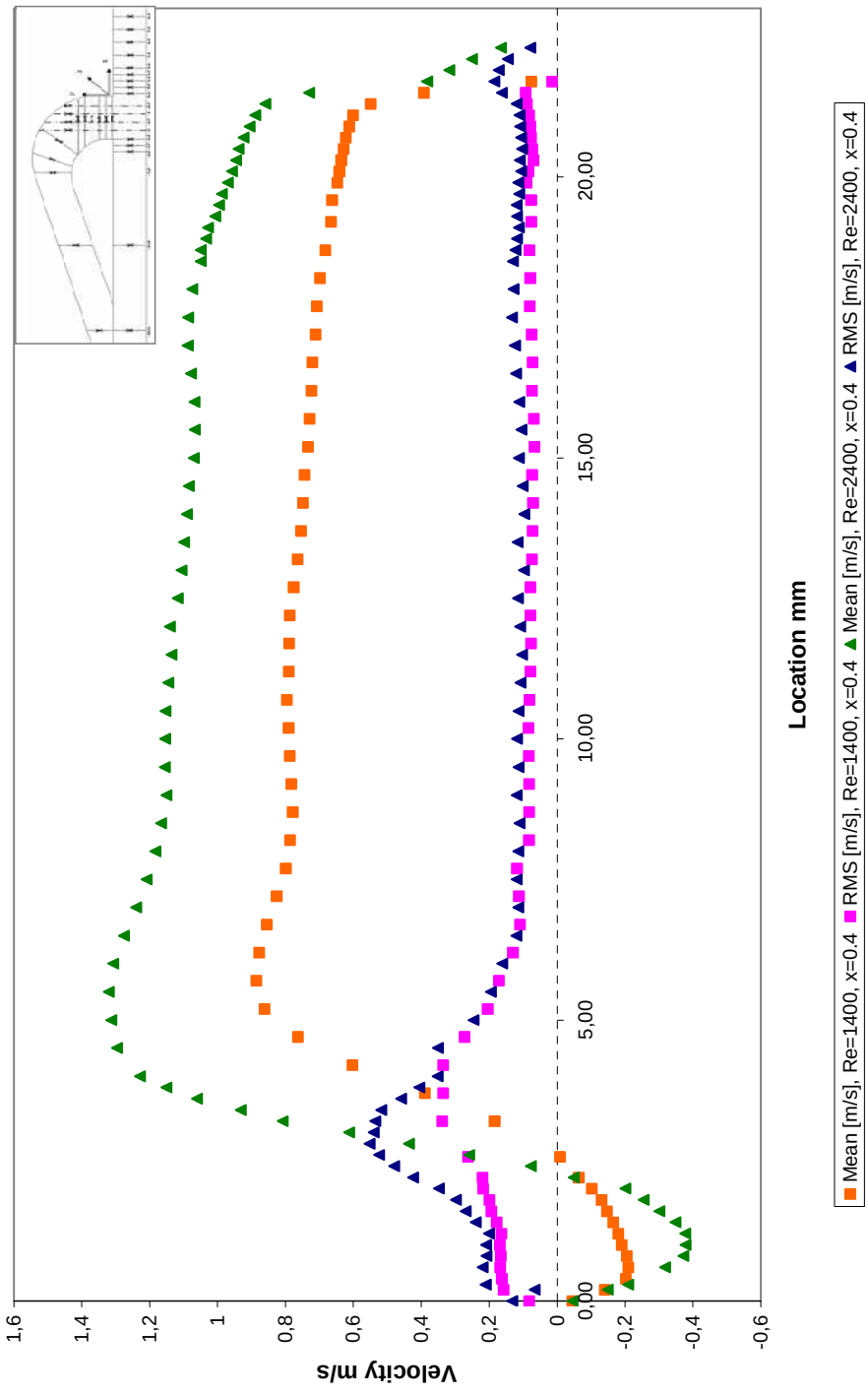

Figure 3.19 Velocity profile measured at the inlet of the PVS Re=1400, 2400, x=0.4

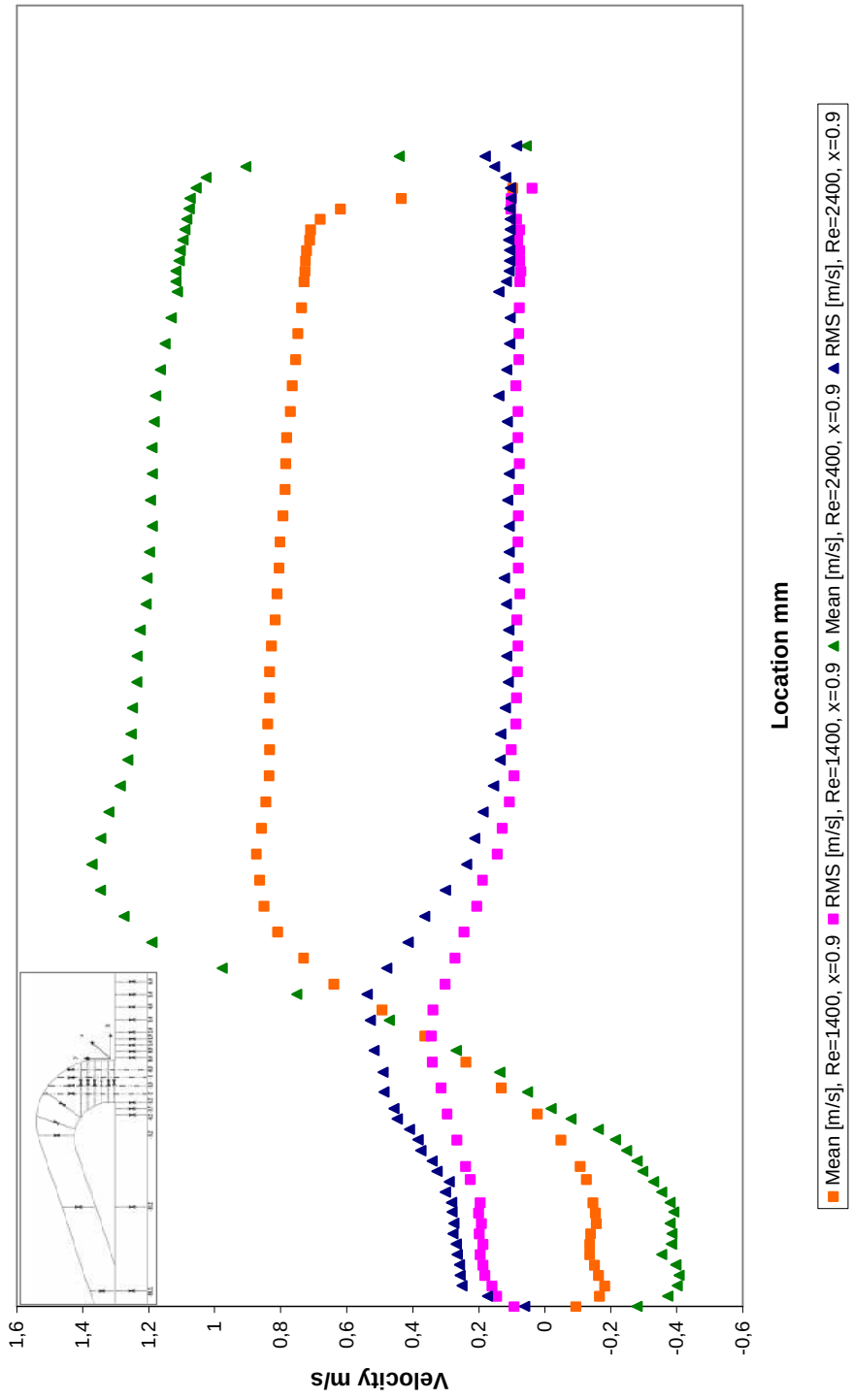

Figure 3.20 Velocity profile measured at the inlet of the PVS Re=1400, 2400, x=0.9

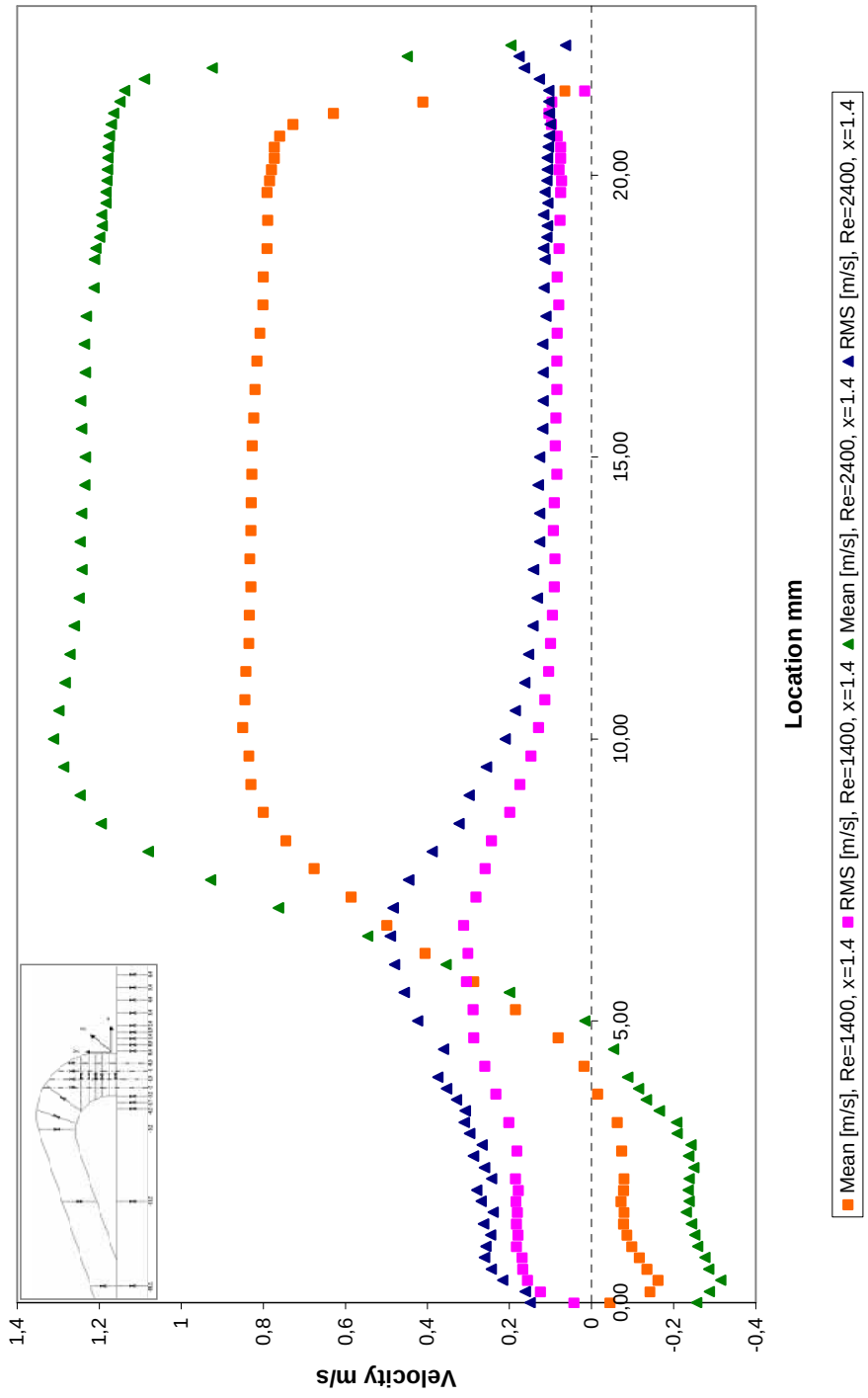

Figure 3.21 Velocity profile measured at the inlet of the PVS Re=1400, 2400, x=1.4

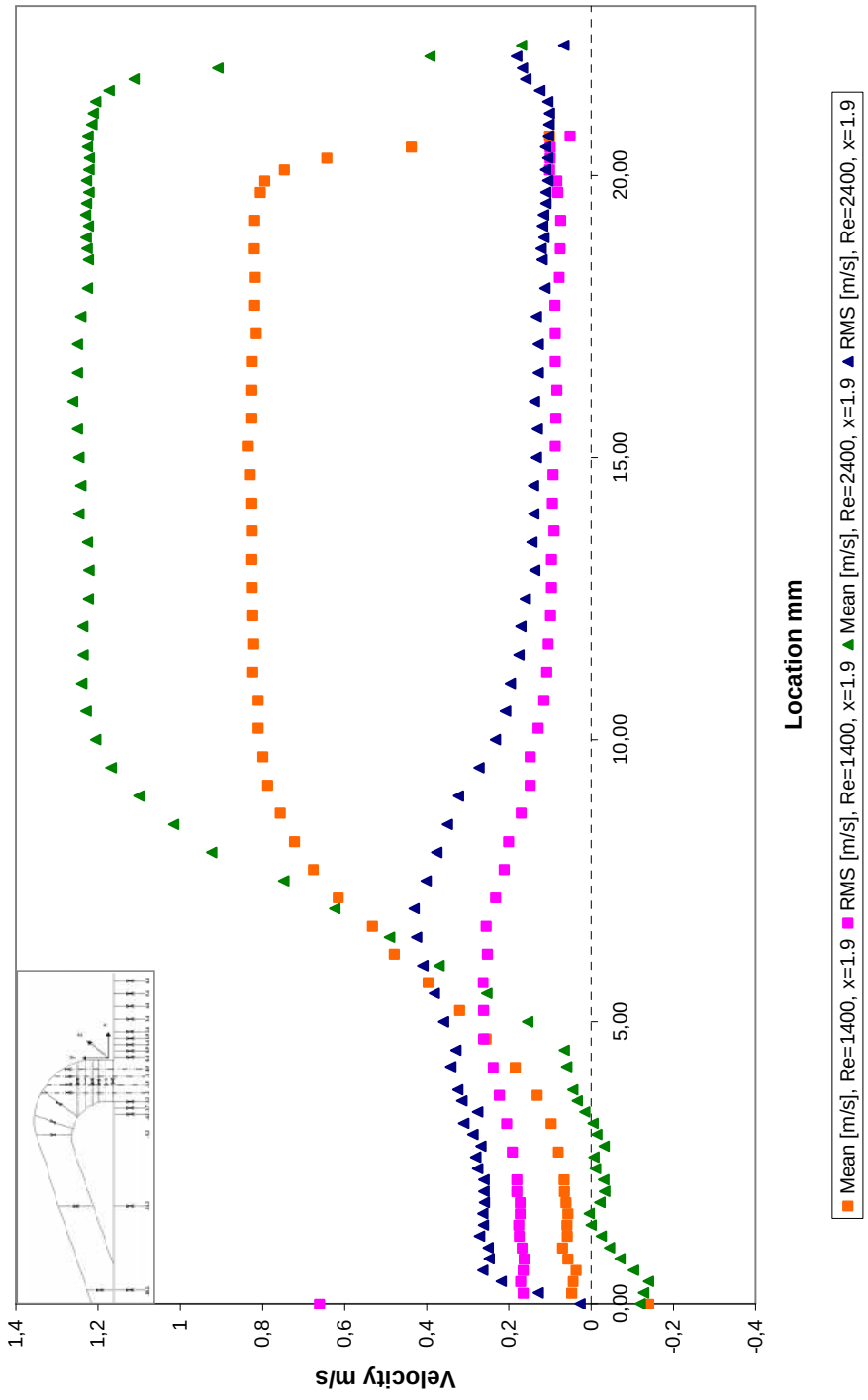

Figure 3.22 Velocity profile measured at the inlet of the PVS Re=1400, 2400, x=1.9

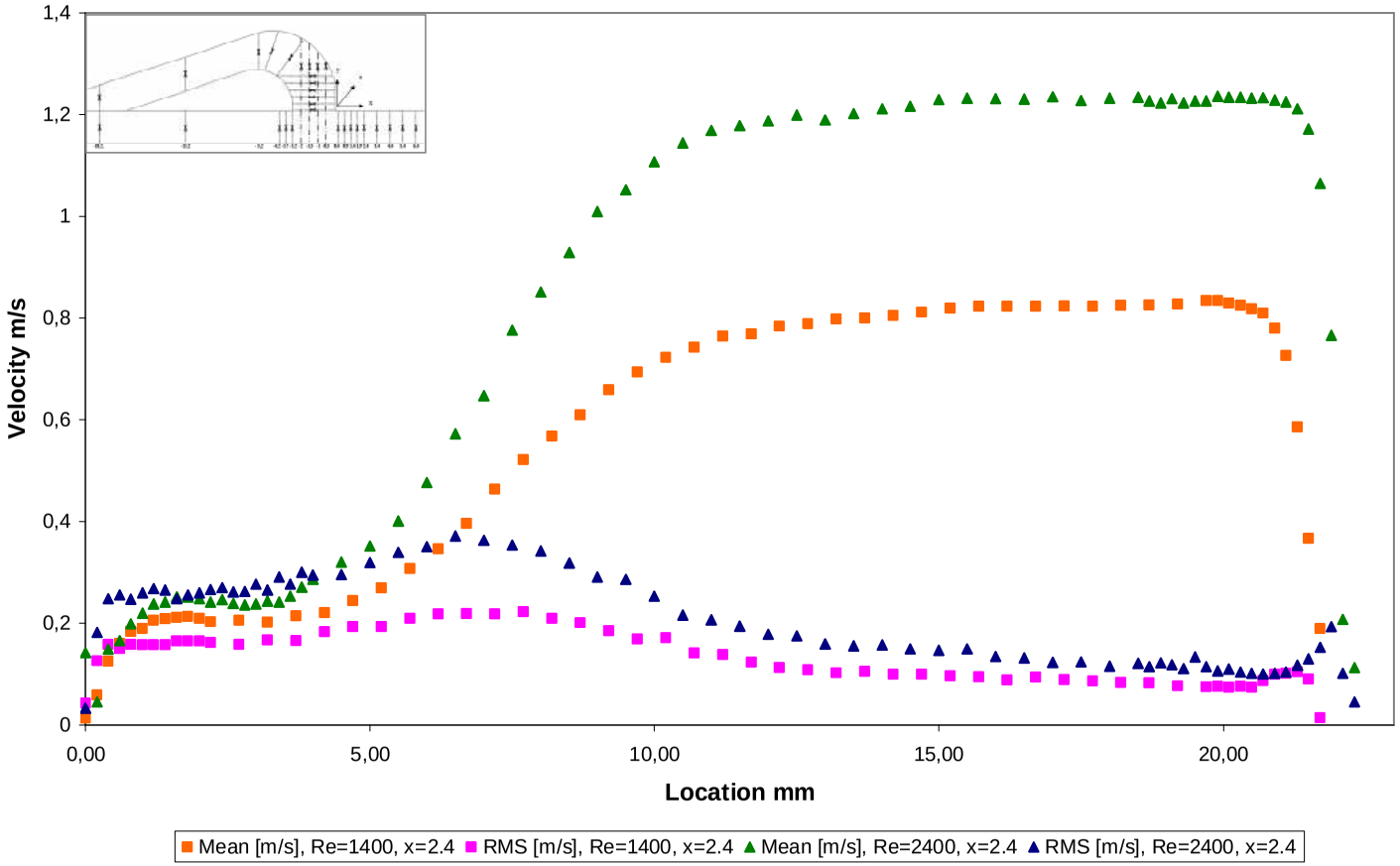

Figure 3.23 Velocity profile measured at the inlet of the PVS Re=1400, 2400, x=2.4

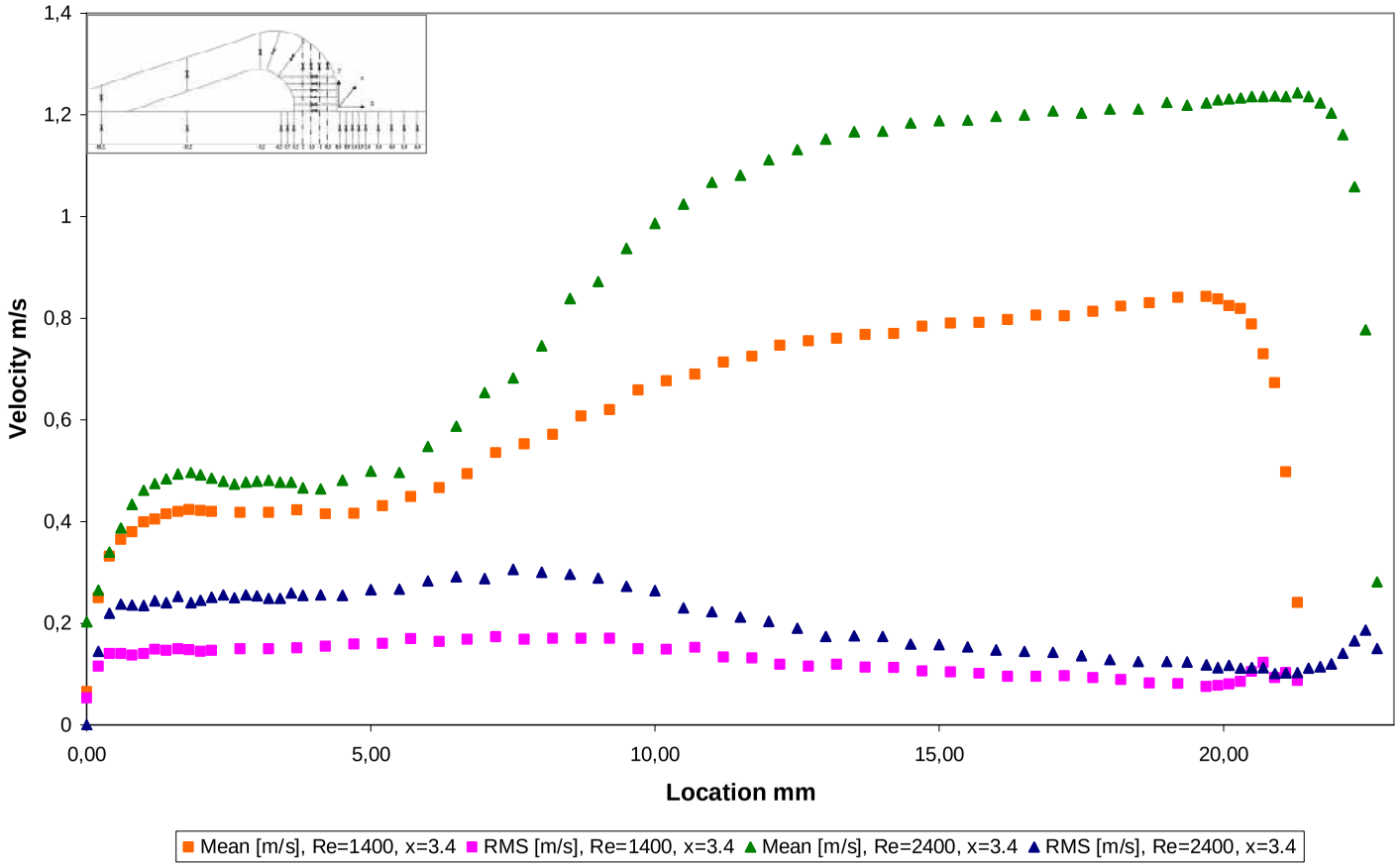

Figure 3.24 Velocity profile measured at the inlet of the PVS Re=1400, 2400, x=3.4

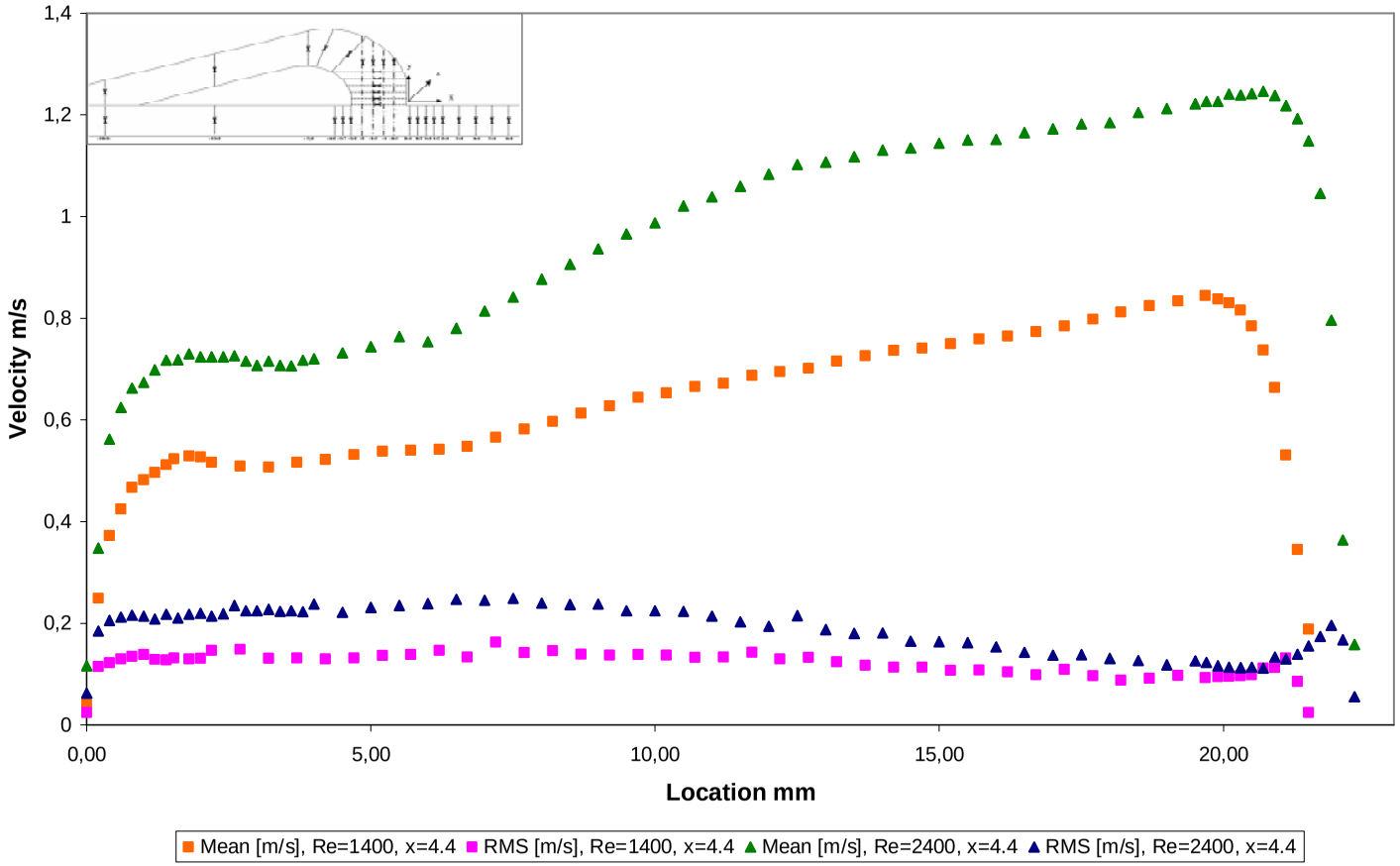

Figure 3.25 Velocity profile measured at the inlet of the PVS Re=1400, 2400, x=4.4

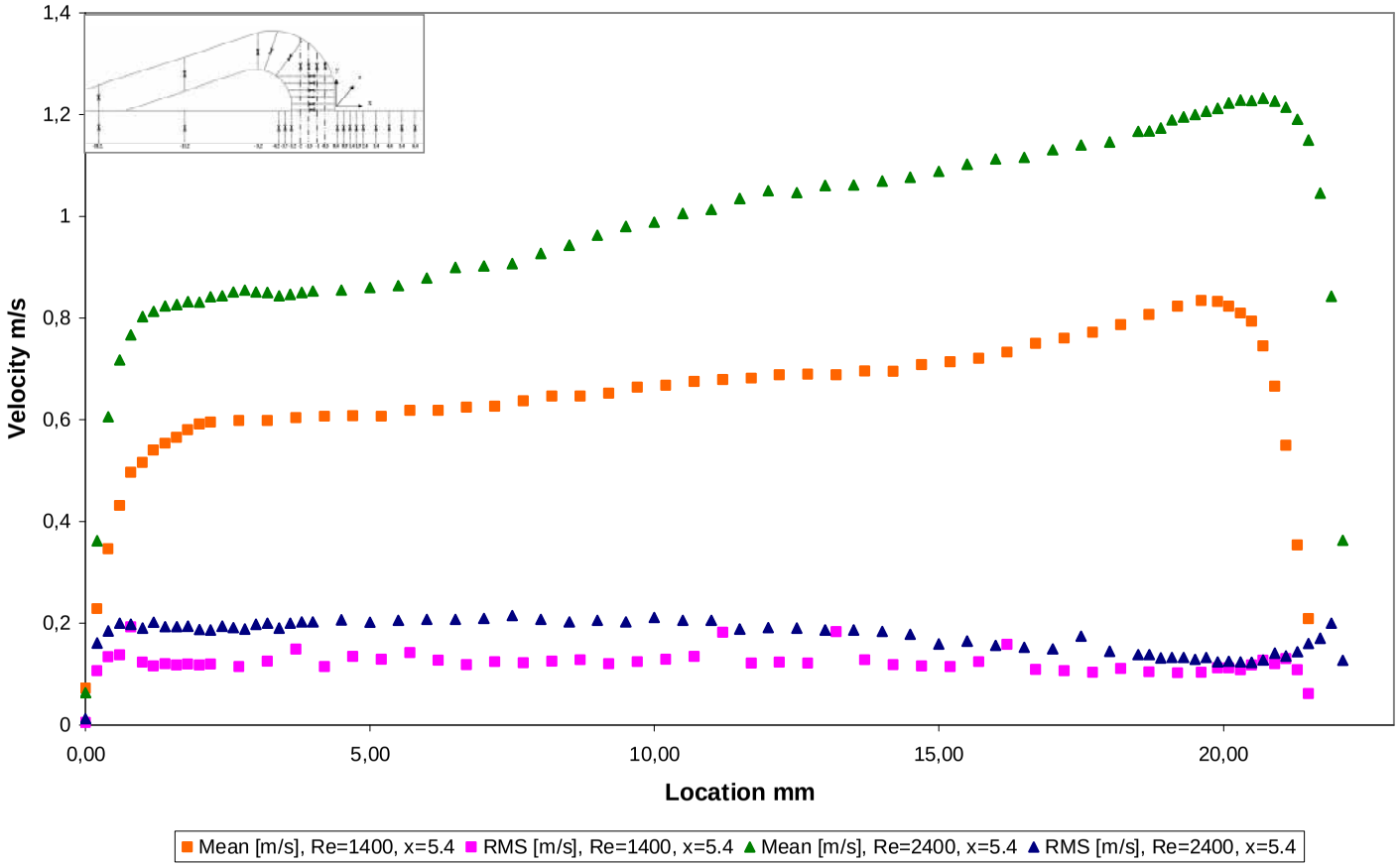

Figure 3.26 Velocity profile measured at the inlet of the PVS Re=1400, 2400, x=5.4

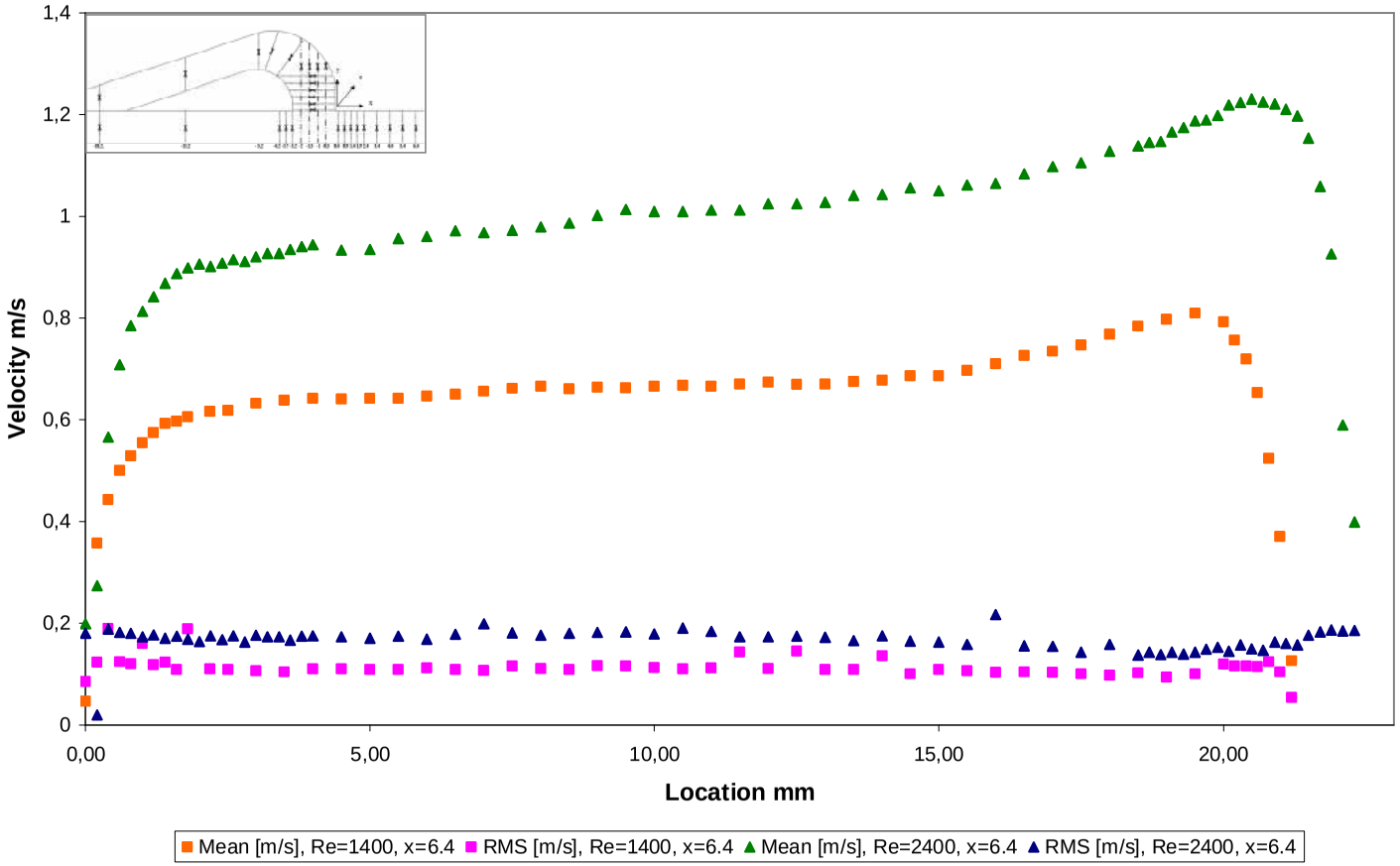

Figure 3.27 Velocity profile measured at the inlet of the PVS Re=1400, 2400, x=6.4

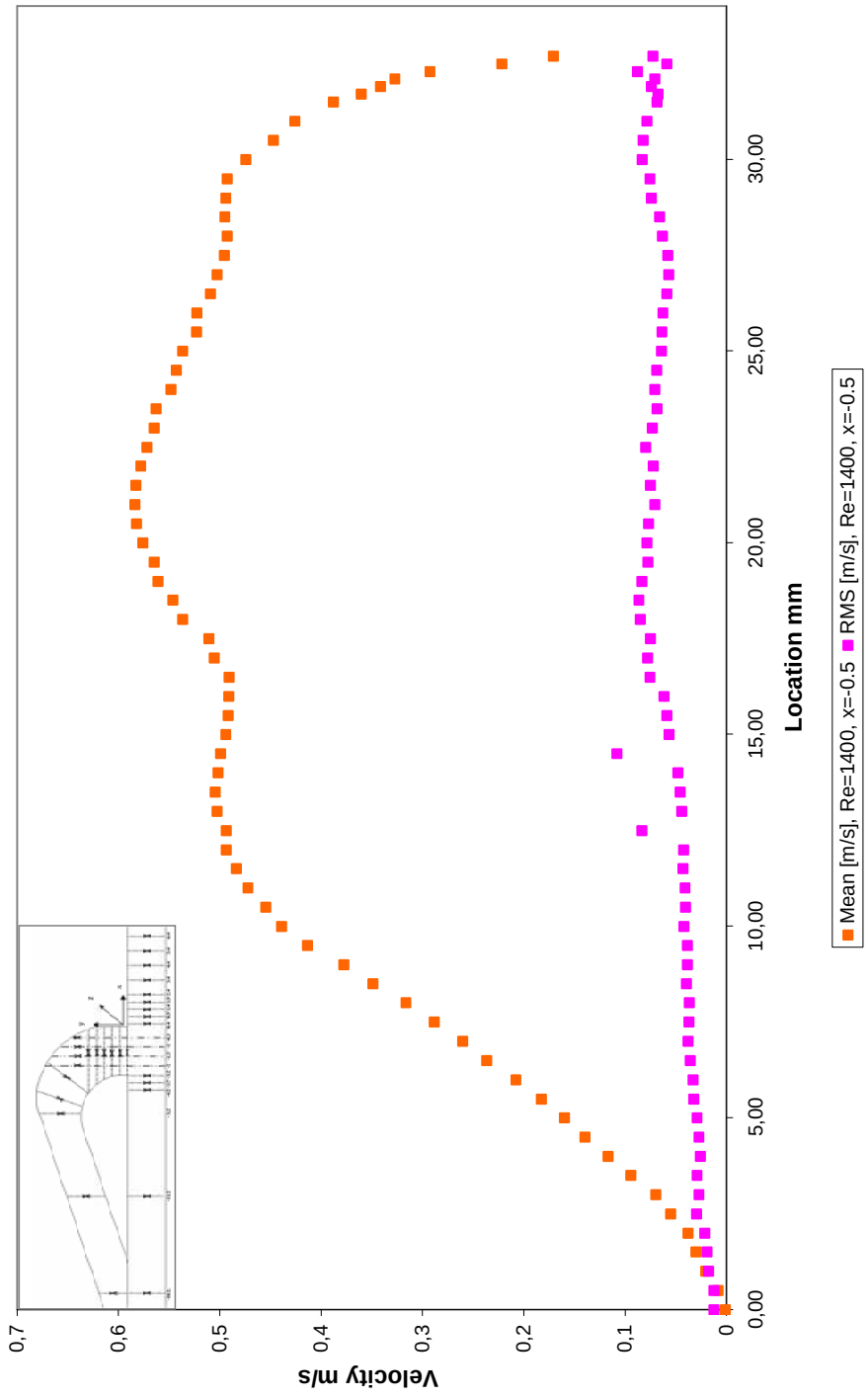

Figure 3.28 Velocity profile measured at the inlet of the VA Re=1400 , x=-0.5

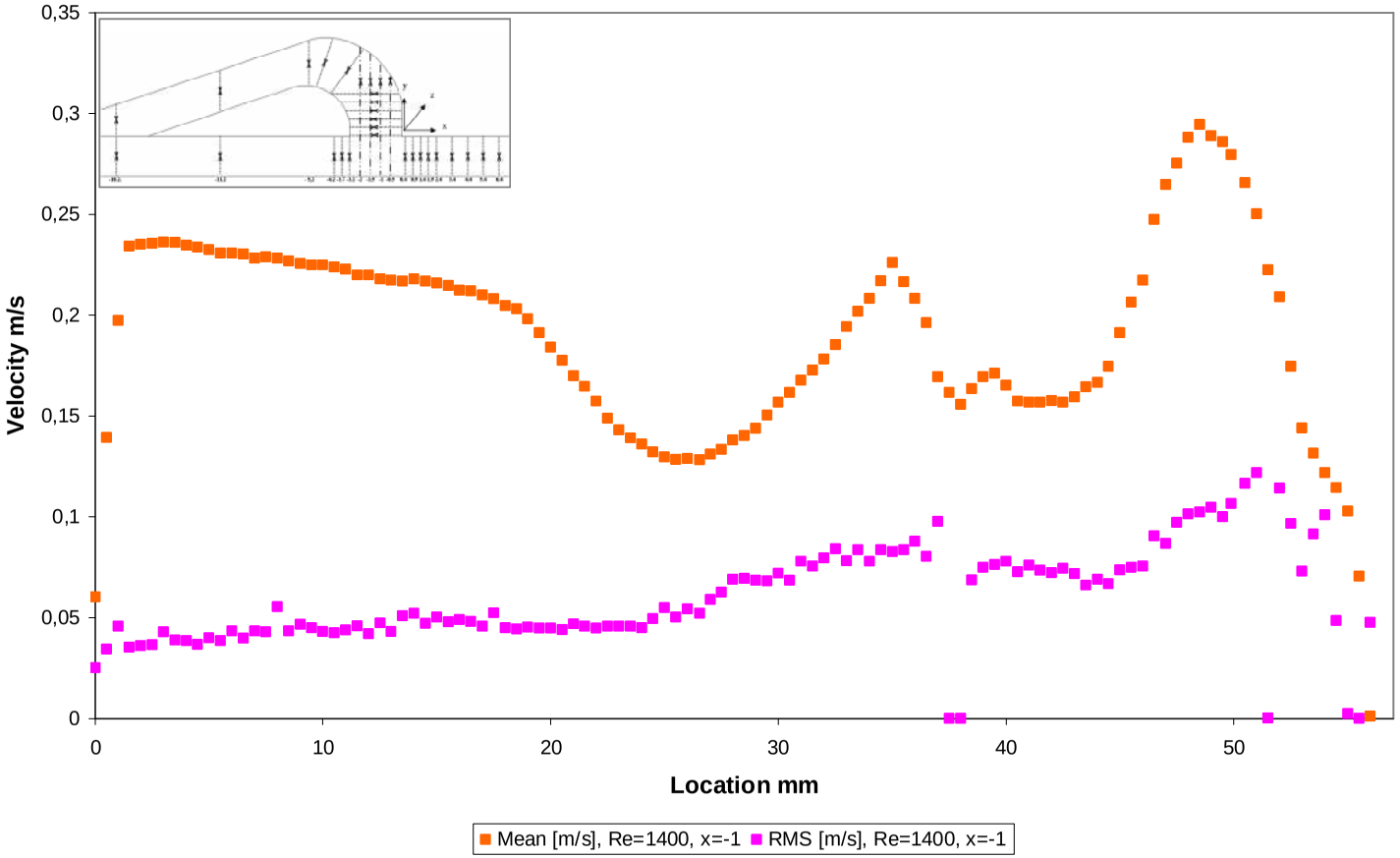

Figure 3.29 Velocity profile measured at the inlet of the VA Re=1400 , x=-1

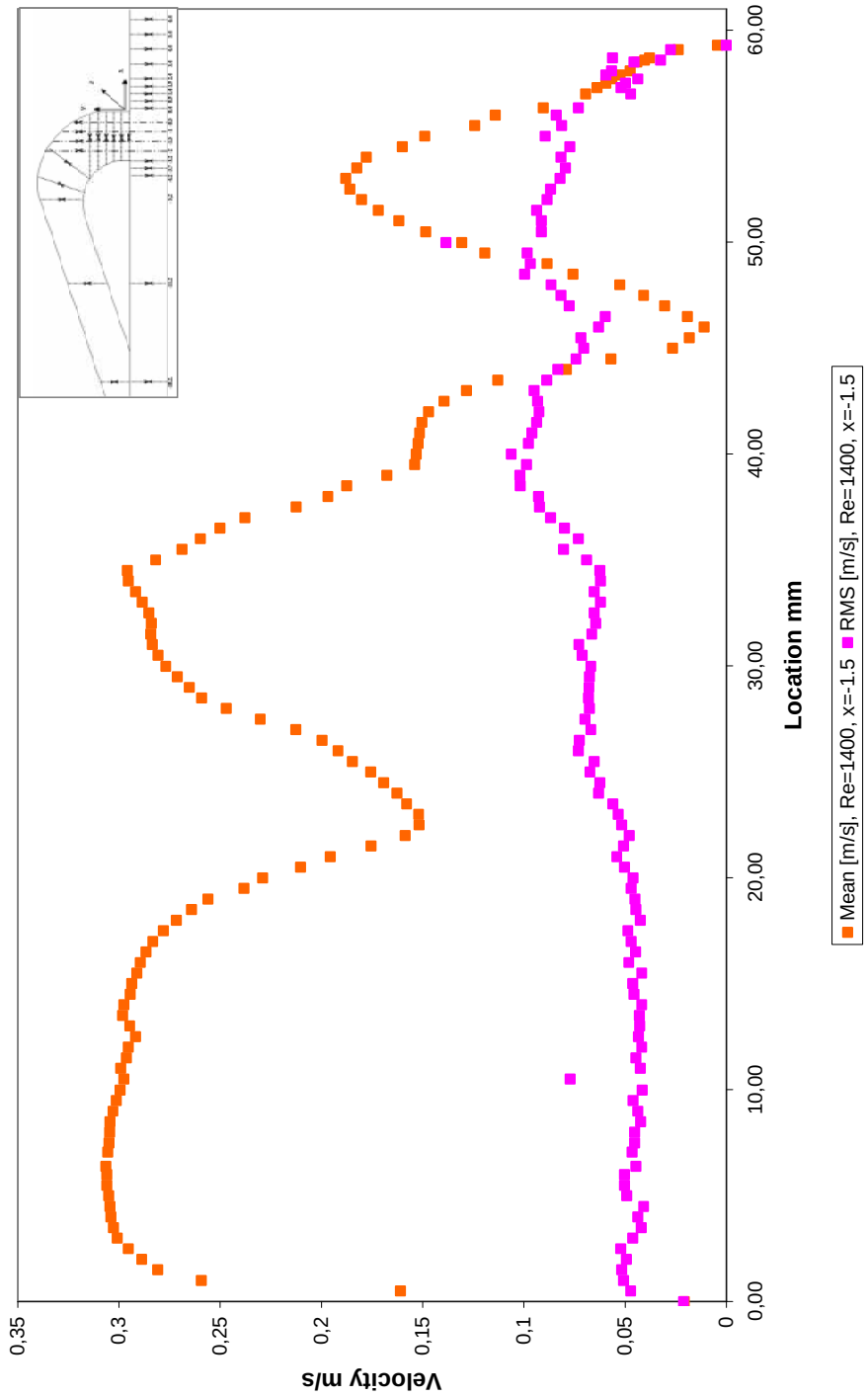

Figure 3.30 Velocity profile measured at the inlet of the VA Re=1400 , x=-1.5

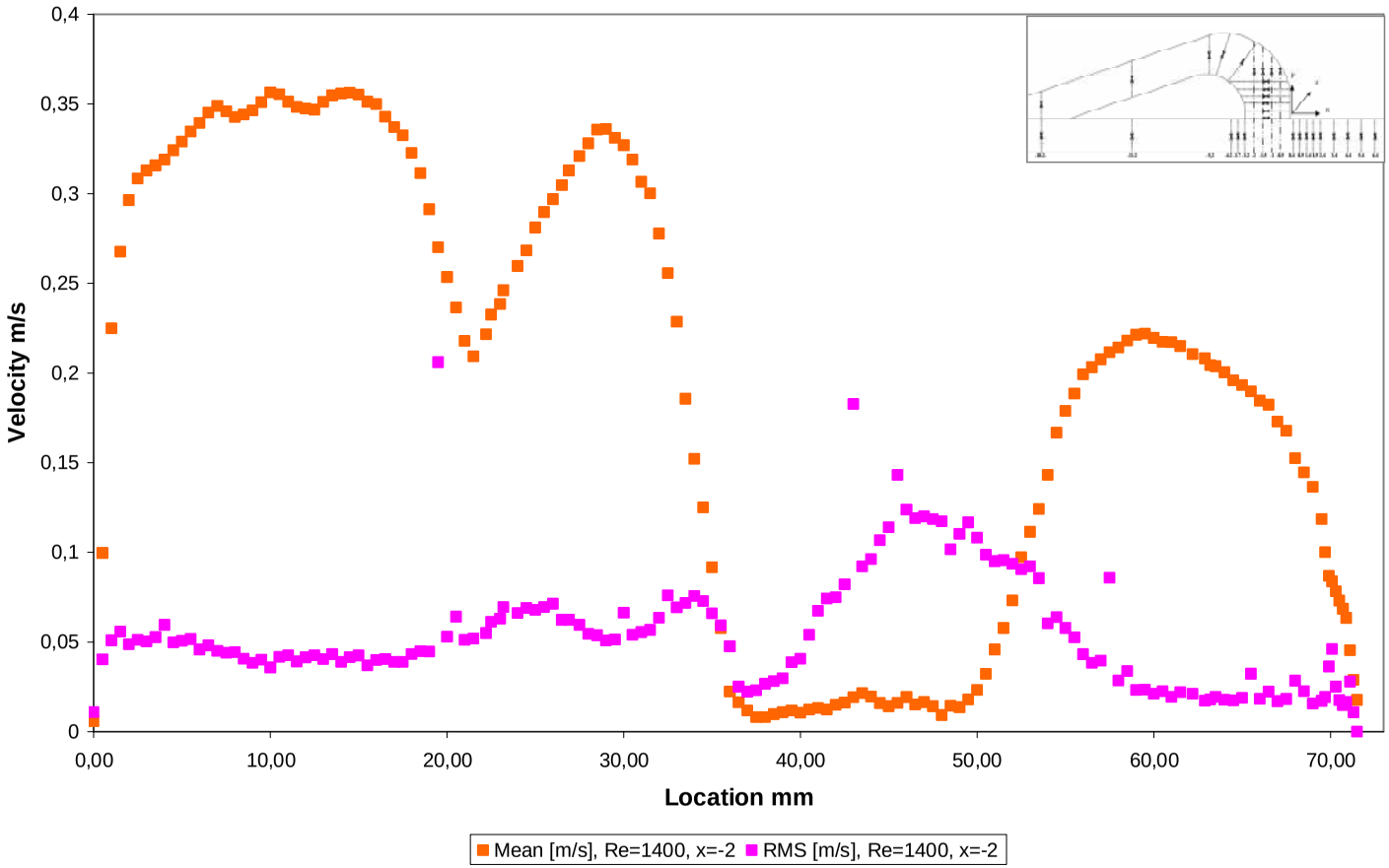

Figure 3.31 Velocity profile measured at the inlet of the VA Re=1400 , x=-2

3.2 WALL SHEAR STRESS CALCULATIONS (Re=1400)

The shear stress value near the wall is the WSS, where IH development is associated with. Normal WSS values are below 0.76 Pa for veins and between 1 and 3 Pa in large arteries and between 2 and 6 Pa in arterioles [36]. WSS values in arteries and below 1 Pa are associated with IH development [37]. As well as WSS values above 35 Pa [38].

When a vascular access is constructed, flow through the vessels of the access increases. Increases blood flow results in increased WSS for a constant vessel diameters [39]. For arteries it is known that they remodel to maintain WSS at the normal level, about 1.5 Pa [40].

Velocity measurements near to the walls of graft, DVS, PVS and anastomoses were taken at 26 locations (Figure 3.32). Wall shear stress was calculated from the product of the instantaneous velocity gradient at the wall. The intantenous velocity gradient at the wall was calculated taken three velocity measurements. The velocity measurements were done at the points of -4.2, to +2.4 for floor, -4.2 to -3.2 for DVS, 0.4 to 2.4 for PVS and 0 to 1 for graft (in the direction of x). In figure 3.33 the trend observed was change of WSSs from 0.55 N/m^2 to 10.93N/m^2moving distal to proximal along the artery floor. In figure 3.34 WSSs values were in the range of 0.79 and 1.56 N/m^2. In figure 3.35, the mean WSSs transitioned between 3.13 to 2.28N/m^2. WSSs varied range of 0D to 1D along the graft and became 2.61 N/m^2 (Figure 3.36). In figure 3.37, the mean WSSs values were in the range of 09 to 1.63 N/m^2.

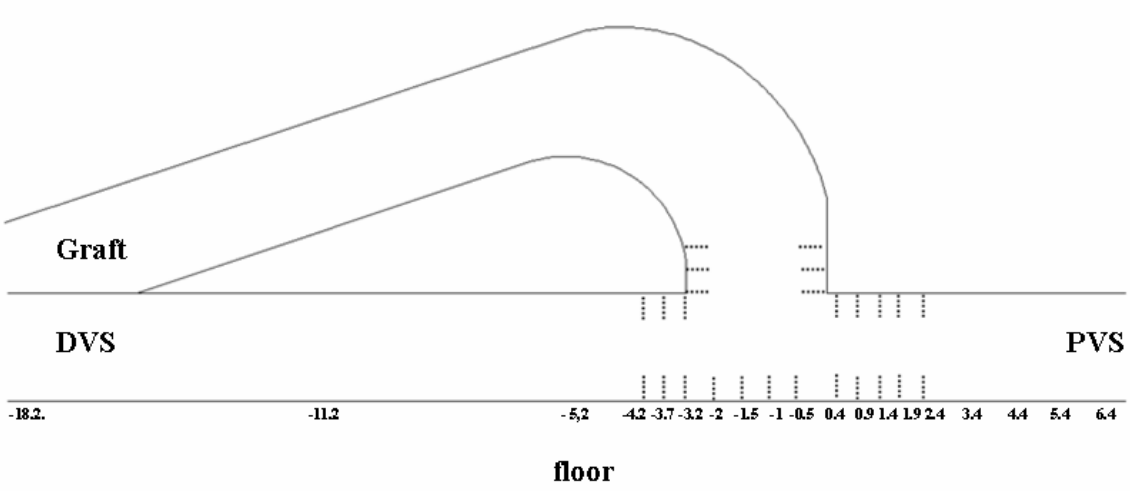

Figure 3.32 Wall shear stress distribution longitudinal sections is dispayed from the PVS, DVS, and graft

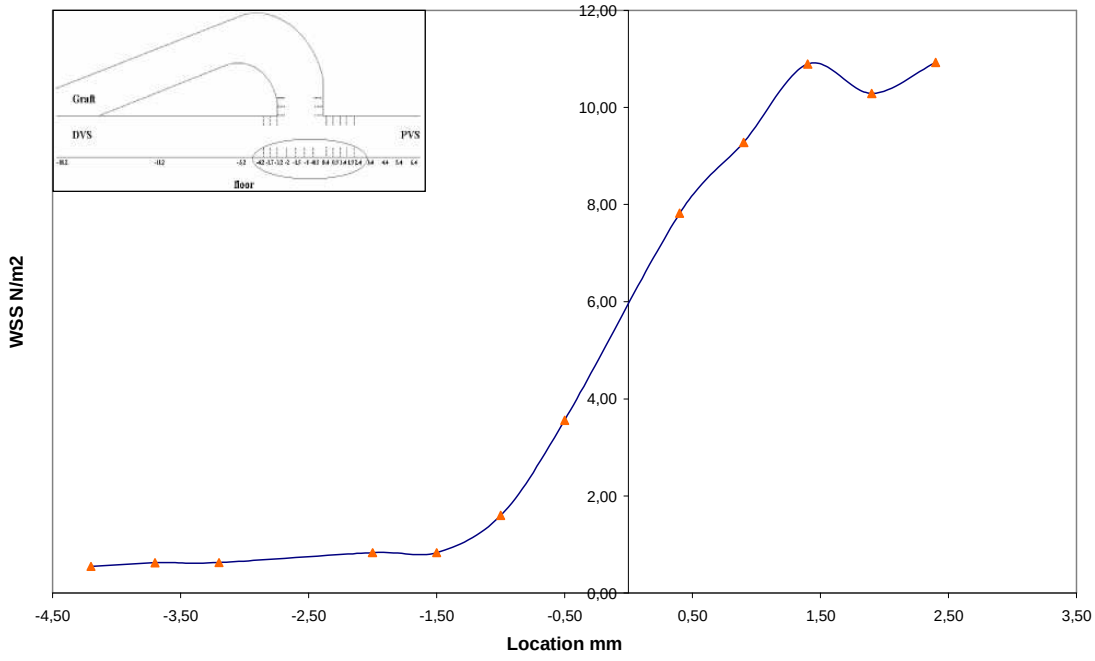

Figure 3.33 WSS estimation along the floor side of VA at Re=1400

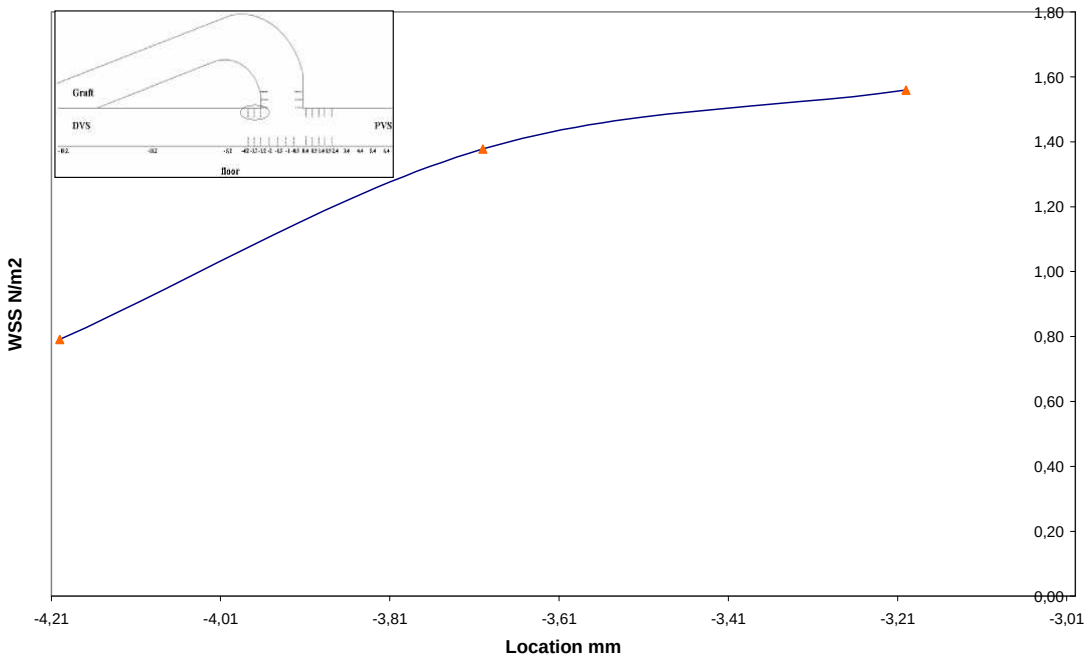

Figure 3.34 WSS estimation at the DVS at Re=1400

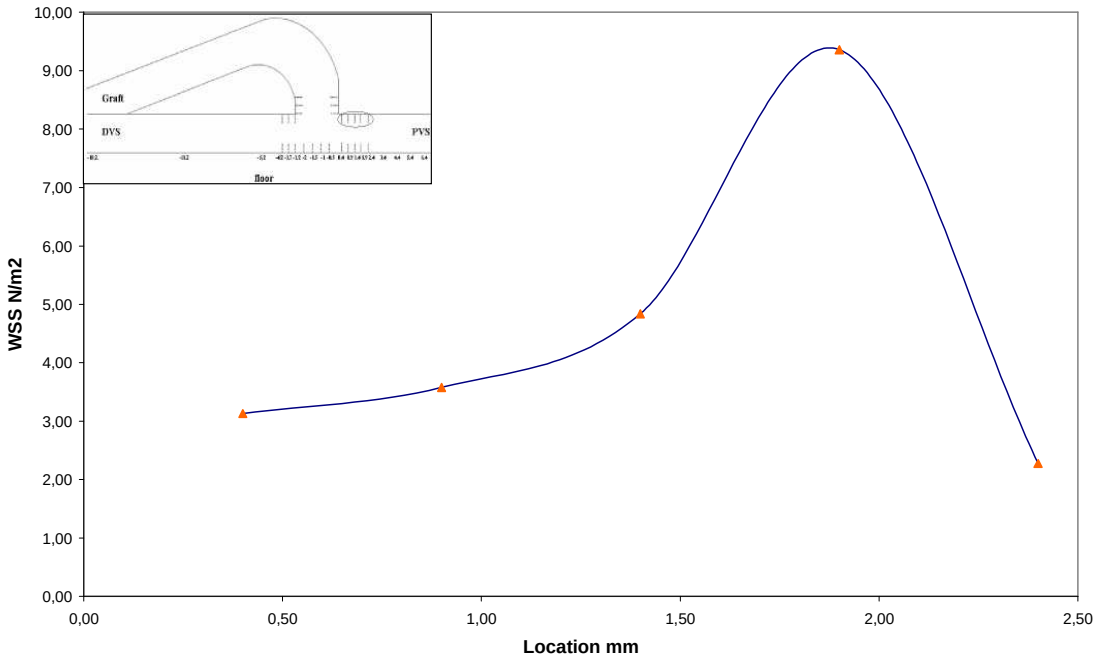

Figure 3.35 WSS estimation at the PVS at Re=1400

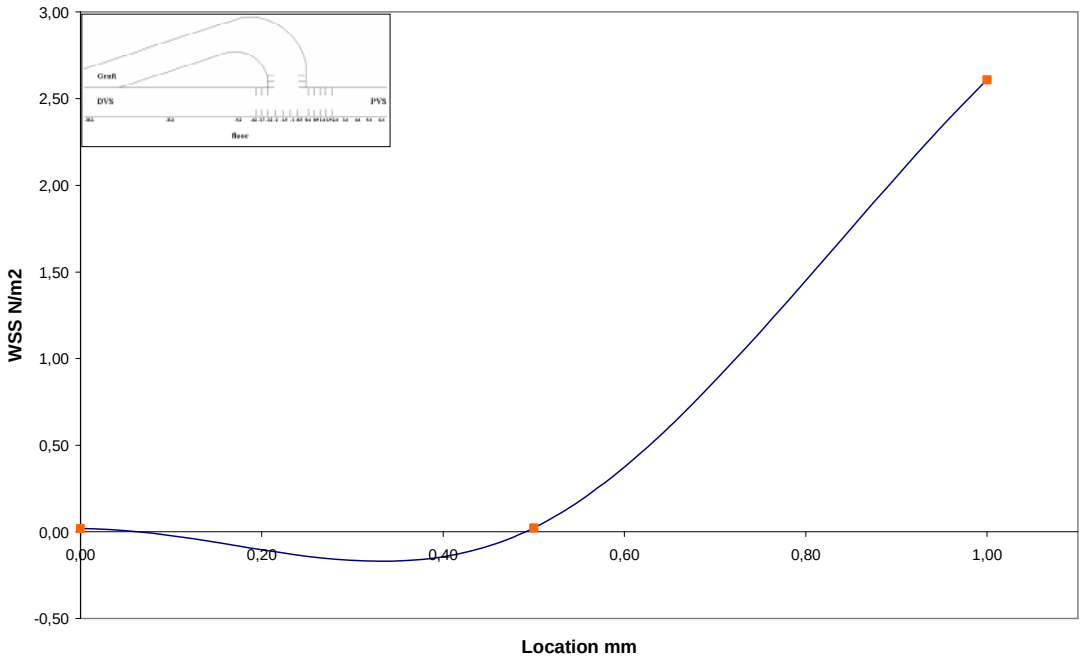

Figure 3.36 WSS estimation at the graft at Re=1400

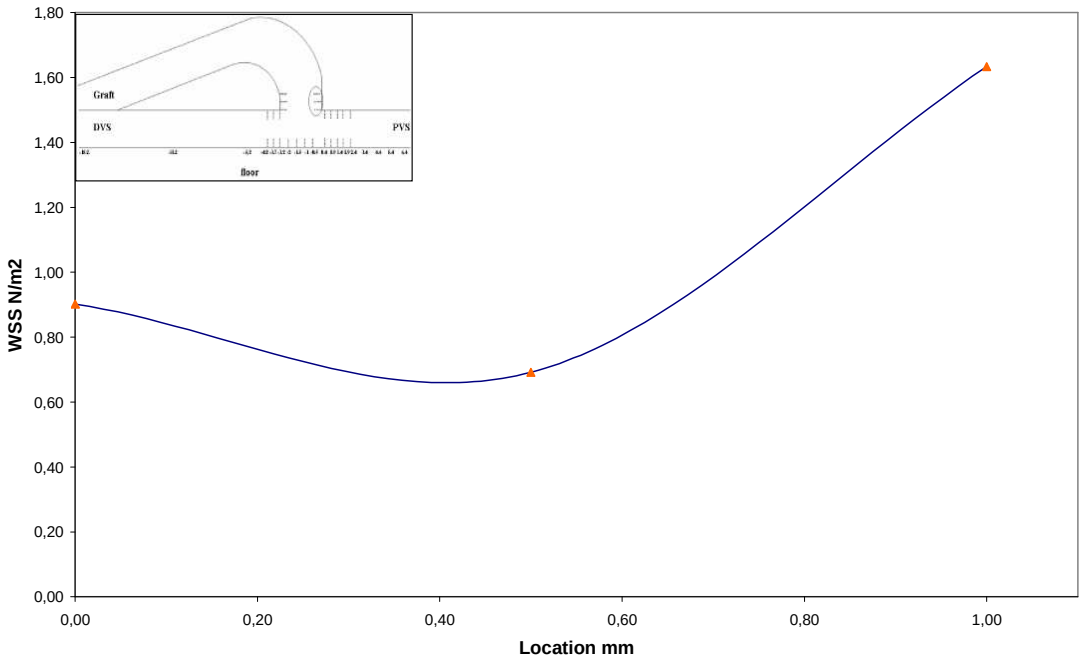

Figure 3.37 WSS estimation at the graft at Re=1400

3.3 WALL SHEAR STRESS CALCULATIONS (Re=2400)

Near wall velocity measurements were taken at 22 locations along the graft, distal and proximal vein segments (Figure 3.32). Wall shear stress was obtained from the product of the instantaneous velocity gradient at the wall. The intantenous velocity gradient at the wall was estimated three velocity measurements near the wall. The velocity measurements nearest to the wall ranged from -4.2 to -3.2 for distal vein segment, from 0.4 to 2.4 for proximal vein segment, from 0 to 1 for graft. In figure 3.38 the trend observed was change of WSSs from 0.8 to 27.9 N/m^2 moving distal to proximal along the artery floor. In figure 3.39 WSSs values were in the range of 1.1 and 0.5 N/m^2. In figure 3.40, the mean WSSs transitioned between 5.21 to 4.86N/m^2. WSSs varied range of 0D to 1D along the graft and became 0.5 N/m^2 (Figure 3.41). In figure 3.42, the mean WSSs values were in the range of 2.77 to 1.93 N/m^2.

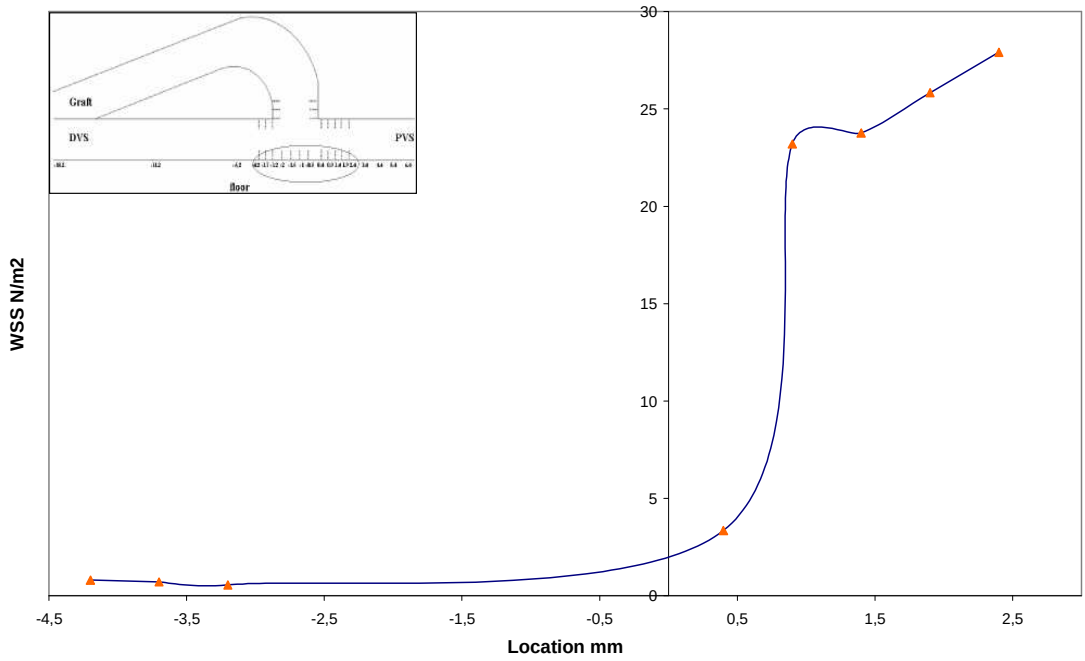

Figure 3.38 WSS estimation along the VA at Re=2400

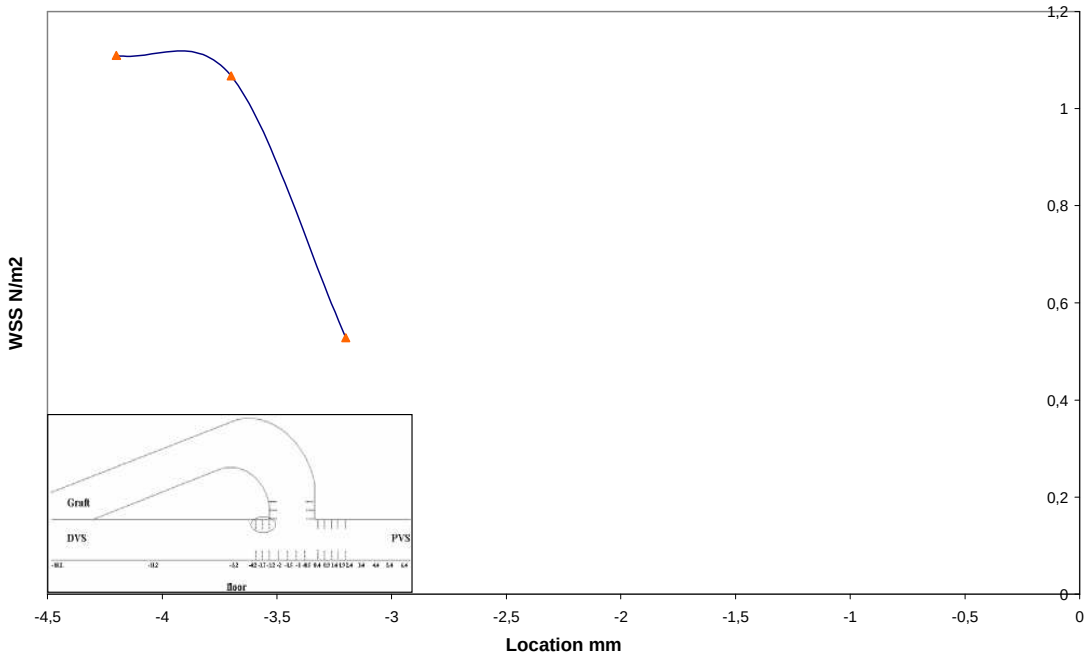

Figure 3.39 WSS estimation at the DVS at Re=2400

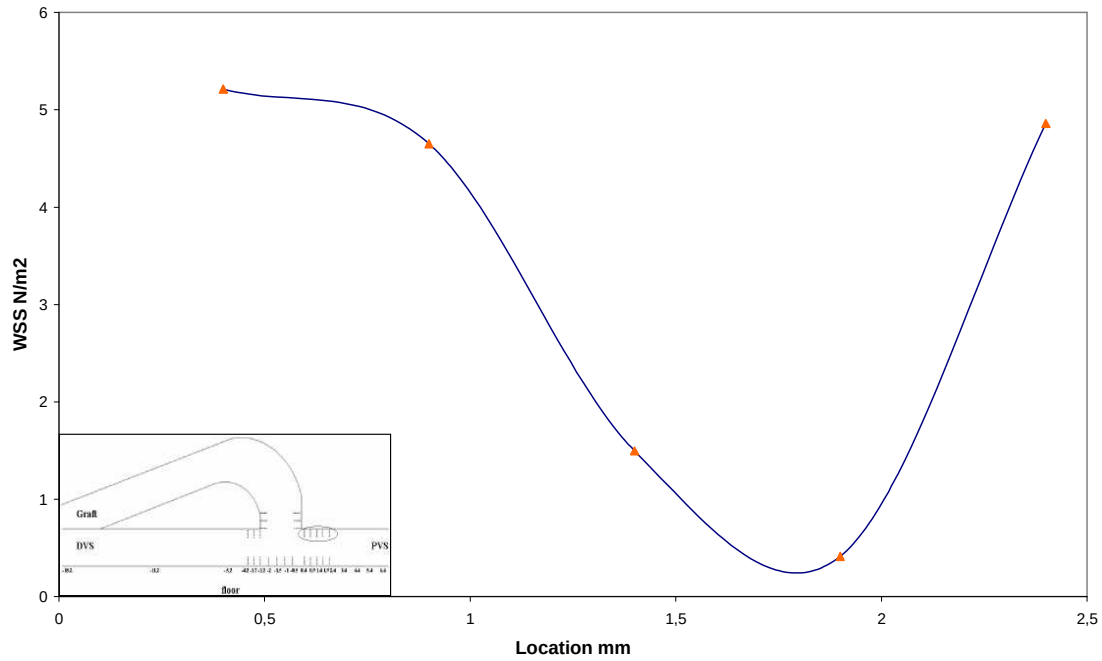

Figure 3.40 WSS estimation at the PVS at Re=2400

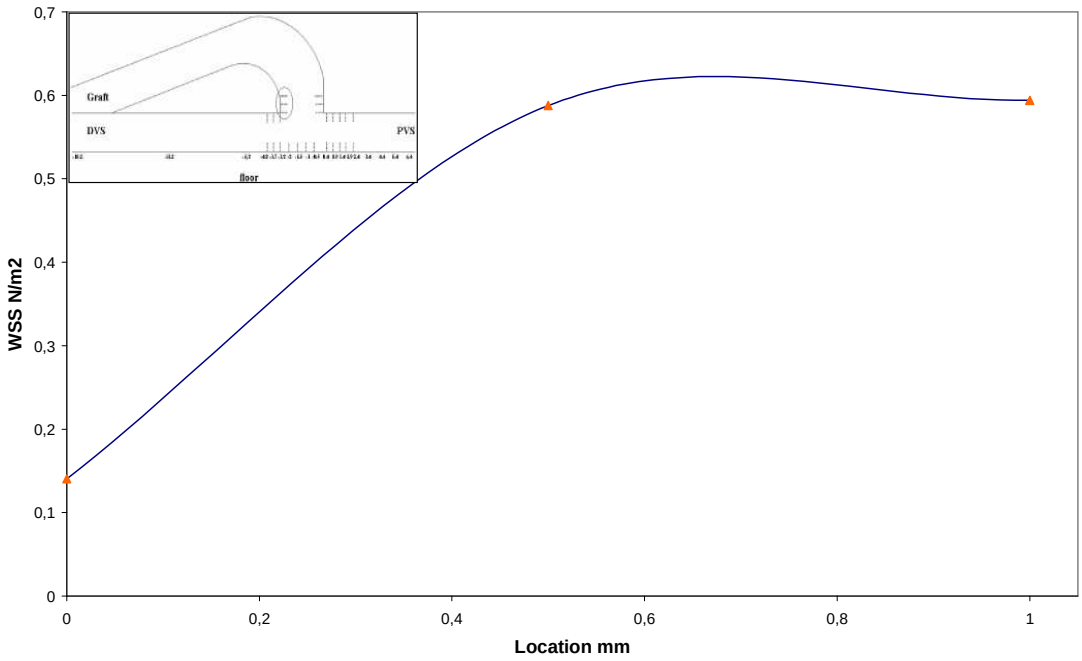

Figure 3.41 WSS estimation at the inner graft at Re=2400

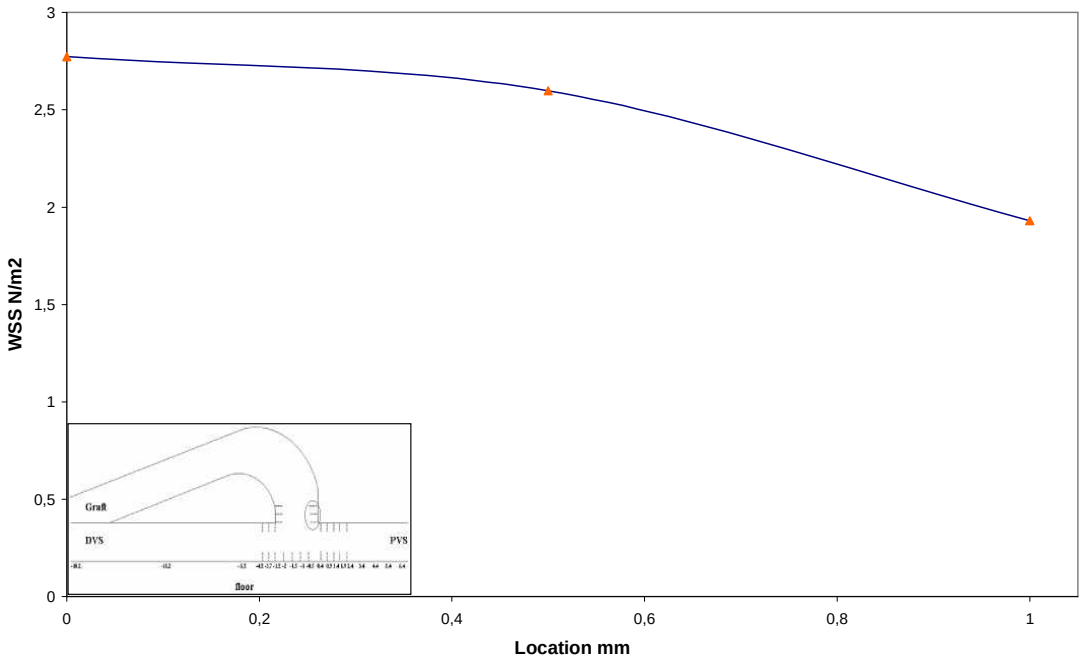

Figure 3.42 WSS estimation at the outer graft at Re=2400

CHAPTER 4

CONCLUSION

The objective of these to characterize the flow field within the venous anastomosis of a dialysis patient's AV graft since fluid dynamics has been implicated as a cause graft failure. The flow field was examined in detail using LDA meaurements inside an in vitro model of the venous anastomosis under steady flow condition.

Flow velocity measurements were done inside and AV graft to vein connections at two Reynolds numbers of 1400 and 2400 values under steady flow conditions. They represent the maksimum and average flow Reynolds values in pulsatile flow conditions. The flow measurements were at eighteen points on the floor side of the anastomosis, eleven points inside the graft. Mean velocity values and fluctuation velocity values were calculated. WSS were calculated in twenty six points inside graft and floor side of the anastomosis. WSS values along the floor vary from 0.5 to 11 N/m^2 for Re= 1400 and from 1 to 28 N/m^2 for Re=2400. The flow was determined as blunt at the inlet of the graft and progresses to the M shaped profiles inside the curve of the graft then continued upto the inlet of the graft to the anastomosis region. The flow velocity profiles were parabolic at Reynolds number of 1400 and 2400. The flow entered to the anastomosis region slightly skewed to the hood. The flow region inside the anastomosis is chaotic due to the mixture of the flow coming from graft and DVS. Two streams from graft and DVS merge inside the anastomosis and exit through the PVS. At the entrance of the PVS, the velocity profile becomes more blunt with high velocity near the hood and floor. Flow was separated at the inlet of the PVS part. Strong secondary flow was found in anastomosis and PVS. The separation region was detected at the toe side of the PVS at two Reynolds number. The maximum negative velocity measured in separation

bubble was -0.37 m/s which is small compared to the maximum value of mean velocity, 0.77 m/s at x/D=+0.4 for Re=2400. The length of the separation was almost one vein diameter long. Turbulence levels were found higher at the inlet of the PVS. These regions are considered critical regions for medical applications because of the lower shear stress values and higher turbulence due to the higher inertial forces. The blockage of the graft was mostly seen in this region. We find that this model was implanted very poor geometrical approach. The patency rate for these types geometrical connections will be very low.

The results of this study show the flow field inside an AV graft to be complex. The velocity flow field was found to be turbulent with a region of a separated flow which created a WSS region. These velocity flow patterns may contribute to the development and localization of inimal hyperplasia.

To fully understand the relationship between hemodynamics and graft failure will require further investigation of the flow field inside an AV graft under the possible different flow and geometrical conditions.

REFERENCES

[1] B. Ene-Iordache, S. Bruno, A. Remuzzi and G. Remuzzi, "*Effect of Hemodynamic Conditions on Arteriovenous Fistula for Hemodialysis Access"*, *Hemodialysis Technology*, *Contributions to Nephrology*, Vol. 137, pp. 54-59, 2002.

[2] Dantec Dynamics, July 2007 http://www.dantecdynamics.com/Default.aspx?ID=1046

[3] F. Loth, P. F. Fischer, N. Arslan, C. D. Bertram, S. E. Lee, T. J. Royston, W. E. Shaalan and H. S. Bassiouny, "*Transitional Flow at the Venous Anastomosis of an Arteriovenous Graft: Potential Activation of the ERK1/2 Mechanotranduction Pathway*", *Journal of Biomechanical Engineering*, Vol. 125, pp. 1144-1157, February 2003.

[4] F. Loth, S. A. Jones, C. K. Zarins, D. P. Giddens, R. F. Nassar, S. Glakov and H. S. Bassiouny, "*Relative Contribution of Wall Shear Stress and Injury in Experimental Intimal Thickening at PTFE End-to-Side Arterial Anastomoses*", *Journal of Biomechanical Engineering*, Vol.124, pp. 44-51, February 2002.

[5] F. W. LoGerfo, T. Soncrant, T. Teel and C. F. Dewey, "*Boundary Layer Separation in Models of Side-to-End Arterial Anastomoses*", *Arch Surg*, Vol. 114, pp. 1369-1373, December 1979.

[6] Fry, D. L."*Aute Vascular Endothelial Changes Associated With Increased Blood Belocity Gradients"*, *Circulat*. Res. Vol. 22, 165-197, 1968.

[7] H. Bassioumy, P. Fisher, F. Loth, and T. J. Royston, "*Pathobiology and Therapy of Venous Inimal Hyperplasia*", *National Institue of Health*, 2002-2006.

[8] I. V. Tricht, D. D. Wachter, D. Vanhercke, J. Tordoir and P. Verdonck, "*Assesment of Stenosis in Vascular Access Grafts*", *Artificial Organs*, Vol. 28, (7), pp 617-622, 2004.

[9] I. V. Tricht, D. D. Wachter, J. Tordoir and P. Verdonck, "*Hemodynamics in a Compliant Hydraulic In Vitro Model of Straight Versus Tapered PTFE Arteriovenous Graft*", *Journal of Surgical Research*, Vol. 116, pp. 297-304, 2004.

[10] I. V. Tricht, D. D. Wachter, J. Tordoir, and P. Verdonck, "Hemodynamics and Complications Encounterde with Arteriovenous Fistulas and Grafts as Vascular Access for Hemodialysis: A Review", Annuals *of Biomedical Engineering*, Vol. 33, (9), pp. 1142-1157, 2005.

[11] htttp://www.mayoclinic.com, 1998-2008

[12] Türk Nefroloji Derneği Merkez Bilgileri Broşürü, Dönem 2003.

[13] I. V. Tricht, D. D. Wachter, J. Tordoir, D. Vanhercke and P. Verdonck, "*Experimental Analysis of the Hemodynamics in Punctured Vascular Access Grafts*", *ASAIO Journal*, Vol. 51, pp. 352-359, 2005.

[14] I. V. Tricht, D. D. Wachter, J. Tordoir, P. Verdonck, "*Comparison of the Hemodynamics in 6 mm and 4-7 mm Hemodialysis Grafts by Means of CFD*", *Journal of Biomechanics*, Vol.39, pp. 226-236, 2006.

[15] J. C. Stettler and A. K. M. Fazle Hussain, "*On Transition of the Pulsatile Pipe Flow*", *J. Fluid Mech.*, Vol. 170, pp. 169-197, February 1986.

[16] M. C. S. Shu and N. H. C. Hwang, "*Haemodynamics of Angioaccess Venous Anastomoses*", October, 1990.

[17] M. C. S. Shu, G. P. Noon and N. H. C. Hwang, "*Flow Profiles and Wall Shear Stress Distribution at a Hemodialysis Venous Anastomosis: Preliminary Study*", *Biorheology*, Vol. 24, pp. 723-735, 1987.

[18] M. C. S. Shu, G. P. Noon, and N. H. C. Hwang, "*Phasic Flow Pattern at a Hemodialysis Venous Anastomosis*", *Biorheology*, Vol. 24, pp. 711-722, 1987.

[19] M. D. Deshpande and D. P. Giddens, "*Turbulence Measurements in a Constricted Tube*", *Journal of Fluid Mechanics*, Vol. 97, pp. 65-89, 1990.

[20] M. F. Fillinger, D. B. Kerns and R. A. Schwarz, "*Hemodynamics and Intimal Hyperplasia*" Chapter 2 of Vascular Access for Hemodialysis-II,

W. L. Gore & Associates, Inc., and Precept Press, Inc., (B. G. Sommer and M. L. Henry, Eds.), pp. 21-51, 1991."

[21] M. F. Fillinger, D. B. Kerns, D. Bruch, E. R. Reintz and R. A. Schwarz, "*Does the End-to-End Venous Anastomosis Offer a Functional Advantage Over the End-to-Side Venous Anastomosis in High-Output Arteriovenous Grafts?*", *Journal of Vascular Surgery*, Vol. 12, pp. 676-690, 1990.

[22] M. F. Fillinger, E. R. Reinitz, R. A. Schwartz, D. E. Resetarits, A. M. Paskanik, D. Brunch, C. E. Bredenberg, "*Graft Geometry and Venous Intimal-Medial Hyperplasia in Arteriovenous Loop Grafts*" *Journal of Vascular Surgery*, Vol. 11, No. 4, April 1990.

[23] M. F. Fillinger, E. R. Reinitz, R. A. Schwartz, D. E. Resetarits, A. M. Paskanik and C. E. Bredenberg, "*Beneficial Effects of Banding On Venous Intimal-Medial Hyperplasia in Arteriovenous Loop Grafts*", *The American Journal of Surgery*, Vol. 158, pp. 87-94, 1989.

[24] M. H.Kroll, J. D. Heliums, L. V. McIntire, A. I. Schafer, and J. L. Moake, "*Platelets and Shear Stress*", Blood Vol. 88(5), pp. 1525-1541,1996.

[25] N. Arslan, "*Experimental Characterization of Transitional Unsteady Flow Inside a Graft-to-Vein Junction*" Ph.D. Thesis, The University of Illinois at Chicago, 1999.

[26] N. Arslan, F. Loth, C. D. Bertram, H. S. Bassiouny, "*Transitional Flow Field Characterization inside an Arteriovenous Graft-to-Vein Anastomosis under Pulsatile Flow Conditions*", *Journal of Mechanics B/Fluids*, Vol. 24, pp. 353-365, 2005.

[27] National Kidney and Urological Diseases Information Clearinghouse, May 2006
http://kidney.niddk.nih.gov/kudiseases/pubs/transplant/

[28] Novoste, 2002-2006
http://www.novoste.com/patient/pat_graft.html

[29] P. E. Hughes and T. V. How, "*Flow Structures at the Proximal Side-to-End Anastomosis. Influence of Geometry and Flow Division*", *Journal of Biomechanical Engineering*, Vol. 117, May 1995.

[30] P. Miller, K. Danielson, G. Moody, A. Slifka, E. Drexer and J. Hertzberg, "*Matching Index of Refraction Using a diethyl phthalate/ethanol solution*

for In Vivo Cardiovascular Models", *Experiments in Fluids*, Vol. 41, pp. 375-381, June 2006.

[31] R. Y. Kanterman, T. M. Vesely, T. K Pilgram, B. W. Guy, D. W. Windus, and D. Piscus, "*Dialysis Access Grafts: Anatomic Location of Venous Stenosis and Results of Angioplasty*", *Radiology*, Vol. 195, pp. 135-139, 1995.

[32] S. Glakov, "*Intimal Hyperplasia, Vascular Modeling, and the Restenosis Problem*", *Circulation*, Vol. 89 (6), pp. 2888-2891, 1994.

[33] S. J. Schwab, "*Vascular Access for Hemodialysis*", *Kidney Int*., Vol. 55, pp. 2078-2090, 1999.

[34] S. S. White, C. K. Zarins, D. P. Giddens, H. Bassiouny, F. Loth, S. A. Jones and S. Glakov, "*Hemodynamic Patterns in Two Models of End-to-Side Vascular Graft Anastomoses: Effects of Pulsatility, Flow Division, Reynolds Number, and Hood Length*", *Journal of Biomechanical Engineering*, Vol. 115, pp. 104-111, February 1993.

[35] S. Unikrishnan, T. N. Huynh, B. C. Brott, Y. Ito, C. H. Cheng, A. M. Shih, M. Allon and A. S. Anayiotos, "*Turbulent Flow Evaluation of the Venous Needle During Hemodialysis*", *Journal of Biomechanical Engineering*, Vol. 127, December 2005.

[36] T. A Salam, A. B. Lumsden, W. D. Suggs, and D. N. Ku, "*Low Shear Stress Promotes Intimal Hyperplasia Thiskening*", *J. Vasc. Invest*., Vol. 2, 12-22, 1996.

[37] T. Kapoian and R. A. Sherman, "*A Brief History of Vascular Access for Hemodalysis: An Unfinished Story*", *Semin Nefhrol*., Vol. 3(17), pp. 239-245,1997.

[38] The Dow Chemical Company, 1995-2008 http://www.dow.com/glycerine/resources/table18.htm

[39] S. W. Lee, P. F. Fischer, F. Loth, T. J. Royston, J. K. Grogan and H. S. Bassiouny, "*Flow-Induced Vein-Wall Vibration in an Arteriovenous Graft*", *Journal of Fluid and Structures*, Vol. 20, pp. 837-852, 2005.

[40] United States Renal Data system (USRDS), September, 17, 2007. http://www.usrds.org